

Phytosulfokine receptors mediate stomatal closure in response to abscisic acid by controlling reactive oxygen species levels in guard cells

Dissertation

zur Erlangung des Doktorgrades

der Mathematisch-Naturwissenschaftlichen Fakultät

der Christian-Albrechts-Universität zu Kiel

vorgelegt von

Lena Anna Carstens

Kiel, Oktober 2021

Erste Gutachterin: Prof. Dr. Margret Sauter

Zweite Gutachterin: Prof. Dr. Jennifer Selinski

Tag der mündlichen Prüfung: 10.12.2021

TABLE OF CONTENTS

LIST OF ABBREVIATIONS.....	1
SUMMARY.....	3
ZUSAMMENFASSUNG.....	4
1 INTRODUCTION.....	6
1.1 Peptide signaling.....	6
1.2 PSK signaling.....	7
1.2.1 From <i>PSK</i> precursor gene to biological active PSK peptide.....	7
1.2.2 PSK perception	8
1.2.3 PSKR signaling promotes plant growth, development and biotic stress responses	10
1.3 ABA mediates stomatal closure in response to drought.....	11
1.3.1 ABA – from biosynthesis to signal transduction in guard cells.....	12
1.3.2 Elevation of Ca ²⁺ and ROS lead to stomatal closure	13
1.4 Drought and osmotic stress regulation by PSK/PSKR signaling	17
1.5 Objectives	18
2 MATERIAL AND METHODS.....	19
2.1 Material.....	19
2.2 Methods	21
2.2.1 Plant propagation.....	21
2.2.2 Molecular biological techniques	23
2.2.3 Microbiological techniques.....	29
2.2.4 Histochemical techniques	31
2.2.5 Plant physiological techniques.....	31
2.2.6 Protein analysis techniques	34
2.2.7 Microscopy techniques	36
3 RESULTS.....	37
3.1 Phytosulfokine signaling is required for stomatal closure	37
3.1.1 Expression analysis of PSK precursor and receptor genes.....	37
3.1.2 Protein expression of PSKR1 and PSKR2.....	39
3.1.3 The knockout of <i>PSKR1</i> and <i>PSKR2</i> results in higher leaf transpiration.....	40
3.1.4 PSK receptor signaling is required for ABA-mediated stomatal closure	41

3.1.5	The PSK peptide can restore impaired stomatal closure in <i>tpst-1</i>	43
3.2	PSKR signaling is required for the accumulation of ROS in guard cells in response to ABA likely via regulation of RBOH.....	44
3.2.1	PSKR signaling maintains ROS levels in ABA- or mannitol-stressed leaves	44
3.2.2	PSKR signaling is required for ABA-induced H ₂ O ₂ accumulation in guard cells	47
3.2.3	<i>RBOHD</i> and <i>RBOHF</i> are not transcriptional regulated by PSKRs in response to osmotic stress or ABA.....	50
3.2.4	<i>RBOHD/F</i> and <i>PSKR1</i> proteins exist in proximity at the plasma membrane.	51
3.2.5	<i>PSKR1</i> phosphorylates <i>RBOHD</i> and <i>RBOHF</i> <i>in vitro</i>	53
3.3	The aquaporin <i>PIP2;1</i> as a possible target of PSKR signaling.....	57
3.3.1	The aquaporin <i>PIP2;1</i> contributes to PSK-induced protoplast expansion	57
3.3.2	Transcripts of <i>PIP2;1</i> are not regulated by <i>PSKRs</i>	58
3.3.3	Phosphorylation of S280/S283 at the C-terminus of <i>PIP2;1</i> is not of importance for stomatal closure	59
3.3.4	<i>PSKR1</i> kinase regulates <i>PIP2;1</i> through phosphorylation.....	60
3.4	Expression analysis of <i>CNGCs</i> in guard cells.....	62
3.4.1	Specific expressions of <i>CNGCs</i> in <i>Arabidopsis</i>	63
3.4.2	Knockout of <i>CNGCs</i> with the CRISPR/Cas9 technology	66
4	DISCUSSION	68
4.1	Transpiration control of leaves via stomatal closure by PSKR signaling	68
4.2	Interplay between PSKR and ROS signaling during ABA-induced stomatal closure	70
4.2.1	Regulation of <i>RBOH</i> by PSKR kinase <i>in vitro</i>	72
4.2.2	The aquaporin <i>PIP2;1</i> as part of the PSKR signaling complex.....	73
4.2.3	PSKRs could increase cellular Ca ²⁺ by activating <i>CNGCs</i> in guard cells	75
4.3	Conclusion	77
5	LIST OF REFERENCES	78
	APPENDIX.....	97
	ACKNOWLEDGEMENT	117
	EIDESSTATTLICHE ERKLÄRUNG	118

LIST OF ABBREVIATIONS

Chemicals

APS	ammonium persulfate	IPTG	isopropyl- β -D-thiogalactopyranoside
DAB	3,3'-diaminobenzidine		
EDTA	ethylenediaminetetraacetic acid	LB	lysogeny broth
EtOH	ethanol	MES	2-(N-morpholino)-ethanesulfonic acid
HCl	hydrogen chloride	MS	Murashige & Skoog
H ₂ DCF-DA	2',7''-dichlorodihydro-fluorescein diacetate	NBT	nitro blue tetrazolium chloride
HEPES	4-(2-hydroxyethyl)-1-piperazineethanesulfonic acid	SDS	sodium dodecylsulfate
		TAE	Tris-acetate-EDTA
H ₂ O ₂	hydrogen peroxide	TE	Tris-EDTA
		YEP	yeast extract peptone

Proteins and peptides

AHA	ARABIDOPSIS H ⁺ -ATPase	PSK	phytosulfokine
		PSKR	PSK RECEPTOR
BAK1	BRI1-ASSOCIATED KINASE 1	PSY1	PEPTIDE CONTAINING SULFATED TYROSINE
BR	brassinosteroid	RBOH	RESPIRATORY BURST OXIDASE HOMOLOG
BRI1	BRASSINOSTEROID SENSITIVE 1	RGF1	ROOT MERISTEM GROWTH FACTOR 1
CPK	CALCIUM-DEPENDENT PROTEIN KINASES	RLP44	RECEPTOR-LIKE PROTEIN 44
CNGC	CYCLIC NUCLEOTIDE-GATED CHANNEL	SLAC1	SLOW ANION CHANNEL-ASSOCIATED 1
flg22	22 aa fragment of flagellin	TPST	TYROSYL PROTEIN SULFOTRANSFERASE
OST1	OPEN STOMATA 1		
PIP	PLASMA MEMBRANE INTRINSIC PROTEIN		

Molecular biological terms

A	alanine	GC	guanylate cyclase
ABA	abscisic acid	GFP	green fluorescent protein
ATP	adenosine triphosphate	GUS	β -glucoronidase
CaM	calmodulin	6xHIS	6x-Histidine-tag
cDNA	complementary DNA	KD	kinase domain
cGMP	cyclic guanosine monophosphate	LRR	leucine-rich repeat
cNMP	cyclic nucleotide monophosphate	LRR-RLK	LRR-receptor like kinase
D	aspartatic acid	MBP	maltose-binding protein
DNA	desoxyribonucleic acid	mRNA	messenger RNA
dNTP	desoxyribonucleoside triphosphate	PAGE	polyacrylamide gel electrophoresis
EF	calcium binding motif (E-helix-loop-F-helix)	PCR	polymerase chain reaction
FRET-AB	Förster resonance energy transfer – acceptor photobleaching	ROS	reactive oxygen species
gDNA	genomic DNA	RT	room temperature
		RT-PCR	reverse transcriptase PCR
		RT-qPCR	real-time quantitative PCR
		RNA	ribonucleic acid
		S	serine

SUMMARY

Plants are exposed to multiple abiotic and biotic stresses and have to perceive, integrate and respond to environmental signals due to their sessile lifestyle. To coordinate and integrate stress signals at the tissue and organ level, plants require cell-to-cell communication. Phytohormones, including peptide hormones, are essential components in plant signaling processes. Phytosulfokine (PSK) is a peptide hormone that promotes growth in *Arabidopsis thaliana* by enhancing cell expansion. It was recently shown to also maintain growth and delay leaf senescence under drought conditions. This study shows that PSK signaling not only controls leaf growth under drought stress but also transpiration by mediating stomatal closure to prevent water loss. Transcriptome and promoter-reporter analyses revealed expression of *PSK4*, *PSKR1* and *PSKR2* in guard cells suggesting a role of PSK receptor (PSKR) signaling in stoma regulation. The PSKR null mutant *pskr1-3 pskr2-1* was impaired in stomatal closure induced by the drought signaling hormone abscisic acid (ABA) and leaves showed greater water loss compared to wild type. High ABA concentrations enable the activation of OPEN STOMATA 1 (OST1) kinase, which targets multiple ion channels, causing a change in osmotic potential that leads to water efflux. Simultaneously, OST1 activates ROS production via RESPIRATORY BURST OXYDASE HOMOLOG D (RBOHD) and RBOHF, which in turn promotes Ca^{2+} signaling to maintain stomatal closure. To elucidate the molecular mechanism by which PSKR signaling mediates stoma closure, ROS accumulation in response to the drought signal ABA was analyzed with an H_2O_2 -sensitive dye. Guard cells of *pskr1-3 pskr2-1* plants accumulated less ROS when treated with ABA and stomatal closure of *pskr1-3 pskr2-1* was restored with the application of H_2O_2 . Since ROS accumulation in guard cells depends on activation of NADPH oxidases RBOHD/F at the plasma membrane, we tested the hypothesis that RBOHD/F are activated by PSKRs. Förster Resonance Energy Transfer (FRET) analyses revealed proximity of PSKR1 and RBOHD and of PSKR1 and RBOHF *in situ*. In addition, the kinase domain of PSKR1 phosphorylated ectopically expressed intracellular peptides of RBOHD and RBOHF *in vitro*, indicating that RBOHD/F may be substrates of PSKR1. Stoma closure requires rapid water movement out of guard cells and uptake of H_2O_2 . The entry of H_2O_2 into guard cells is facilitated by the aquaporin PLASMA MEMBRANE INTRINSIC PROTEIN 2;1 (PIP2;1) that could also be a target of PSKRs. A kinase assay revealed phosphorylation of PIP2;1 by PSKR1 kinase *in vitro* providing first evidence that PSKR1 may control H_2O_2 uptake into guard cells. Taken together, PSKR signaling is required for ABA-mediated stomatal closure by controlling ABA-induced ROS accumulation in guard cells possibly through direct phosphorylation of RBOHD/F and/or PIP2;1 at the plasma membrane.

ZUSAMMENFASSUNG

Pflanzen sind zahlreichen abiotischen und biotischen Stressfaktoren ausgesetzt und müssen aufgrund ihrer sessilen Lebensweise Umweltsignale wahrnehmen, integrieren und darauf reagieren. Um Stresssignale auf Gewebe- und Organebene zu koordinieren und zu integrieren, benötigen Pflanzen eine Kommunikation von Zelle zu Zelle. Phytohormone, einschließlich Peptidhormone, sind wesentliche Bestandteile der pflanzlichen Signalprozesse. Phytosulfokin (PSK) ist ein Peptidhormon, das das Wachstum von *Arabidopsis thaliana* fördert, indem es die Zellexpansion anregt. Kürzlich wurde gezeigt, dass es auch das Wachstum aufrechterhält und die Blattseneszenz unter Trockenheitsbedingungen verzögert. Diese Studie zeigt, dass die PSK-Signalübertragung nicht nur das Blattwachstum unter Trockenstress steuert, sondern auch die Transpiration, indem sie die Schließung der Stomata vermittelt, um Wasserverluste zu verhindern. Transkriptom- und Promotor-Reporter-Analysen ergaben eine Expression von *PSK4*, *PSKR1* und *PSKR2* in Schließzellen, was auf eine Rolle der PSK-Rezeptor (PSKR)-Signalübertragung bei der Stomaregulierung schließen lässt. Die Schließung der Stomata durch das Trockenstresshormon Abscisinsäure (ABA) war in der PSKR-Nullmutante *pskr1-3 pskr2-1* beeinträchtigt, und die Blätter zeigten im Vergleich zum Wildtyp einen größeren Wasserverlust. Hohe ABA-Konzentrationen ermöglichen die Aktivierung der OPEN STOMATA 1 (OST1) Kinase, die mehrere Ionenkanäle reguliert und eine Veränderung des osmotischen Potenzials bewirkt, was zu einem Wasserausstrom führt. Gleichzeitig aktiviert OST1 die ROS-Produktion über RESPIRATORY BURST OXYDASE HOMOLOG D (RBOHD) und RBOHF, was wiederum die Ca^{2+} Signalübertragung zur Aufrechterhaltung des Stomaschlusses fördert. Um den molekularen Mechanismus aufzuklären, durch den der PSKR-Signalweg den Stomaschluss vermittelt, wurde die ROS-Akkumulation als Reaktion auf das Trockenstresssignal ABA mit einem H_2O_2 -sensitiven Farbstoff analysiert. Die Schließzellen von *pskr1-3 pskr2-1* Pflanzen akkumulierten weniger ROS, wenn sie mit ABA behandelt wurden, und der Stomaschluss von *pskr1-3 pskr2-1* wurde durch die Zugabe von H_2O_2 wiederhergestellt. Da die ROS-Akkumulation in Schließzellen von der Aktivierung der NADPH-Oxidasen RBOHD/F an der Plasmamembran abhängt, haben wir die Hypothese getestet, dass RBOHD/F durch PSK Rezeptoren aktiviert werden. Förster-Resonanzenergietransfer (FRET) Analysen zeigten die Nähe von PSKR1 und RBOHD sowie von PSKR1 und RBOHF *in situ*. Darüber hinaus phosphorylierte die Kinasedomäne von PSKR1 ektopisch exprimierte intrazelluläre Peptide von RBOHD und RBOHF *in vitro*, was darauf hindeutet, dass RBOHD/F möglicherweise Substrate von PSKR1 sind. Der Stomaschluss erfordert eine schnelle Wasserbewegung aus den Schließzellen und die Aufnahme von H_2O_2 . Der Eintritt von H_2O_2 in die Schließzellen wird durch das Aquaporin PLASMA MEMBRANE INTRINSIC PROTEIN 2;1

(PIP₂;1) erleichtert, das auch ein Ziel von PSK Rezeptoren sein könnte. Ein Kinase-Assay zeigte die Phosphorylierung von PIP₂;1 durch die PSKR1-Kinase *in vitro* und lieferte damit erste Hinweise darauf, dass PSKR1 die H₂O₂-Aufnahme in die Schließzellen steuern könnte. Zusammenfassend lässt sich sagen, dass die PSKR-Signalübertragung für die ABA-vermittelte Schließung der Stomata erforderlich ist, indem sie die ABA-induzierte ROS-Akkumulation in den Schließzellen kontrolliert, möglicherweise durch direkte Phosphorylierung von RBOHD/F und/oder PIP₂;1 an der Plasmamembran.

1 INTRODUCTION

1.1 Peptide signaling

Higher plants are multicellular organisms where growth and development must be flexibly coordinated, due to their sessile lifestyle. Therefore, plants require well-organized cell-to-cell communication to respond to a changing environment. Well-studied is the involvement of phytohormones, such as cytokinin, abscisic acid (ABA), gibberellin, ethylene, jasmonate, salicylic acid and brassinosteroids (Zhao et al., 2021). The number of known hormones that contribute to cell signaling in plants has largely increased since the discovery of peptide hormones and their functions (Gancheva et al., 2019).

Plant peptide hormones can be divided into two classes: secreted peptides and non-secreted peptides, with the N-terminal secretory sequence determining the classification. The small number of non-secreted peptides is known to function in plant development and defense against pathogens. Evidence suggests that non-secreted peptides exit the cell through injured cells and thus contribute to cell-to-cell communication in pathogen defense (Gancheva et al., 2019; Yamaguchi et al., 2006). However, cell-to-cell communication is mostly fine-tuned by peptide hormones that are secreted and can be perceived by neighboring cells (Matsubayashi, 2014). Based on structural differences, secreted peptides can be further divided into post-translationally modified small peptides and cysteine-rich peptides (Matsubayashi, 2014; Tavormina et al., 2015). Post-translational modifications can be tyrosine sulfation, proline hydroxylation and hydroxyproline glycosylation, resulting in fully active peptide hormones which are required in developmental processes like meristem maintenance, organ abscission, embryogenesis, cell elongation, cell proliferation and differentiation, gravitropism and response to biotic and abiotic stimuli (Ghorbani, 2014; Stührwohltd et al., 2021). In recent years several peptides were identified that regulate osmotic stress responses. CAP-DERIVED PEPTIDE 1 (CAPE1) is a negative regulator of salt tolerance, by inhibiting the expression of salt tolerance genes that regulate osmolyte production, detoxification, stomatal closure control and cell membrane protection (Chien et al., 2015; Chen et al., 2020). From the ELICITOR PEPTIDE PRECURSORS (PROPEPs) that were first identified as immune-response peptides, PROPEP3 is highly induced by salt stress. The loss-of-function of the PROPEP3 precursor gene leads to salt hypersensitivity that can be rescued with the PEP3 phytocytokine (Nakaminami et al., 2018). PATHOGEN-ASSOCIATED MOLECULAR PATTERN-INDUCED PEPTIDE (PIP1) is known as an elicitor for immune responses (Hou et al., 2014). It closes stomata in a dose-dependent manner in response to pathogen attacks (Shen et al., 2020). The CLAVATA3/EMBRYO-SURROUNDING REGION-RELATED 25 (CLE25) peptide acts as a long-distance signal in response to drought stress. The peptide transmits

the dehydration signal from root to shoot through the vascular tissue, binds to BARELY ANY MERISTEM (BAM) receptors and thereby promotes ABA biosynthesis in leaves and thus stomatal closure (Takahashi et al., 2018). PHYTOSULFOKINE (PSK) contributes to drought and osmotic stress responses such as the drought-dependent flower drop in tomato (Reichardt et al., 2020) and root and shoot growth in *Arabidopsis thaliana* during osmotic stress (Stührwohldt et al., 2021).

1.2 PSK signaling

1.2.1 From PSK precursor gene to biological active PSK peptide

The secreted peptide PSK was first described in *Asparagus officinalis*, as the factor that is responsible for the proliferation in suspension-cultured cells kept at low density (Matsubayashi and Sakagami, 1996). In *Arabidopsis*, the PSK pre-pro-protein, containing the PSK domain YIYTQ, is encoded by five precursor genes, *PSK1-5*. All precursor genes are expressed throughout organs, tissues and developmental stages of the plant (Kutschmar et al., 2009; Stührwohldt et al., 2011). Two other loci are annotated as PSK precursor genes, the pseudogene *PSK6*, encoding the PSK-related sequence YIYTH, and *At2g22942*, encoding two canonical PSK sequences. The expression of both genes is very low and the biological functions remain to be described (Kaufmann and Sauter, 2019).

An N-terminal signal peptide targets the PSK pre-pro-protein to the endoplasmic reticulum (Lorbiecke and Sauter, 2002), where it gets cleaved. In the cis-Golgi network, the enzyme TYROSYL PROTEIN SULFOTRANSFERASE (TPST) mediates the posttranslational modification of PSK pro-proteins by catalyzing the transfer of sulfate from 3' phosphoadenosine 5'-phosphosulfate (PAPS) to the hydroxyl group of tyrosine (Komori et al., 2009; Moore, 2003). Sulfation of the two tyrosine residues within the PSK domain is required for the full biological activity of the PSK peptide (Matsubayashi et al., 1996; Kutschmar et al., 2009). In *Arabidopsis*, *TPST* is the only known gene with that biological function and is responsible for the sulfation of other peptide hormones such as PLANT PEPTIDE CONTAINING SULFATED TYROSINE 1 (PSY1) and ROOT MERISTEM GROWTH FACTOR 1 (RGF1) (Kaufmann and Sauter, 2019). The loss-of-function mutant *tpst-1* shows a pleiotropic phenotype that can be rescued with the application of all three peptide hormones (Matsuzaki et al., 2010), showing the importance of sulfated peptide signaling.

The disulfated PSK pro-protein is secreted into the apoplast, where it must be proteolytically processed to produce the mature functional peptide (Matsubayashi, 2011). So far it is not

fully clear which enzymes are responsible for the proteolytic cleavage of PSK but most likely, SUBTILISIN-LIKE SERINE PROTEASEs (SBTs) are involved. The pro-protein of PSK4 is proteolytically processed by SBT1.1 *in vivo* (Srivastava et al., 2008) and the pro-peptide of PSK1 is processed at its C-terminal site by SBT3.8 (Stührwohldt et al., 2021).

1.2.2 PSK perception

PSK is perceived by membrane-bound PSK receptors (PSKRs) that are encoded by two genes in Arabidopsis. Based on sequence homology to the first characterized PSK receptor in carrot (*DcPSKR1*), *PSKR1* and *PSKR2* were identified (Matsubayashi et al., 2002; Matsubayashi, 2006; Amano et al., 2007). They belong to the group of leucine-rich repeat receptor-like kinases (LRR-RLKs), the largest group of RLKs with over 200 members in Arabidopsis. They are characterized by a cytoplasmic protein kinase domain and an extracellular LRR domain that is arranged in tandem repeats of conserved leucines (Shiu and Bleecker, 2001, 2003). CLAVATA1 (CLV1), BRASSINOSTEROID SENSITIVE 1 (BRI1) and FLAGELLIN-SENSITIVE 2 (FLS2) are related LRR-RLKs that regulate growth, development and defense against pathogens (Ogawa et al., 2008; Kinoshita et al., 2005; Chinchilla et al., 2006).

The extracellular LRR domain of PSKR1 and PSKR2 contains 21 LRRs with an island domain that binds PSK (Amano et al., 2007). Hydrogen bonds, van der Waals packing and the two sulfates of PSK are needed for the binding between PSK and PSKR1. The required binding residues of PSKR1 are conserved in PSKR2, suggesting similar PSK recognition (Wang et al., 2015b). The root phenotype of the *tpst-1 pskr1-3 pskr2-1* triple mutant revealed a synergistic effect of ligand and receptor knockout, suggesting an activation of the receptor without the ligand (Kaufmann et al., 2021). The extracellular LRR domain is connected through a transmembrane domain with the intracellular kinase domain (KD), which harbors a guanylate cyclase (GC) and a calmodulin-binding (CaM) site (Kwezi et al., 2011). Point mutations in either one of these functional domains in PSKR1 lead to loss of receptor function, indicating the need of all three functional domains for the signal transduction (Hartmann et al., 2014; Ladwig et al., 2015).

PSKR1 is part of a multimeric protein complex at the plasma membrane that includes the co-receptor BRI1-ASSOCIATED KINASE 1 (BAK1), proton pumping ARABIDOPSIS H⁺-ATPase 1 and 2 (AHA1/2) and the cation channel CYCLIC NUCLEOTIDE-GATED CHANNEL17 (CNGC17) (Ladwig et al., 2015) (Figure 1). BAK1 is a member of the SOMATIC EMBRYOGENESIS RECEPTOR-LIKE KINASE (SERK) family and is also named SERK3. BAK1/SERK3 and other SERKs have been characterized as co-receptor for LRR-RLKs such as PSKR1, BRI1 and FLS2 (Rusinova et al., 2004;

Chinchilla et al., 2009; Ladwig et al., 2015). Crystal structure analysis of PSKR1 reveals that PSK is not required at the binding site of the receptor with its coreceptor, but PSK binding stabilizes the PSKR island domain, which supports the heterodimerization between PSKR1 and SERK1, SERK2 and BAK1 (Wang et al., 2015b). Essential for PSKR1 activity is its phosphorylation (Hartmann et al., 2014) and PSKR1 and PSKR2 were shown to be phosphorylated by BAK1 (Kaufmann, 2018). AHA1/2 are the most abundant proton pumps in the plasma membrane in Arabidopsis, and their loss-of-function mutation is lethal (Haruta et al., 2010). Proton pumps in the plasma membrane maintain an electrochemical gradient across the plasma membrane that is required to promote the transport of solutes by secondary transporters. AHA activity drives cell expansion by acidifying the extracellular matrix (Haruta et al., 2010; Hager, 2003). The C-terminus of AHAs is targeted by RLKs, such as BRI1, PSY1R and PSKR1 (Caesar et al., 2011; Fuglsang et al., 2014; Kaufmann, 2018) and phosphorylation leads to AHA activation. CNGC17 belongs to the CNGC family, with 20 members in Arabidopsis that are identified as cation channels (Leng et al., 1999). The CNGCs are separated in 5 groups and CNGC17 belongs to group III together with CNGC14, CNGC15, CNGC16 and CNGC18 (Talke et al., 2003). Bioinformatic analysis predicted a CaM-binding domain and a cyclic-nucleotide binding domain (CNBD) at the C-terminus of plant CNGCs (Talke et al., 2003). Biochemical analysis of a related protein in tobacco (*NtCBP4*) indicates an overlap of CaM-binding domain and CNBD (Arazi et al., 2000). Ectopic expression of CNGC2 in Human Embryonic Kidney (HEK) cells resulted in Ca^{2+} elevation and CaM binding whereas binding of cNMP was blocked supporting the biochemical analysis in tobacco (Hua et al., 2003). In contrast to CNGC2, the CaM-binding site of CNGC20 does not overlap with the cNMP binding site (Fischer et al., 2013) and CNGC12 harbors multiple CaM-binding domains at the N- and C-termini (DeFalco et al., 2016), indicating that further analyses of the functional domains of CNGCs are required. In the nanocluster with PSKR1, CNGC17 was shown to be important for PSK-dependent growth promotion. PSK-induced protoplast expansion was shown to depend on the second messenger cGMP and CNGC17, showing that PSKR1 with its GC domain possibly synthesizes cGMP that binds to CNGC17 for its activation (Ladwig et al., 2015).

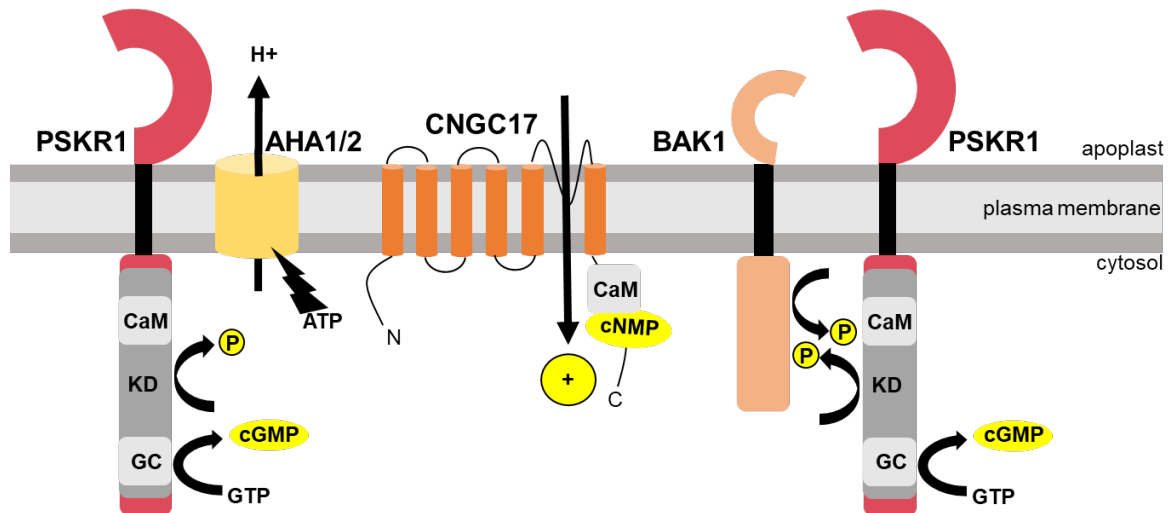


Figure 1: Schematic representation of the nanocluster with PSKR1 (based on Ladwig et al., 2015).

PSKR1 exists in a larger protein complex at the plasma membrane that includes the co-receptor BAK1, the proton pumps AHA1/2 and the cation channel CNGC17. PSKR1 harbors a functional GC domain, a CaM binding site and a kinase domain (KD) (Kwezi et al., 2011; Hartmann et al., 2014). PSKR1 directly interacts with AHA1/2 and BAK1, while AHA1/2 and BAK1 interact with CNGC17, which harbors an overlapping CaM and cNMP binding site at the C-terminus (Talke et al., 2003; Ladwig et al., 2015).

1.2.3 PSKR signaling promotes plant growth, development and biotic stress responses

The importance of PSKR signaling is evident in loss-of-function mutants with defects in root and shoot growth, pollen tube guidance and immune responses against pathogens. PSK was first identified as a mitogenic factor in suspension-cultured cells derived from mesophyll cells of *Asparagus officinalis*, in which it induces proliferation when kept at low density, indicating that PSK is an autocrine-type cell growth factor (Matsubayashi et al., 1996). Later studies showed that PSK acts non-cell autonomously (Wheeler and Irving, 2010; Hartmann et al., 2013), demonstrating that PSK acts as both a paracrine and autocrine factor.

PSK was shown to enhance root (Kutschmar et al. 2009), hypocotyl (Stührwohldt et al., 2011) and cotton fiber growth (Han et al., 2014) by promoting cell elongation. It was further shown that protoplast expansion is induced by PSK through PSKR1 (Stührwohldt et al., 2011) and that shoot size is a result of reduced cell size when PSKR signaling is knocked out (Hartmann et al., 2014). Reproduction is influenced by PSK signaling through promotion of germination and pollen tube growth as shown in tobacco and pear (Chen et al., 2000; Kou et al., 2020), as well as pollen tube guidance in Arabidopsis where loss of PSK receptors causes a reduced fertilization success and seed production (Stührwohldt et al., 2015). In addition to sexual reproduction, PSK promotes somatic

embryogenesis in carrot and *C. japonica* (Kobayashi et al., 1999; Igasaki et al., 2003). Furthermore, PSKR signaling, through RECEPTOR-LIKE PROTEIN 44 (RLP44), determines xylem cell fate through maintenance of procambial cell identity (Holzwardt et al., 2018).

Depending on the pathogen, PSK is promoting plant immunity. PSKR signaling has a positive effect on immunity response against necrotrophic pathogens such as *Alternaria brassicicola*, *Botrytis cinerea*, *Sclerotinia sclerotiarum*, *Fusarium oxysporum* and *Ralstonia solanacearum* (Loivamäki et al., 2010; Mosher et al., 2013; Zhang et al., 2018b), whereas PSKR signaling reduces plant immunity against (hemi-)biotrophic pathogens such as *Hyaloperonospora arabidopsidis* and *Pseudomonas syringae* (Loivamäki et al., 2010).

Gene expression profiles identified possible targets of PSKR signaling in reactive oxygen species (ROS) production in *Gossypium hirsutum* (Han et al., 2014), supported by the finding that the ectopic expressed peptide of *PbrPSK2* increases ROS production in pear pollen tubes (Kou et al., 2020). In Arabidopsis, elevated levels of ROS induce transcription factors that control quiescent center cell division and distal stem cell differentiation through PSK signaling (Kong et al., 2018).

Recent studies indicate a role of PSKR signaling in growth maintenance during osmotic stress and drought and provide evidence that PSKR and ABA signaling are dependent on each other (Rajamanickam et al., 2021).

1.3 ABA mediates stomatal closure in response to drought

Drought is caused by water shortage and results in cellular osmotic stress. Plants adapt to drought by a wide range of responses including changes in morphology, such as deep-rooting to reach water and a reduction in shoot growth to reduce the transpiring surface area (Foxy and Fort, 2019). In addition, plants accumulate solutes for cellular osmotic adjustment and regulate water flux (Turner, 2018). During the evolution of terrestrial plants, the development of stomata was an important element for adaptation to dry environmental conditions (Umezawa et al., 2010; Sussmilch et al., 2019). Stomata are regulated pores that allow uptake of CO₂ for photosynthesis and limit water loss through an otherwise gas-impermeable plant surface. Three morphological types of stomata exist, a single guard cell identified in *Funaria* and *Physcomitrella* spp., dumb-bell-shaped stomata with subsidiary cells at the border, seen in monocot plants, and the kidney-shaped form that is seen in most dicot plants (Sussmilch et al., 2019). Stomata are under control of numerous stimuli such as water status, light, CO₂, Ca²⁺, ROS and ABA (Kim et al., 2010; Kwak et al., 2003).

1.3.1 ABA – from biosynthesis to signal transduction in guard cells

ABA is required in plant growth and developmental processes such as promotion of root elongation, inhibition of shoot growth, lateral root formation and seed germination, as well as responses to pathogens, salinity and cold (Finkelstein, 2013; Cardoso et al., 2020). Among multiple processes controlled by ABA, it is the key hormone known to regulate drought responses. This chapter will focus on the regulation of drought stress-induced stomatal closure, to reduce water transpiration.

ABA is a sesquiterpenoid ($C_{15}H_{20}O_4$) whose biosynthesis takes place in five steps. The *ABA DEFICIENT 1 (ABA1)* encodes zeaxanthin epoxidase that catalyzes the formation of zeaxanthin to violaxanthin. *aba1*, is the first ABA-deficient mutant that was described in *Arabidopsis*, has non-dormant seeds and an enhanced water loss compared with wild type (Koorneef et al., 1982; Rock and Zeevaart, 1991; Finkelstein, 2013). Violaxanthin is converted to neoxanthin by ABA4 and through oxidative cleavage by 9-*cis*-epoxycarotenoid dioxygenase (NCED), xanthoxin is produced in plastids (Schwartz et al., 1997). Neoxanthin synthesis is dependent on ABA4, which loss-of-function phenotype has a sufficient ABA synthesis in contrast to *aba1* (North et al., 2007), indicating that an alternative biosynthesis step takes place during the conversion from violaxanthin to xanthoxin. In the cytosol xanthoxin is then further converted through ABA aldehyde oxidase (AAO), encoded by ABA2, to ABA. During that step, the molybdenum cofactor (MoCo) catalyzes the reaction and the loss-of-function of the MoCo sulfuryase impairs ABA biosynthesis (Bittner et al., 2001). For a long time, it was assumed that drought-dependent ABA synthesis occurs in roots and that ABA acts as a long-distance signal that is transported to leaves where it promotes stomatal closure (Davies et al., 2005). Grafting experiments using *Pisum sativum* wild type and a loss-of-function mutant for ABA2 as well as *Solanum lycopersicon* wild type and an AAO mutant revealed that ABA synthesis occurs mainly in leaves and that ABA is transported to roots (McAdam et al., 2016a; Zhang et al., 2018a). Phloem companion cells, guard cells, mesophyll and parenchyma cells around the vascular tissues synthesize ABA (McAdam et al., 2016b; Bauer et al., 2013; Merilo et al., 2018). Aside from synthesis, ABA accumulation occurs through hydrolysis of its glycosyl ester (ABA-GE) (Xu et al., 2012).

ABA binds to PYRABACTIN RESISTANCE 1 (PYR)/PYR1-LIKE (PYL)/REGULATORY COMPONENT OF ABA RECEPTOR (RCAR) receptors, allowing inhibition of PROTEIN PHOSPHATASE 2C (PP2C), which in the absence of ABA is negatively regulating the signal transduction (Park et al., 2009) (Figure 2). The active PP2C inhibits the activation, through dephosphorylation, of the SUCROSE NONFERMENTING-1-RELATED KINASE 2 orthologs (SnRK2s), in guard cells most importantly OPEN STOMATA 1 (OST1/SnRK2.6).

In addition, it inhibits the slow-sustained (S-type) anion channel SLOW ANION CHANNEL-ASSOCIATED 1 (SLAC1) and calcium channels by dephosphorylation, resulting in interruption of the signaling cascade and no closure of the stomata. In the presence of ABA, PYR/PYL/RCAR inhibit PP2C, which results in autophosphorylation of OST1, that leads to phosphorylation of downstream targets, such as the slow-sustained (S-type) and rapid-transient (R-type) anion channels SLAC1 and QUICKLY ACTIVATING ANION CHANNEL 1 (QUAC1) which drive plasma membrane depolarization (Vahisalu et al., 2008; Imes et al., 2013). Subsequently, depolarization activates the voltage-dependent K⁺ efflux channel GUARD CELL OUTWARD RECTIFYING K⁺ CHANNEL (GORK) (Hosy et al., 2003), which decreases cellular K⁺ (Schroeder, 2003). Besides GORK, K⁺ UPTAKE TRANSPORTER 6 (KUP6) supports the efflux of K⁺ (Osakabe et al., 2013). Potassium efflux lowers cell osmotic potential and, consequently, promotes water efflux resulting in stomatal closure. Notably, the control of facilitated water efflux through aquaporins that leads to stomatal closure is not well characterized. In Arabidopsis, ABA-induced stomatal closure is hydraulically supported by the PLASMA MEMBRANE INTRINSIC PROTEIN 2;1 (PIP2;1) that is a target of OST1 (Grondin et al., 2015; Rodrigues et al., 2017). PIP2;1 was also shown to facilitate entry of apoplastic H₂O₂ into guard cells in an ABA-dependent manner (Rodrigues et al., 2017). Conflicting results were obtained with *pip2;1* and *pip2;1-2* knock-out lines that showed wild-type-like ABA-induced stomatal closure (Ceciliato et al., 2019; Wang et al., 2015a), indicating that more research is required to clarify the role of PIP2;1 in ABA-induced stomatal closure.

1.3.2 Elevation of Ca²⁺ and ROS lead to stomatal closure

Despite the OST1-dependent phosphorylation of anion channels SLAC1 and QUAC1, inducing a plasma membrane depolarization, ABA signaling of stoma closure requires the second messengers Ca²⁺ and ROS (Huang et al., 2019; Sierla et al., 2016). Elevation of ROS levels in guard cells is induced by high carbon dioxide concentrations (Chater et al., 2015), ABA and biotic stress (Grondin et al., 2015; Rodrigues et al., 2017; Singh et al., 2017). Besides production of ROS in chloroplasts (Foyer and Harbinson, 1994; Iwai et al., 2019), ROS is produced in the apoplast by NADPH oxidases at the plasma membrane (Kwak et al., 2003). NADPH oxidases in Arabidopsis are termed *RESPIRATORY BURST OXIDASE PROTEINS (RBOHs)* and are encoded by a gene family of 10 genes (*RBOHA–J*) of which *RBOHD* and *RBOHF* are expressed specifically in guard cells and function in ABA-induced ROS production (Torres et al., 1998, 2002; Bánfi et al., 2000; Kwak et al., 2002, 2003).

Transcripts of *RBOHD* and *RBOHF* are increased by ABA, drought, salt and the osmolyte mannitol (Kwak et al., 2003; Kilian et al., 2007). The loss-of-function mutant *rbohD* shows no difference in stomatal closure in response to ABA compared with wild type whereas ABA-induced stomatal closure is slightly impaired in *rbohF* and strongly impaired in the double knockout mutant *rbohD/F* (Kwak et al., 2003), indicating that *RBOHD* and *RBOHF* functional overlap in ABA-induced stomatal closure. At the protein level, RBOHs are activated by elevated cytosolic Ca^{2+} and phosphorylation. RBOHF is phosphorylated by CALCINEURIN B-LIKE (CBL) protein interacting with CBL-INTERACTING PROTEIN KINASES (CIPKs) in a Ca^{2+} -dependent manner (Kimura et al., 2013). Controversial reports exist on how CIPK26 controls ROS production via RBOHF as a negative regulator (Kimura et al., 2013) or as a positive regulator (Drerup et al., 2013). The guard cell-specific kinase OST1 also phosphorylates RBOHF, but the physiological role of the phosphorylation remains to be characterized (Sirichandra et al., 2009). The regulation of RBOHD is well analyzed mainly regarding plant immunity where ROS production is promoted by N-terminal RBOHD phosphorylation mediated by the plant purinoreceptor DOESN'T RESPOND TO NUCLEOTIDES 1 (DORN1), the SERINE/THREONINE KINASE 1 (SIK1), CYSTEINE-RICH RLK 2 (CRK2), BOTRYTIS-INDUCED KINASE 1 (BIK1) and CALCIUM-DEPENDENT PROTEIN KINASE 4-6 (CPK4-6) and CPK11 (Chen et al., 2017; Zhang et al., 2018c; Kimura et al., 2020; Kadota et al., 2014; Dubiella et al., 2013). Protein-protein interaction studies indicate an interaction of RBOHD with OST1 (Acharya et al., 2013) and ROS production is increased after phosphorylation of RBOHD in HEK cells (Ogasawara et al., 2008) which is why OST1 is considered a positive regulator of RBOHD activity.

RBOHs catalyze the transfer of electrons from cytoplasmic NADPH to oxygen in the extracellular space to form the superoxide anion ($\text{O}_2^{\cdot-}$) that is subsequently converted to H_2O_2 by superoxide dismutase (Marino et al., 2012). The resulting H_2O_2 enters the guard cells possibly via the aquaporin PIP2;1 (Rodrigues et al., 2017). MITOGEN ACTIVATED PROTEIN KINASES (MAPKs) are downstream targets of ROS signaling in guard cells (Lee et al., 2016). MPK9 and MPK12 were shown to be activated through ABA and H_2O_2 signaling and to positively regulate stomatal closure (Jammes et al., 2009). Also, the PP2C phosphatases ABI1 and ABI2 play a role in the elevation of H_2O_2 for stomatal closure. Genetic analysis revealed that ROS production was not induced by ABA in *abi1-1* whereas Ca^{2+} elevation in guard cells and H_2O_2 -induced stomatal closure takes place (Murata et al., 2001). Stomatal closure and Ca^{2+} elevation were impaired in *abi2-1* but ROS production was induced with ABA, indicating that ABI1 acts upstream and ABI2 acts downstream of ROS production. However, the exact role of ABI1 and ABI2 remains to be characterized (Murata et al., 2001; Meinhard et al., 2002). The ROS burst in guard cells

activates Ca^{2+} signaling through cytosolic Ca^{2+} elevation and enhanced sensitivity of Ca^{2+} activated proteins, such as CaM, CBL1, CBL9, CPK4-6, CPK11, TWO PORE CHANNEL 1 (TPC1) and RBOHD (Köhler and Blatt, 2002; Kim et al., 2010; Hubbard et al., 2012; Pei et al., 2000; Ogasawara et al., 2008; Rienmüller et al., 2010). Ca^{2+} elevation occurs through plasma membrane-localized Ca^{2+} -permeable non-selective cation channels (I_{Ca}) or release from intracellular Ca^{2+} stores (Kim et al., 2010). The ABA-dependent activation of I_{Ca} channels requires ABA receptors PYR/PYL/RCARs, CPKs and the LRR-RLK GUARD CELL HYDROGEN PEROXIDE-RESISTANT (GHR1) (Munemasa et al., 2015). The H_2O_2 -sensitive GHR1 is activated by ROS and, in turn, activates calcium channels (Hua et al., 2012). To date, the Ca^{2+} -permeable channels that contribute to ABA-mediated stomatal closure have not been identified. The cation channels CNGC5 and CNGC6 are cGMP-activated nonselective Ca^{2+} -permeable cation channels present in Arabidopsis guard cells, but knockout of both genes did not impair I_{Ca} channel activity (Wang et al., 2013). Recent research identified the Ca^{2+} -permeable channel OSCA1.3 to be required for stomatal closure in response to immune signaling but not in response to ABA. OSCA1.3 channel activity is promoted through phosphorylation by BIK1 (Thor et al., 2020). Elevated Ca^{2+} in guard cells activates the S-type anion channel SLAC1 through CPKs and GHR1 (Sierla et al., 2018). PP2Cs were suggested to inhibit Ca^{2+} signaling of ABA-induced stomatal closure through the dephosphorylation of SLAC1 kinases CPK23/21 and OST1 (Geiger et al., 2010) and possibly by dephosphorylating Ca^{2+} permeable I_{Ca} channels to prevent activation by ABA signaling via GHR1 (Murata et al., 2001; Hua et al., 2012). Finally, RBOHs possess Ca^{2+} -binding EF-hand motifs and are controlled by Ca^{2+} -dependent kinases as described above. ABA-mediated stomatal closure is a well-studied complex signaling network of protein kinases, transporters and channels. As described, it also includes second messengers such as Ca^{2+} and H_2O_2 , which play a central role in signal transduction.

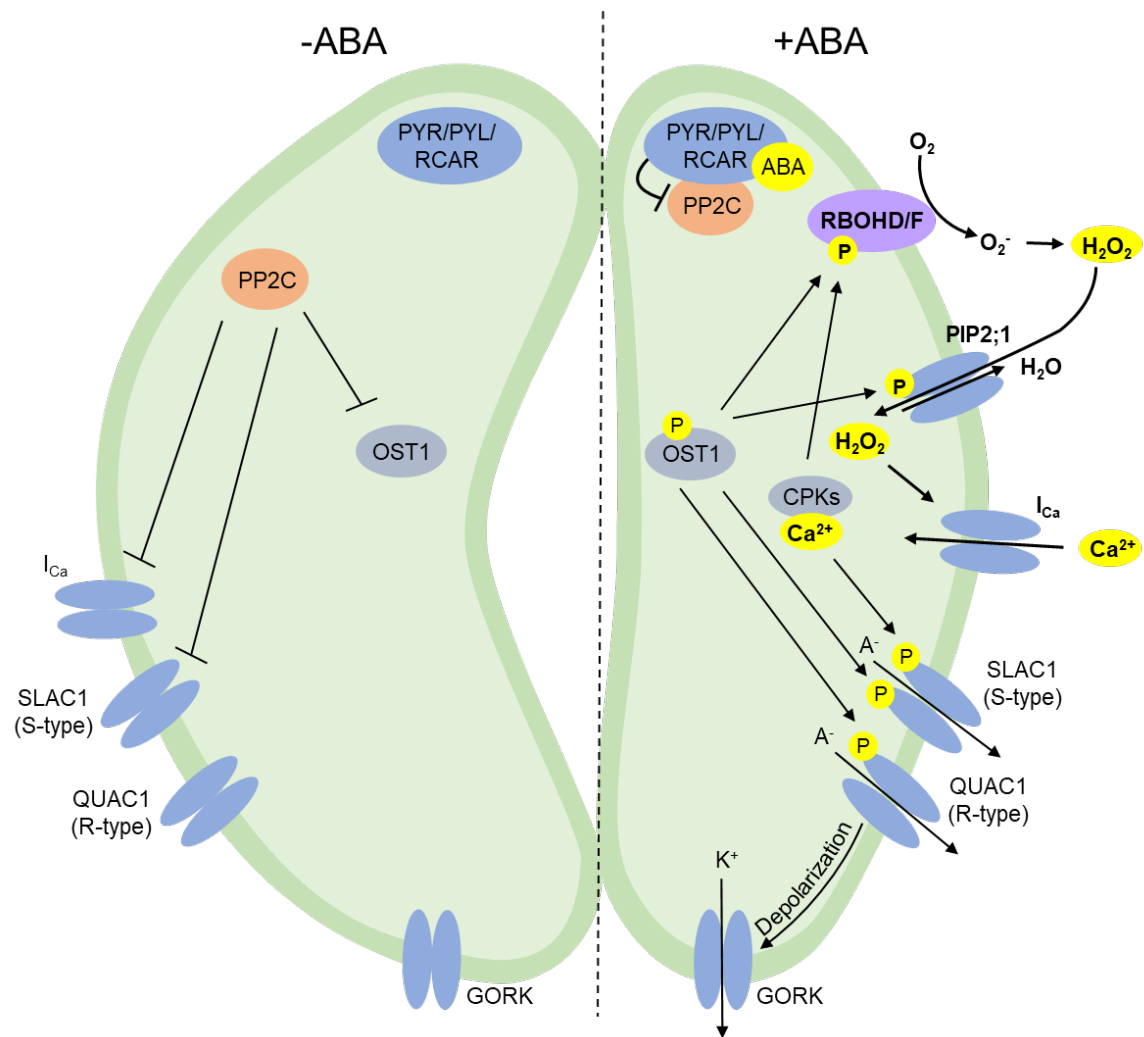


Figure 2: Simplified representation of molecular mechanisms in the absence or presence of ABA in the guard cell.

In the absence of ABA, the protein phosphatase PP2C dephosphorylates the SnRK2 OST1, S-type anion channel SLAC1 and calcium-permeable channels (I_{Ca}) preventing closure of stomata. ABA binds to its PYR/PYL/RCAR receptor which inhibits PP2Cs thus leading to activation of OST1 through autophosphorylation. Activated OST1 phosphorylates SLAC1 and QUAC1, thereby inducing membrane depolarization and activation of the voltage-dependent K^+ efflux channel GORK. Osmotic potential changes and water efflux through PIP2;1 follow. Simultaneously, OST1 activates RBOHD and RBOHF. H_2O_2 enters the cell via PIP2;1 where it activates calcium-permeable non-selective channels (I_{Ca}). A rise in cellular calcium activates CPKs, which are responsible for the activity of RBOHD and RBOHF by phosphorylating them (Wang and Song, 2008; Postiglione and Muday, 2020).

1.4 Drought and osmotic stress regulation by PSK/PSKR signaling

The nanocluster with PSKR1 at the plasma membrane is proposed to regulate cell expansion by activation of proton pumps and subsequent acidification of the cell wall. A controlled osmotic potential ensures water uptake and maintenance of turgor pressure as a driving force for growing plant cells. Recent studies revealed a role of PSKR signaling in maintaining root and shoot growth under mannitol-induced osmotic stress (Stührwohldt et al., 2021; Rajamanickam et al., 2021). Expression of *PSK1*, *PSK3*, *PSK4* and *PSK5* is induced and propeptide processing by SBT3.8 that processes the PSK1 propeptide is required to maintain root growth under high mannitol (200 mM) stress (Stührwohldt et al., 2021). The strong root growth retardation observed in the loss-of-function mutant *sbt3.8* with mannitol is reverted by the application of PSK (Stührwohldt et al., 2021). In addition, PSKR signaling maintains shoot growth under mild osmotic stress (Rajamanickam et al., 2021). *PSK3* and *PSKR1* are upregulated in the shoot under mild osmotic stress imposed by a low concentration (50 mM) of mannitol (Rajamanickam et al., 2021). Both studies show for *Arabidopsis* that root and shoot growth, and survival under mild drought conditions are dependent on PSK/PSKR signaling. Plants that overexpress *SBT3.8* are more tolerant to water shortage compared to wild type (Stührwohldt et al., 2021) and PSKR-deficient plants have smaller shoots, premature leaf senescence and reduced photosynthetic activity when drought-stressed (Rajamanickam et al., 2021). Moreover, PSK signaling promotes drought stress-induced flower drop by inducing pedicel abscission in the tomato inflorescence (Reichardt et al., 2020). The overexpression of *PHYTAPHASE 2 (SIPHYT2)*, shown to process the PSK precursor in tomato, reveals enhanced flower drop when drought-stressed, indicating control of abscission by PSK signaling. In summary, the studies reveal a role of PSK/PSKR signaling in osmotic and drought stress resistance. The molecular mechanisms that provide drought resistance via PSK/PSKR signaling in the shoot remain to be characterized.

1.5 Objectives

Based on the observation that PSKR-deficient *Arabidopsis* plants are more sensitive to drought stress than wild type, with reduced growth and premature leaf senescence, we hypothesized that PSKR signaling may delay senescence by controlling water loss during water shortage. Under water-limiting conditions, transpiration is reduced through closure of stomata with abscisic acid as a key hormone that promotes stomatal closure. To study a role of PSKR signaling in stoma closure, transcriptome and promoter-reporter analyses will provide information on whether PSK and PSKRs are expressed in guard cells. A physiological role of PSKR signaling in stomatal closure will be investigated by comparing stomatal closure induced by ABA as a drought signal in PSK(R) loss-of-function and gain-of-function mutants. Previous results revealed co-immunoprecipitation of PSKR1 with RBOHD and PIP2;1 (AG Sauter, personal communication) suggesting that PSKRs may regulate ROS synthesis by RBOHD/F and/or entry of ROS into guard cells via PIP2;1. A major objective is to investigate whether the PSKR signaling pathway is required for ABA-induced ROS burst during stomatal closure. This will be investigated by histochemical analyses with ROS-sensitive dyes on PSKR-deficient and wild-type plants. To assess whether RBOHD/F and PSKR proteins directly interact at the plasma membrane the Förster-Resonance-Energy-Transfer (FRET) technique will be used. Finally, to look into the biochemical mode of stoma regulation by PSKRs, the hypothesis that RBOHD, RBOHF and/or PIP2;1 are substrates of PSKR that are phosphorylated by PSKR kinase will be tested. We will further test the hypothesis that PSKR signaling regulates ABA-induced stomatal closure through altering Ca^{2+} signaling. Ca^{2+} elevation in guard cells is required during ABA-mediated stomatal closure but the Ca^{2+} channels that mediate calcium influx in guard cells have not yet been identified. Based on the published finding that the cyclic nucleotide-gated cation channel CNGC17 is present in the PSKR nanocluster and is required for PSKR-dependent cell expansion, we will explore if *CNGC17* or other *CNGC* genes are expressed in guard cells and use CRISPR/Cas technology to generate loss-of-function mutants to genetically test their involvement in stoma closure. This work will provide new insights into the molecular mechanisms on how PSKR signaling contributes to drought stress resistance.

2 MATERIAL AND METHODS

2.1 Material

2.1.1 Chemicals, enzymes and equipment

The chemicals and their manufacturers used in this thesis are listed in Appendix Table 1 and were of the commercial grade of analysis (p. A.) unless it is indicated. The compositions of all solutions used in this work are listed in Appendix Table 2. All enzymes were purchased from Thermo Fisher Scientific. The list of equipment that was used in this work is shown in Appendix Table 3. All companies and their registered seat are listed in Appendix Table 4.

2.1.2 DNA and protein markers

To identify the size of DNA fragments on an agarose gel after electrophoresis (2.2.2.7), the Smart Ladder (Eurogentec) and the Ultra-Low Range DNA Ladder (Thermo Fisher Scientific Inc.) were used. Furthermore, the Pierce™ Unstained Protein MW Marker (Thermo Fisher Scientific Inc.) was used to identify the molecular weight of proteins in an SDS PAGE (2.2.6.3). The separation of the predicted markers is shown in Figure 3.

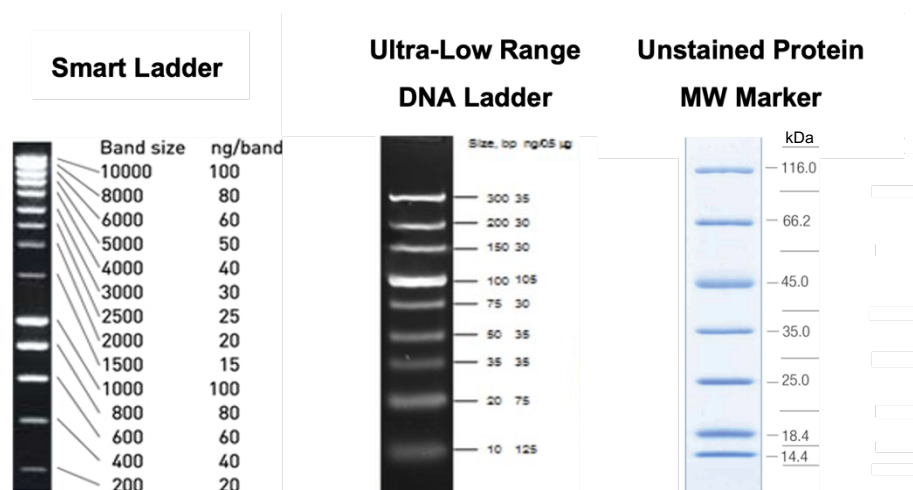


Figure 3: Fragment sizes of used markers (Thermo Fisher Scientific Inc., Eurogentec).

2.1.3 Primers

The primers were purchased from Eurofins Genomics. They were resuspended in ultrapure water at a concentration of 100 μ M. The working solution was diluted to 10 μ M and stored at -20°C. In Appendix Table 5-10, all primers and their usage are listed. The used primers are shown in 5' to 3' prime sequence and restriction sites are marked with an underline character.

2.1.4 Plant material

The plant accessions/genotypes used and generated in this work are listed in Appendix Table 11. All T-DNA insertion lines were obtained from the Nottingham Arabidopsis Stock Centre (NASC).

2.1.5 Media for *in vitro* plant and bacteria growth

The composition of media for *in vitro* plant growth (MS-medium) and bacteria (LB- or YEP-medium) used in this work are listed in Appendix Table 2. For the selection of resistant bacteria one or more antibiotic was added to the medium in the following concentrations:

Ampicillin	100 µg/ml
Gentamycin	30 µg/ml
Kanamycin	50 µg/ml
Rifampicin	50 µg/ml
Spectinomycin	100 µg/ml

2.1.6 Software

Nucleotide and protein sequences were obtained from the National Center for Biotechnology Information (NCBI) (www.ncbi.nlm.nih.gov) or The Arabidopsis Information Resource (TAIR) (www.arabidopsis.org). For *in silico* analysis of DNA sequences, cloning and oligomer design Snapgene (Version 5.0.8, GSL Biotech LLC) was used. Sequence alignments were performed with Clustal Omega (Sievers et al., 2011) and the phylogenetic tree with TreeView (Version: 1.6.6, Roderic D. M. Page, 2001). RNA sequencing data and microarray data were obtained from eFP-seq browser database (Sullivan et al., 2019) and eFP Browser (Winter et al., 2007), respectively. The software for taking microscopy pictures was ZEN 2.3 SP1 FP3 (black) Imaging Software (Version: 14.0.20.201) (Carl Zeiss Microscopy GmbH), Infinity Analyze (Version: 5.6.4) (Olympus Europa SE & Co. KG) and NIS-Elements Imaging Software (Version: 4.40) (Laboratory Imaging s.r.o.). Picture processing was performed with the ImageJ software (Version: 1.53c) (Schindelin et al., 2012). Agarose gel documentation was performed with the Nippon Genetics – Camera Studio (Version 1.0) (NIPPON Genetics EUROPE). All graphs were designed with Origin 2019b (Version: 9.6.5.169, OriginLab Corporation) and the statistic was calculated with the software MiniTab (Version: 16.1, Minitab Ltd.).

2.2 Methods

2.2.1 Plant propagation

2.2.1.1 Propagation of *Arabidopsis thaliana*

Seeds of *A. thaliana* were sown on a 2:1 soil-sand mixture. Seeds were stratified for 2 days at 4°C in the dark and then grown in the growth chamber under long-day conditions (16 h light/70 μM photons $\text{m}^{-2} \text{s}^{-1}$), 22°C and 60% humidity.

For growth on plates, seeds were surfaced sterilized with 2% (v/v) NaOCl for 20 min and 1,400 rpm. Subsequently, the seeds were washed four times with sterile water and placed on MS-medium. When seedlings were analyzed due to treatment, they were first grown on MS-medium for 4 or 7 days. Then, the seedlings were transferred to new plates with MS-medium supplemented with 0.1 μM PSK, 1 μM ABA or 50 mM mannitol as indicated. The seeds were stratified at 4°C for 2 days in the dark, before being transferred to the growth chamber, where they were grown under long-day conditions.

2.2.1.2 Crossing of *Arabidopsis thaliana*

Since *Arabidopsis* is a self-pollinator, the female crossing partner was emasculated before crossing. Therefore, still closed flowers were opened under the binocular and the anthers were removed. Subsequently, already opened flowers that were used as the male crossing partner were grasped with forceps at the flower base and the anthers with pollen were placed in contact with the stigma of the female crossing partner. All flowers that were not hand-pollinated were removed.

2.2.1.3 Stable transformation of *Arabidopsis thaliana*

Following the *floral dip* method (Clough and Bent, 1998), 5-6-week-old *Arabidopsis* plants were transformed with *Agrobacteria*. Before transformation, all siliques and opened flowers were removed. The day before transformation, 3 ml of liquid YEP-medium, with the corresponding antibiotic, was inoculated with a single colony of *Agrobacterium* transformed cells and incubated at 28°C and 250 rpm. The next day, 500 μl of this preculture was taken to inoculate 2.5 ml of liquid YEP-medium with corresponding antibiotics. This culture was then incubated for 4 to 5 hours at 28°C and 250 rpm. The bacterial culture was centrifuged at 2,500 x g for 5 min and the resulting pellet was carefully resuspended in 2 ml of liquid YEP-medium with the addition of 0.06 g sucrose and 1 μl Silwett L-77, and then applied

dropwise to the young flowers of the plants. Plants were kept in the dark at high humidity for 24 h and then transferred back to normal growing conditions.

2.2.1.4 Propagation of *Nicotiana benthamiana*

Seeds of *N. benthamiana* were sown on a 2:1 soil-sand mixture and grown in the growth chamber (14 h light/150 μM photons $\text{m}^{-2} \text{s}^{-1}$ at 23°C, 10 h darkness at 20°C and 60% humidity).

2.2.1.5 Transient expression of fusion proteins in *N. benthamiana* leaves

Four- to five-week-old *N. benthamiana* plants were used for *Agrobacterium* infiltration. Post infiltration 30 ml YEP-medium with corresponding antibiotics were inoculated with glycerol stocks of fusion proteins and incubated overnight at 28°C and 230 rpm. Cells were harvested by centrifugation for 10 min, 3200 x g. Subsequently, the cells were gently resuspended in infiltration medium until optical density (OD_{600}) of 0.8 was reached. The adjusted *Agrobacterium* solutions of the protein of interest were mixed in different combinations together with the suppressor of post-transcriptional gene silencing P19 in a 1:1:1 ratio and incubated for 1 hour at room temperature. Two leaves (marked in Figure 4) of each plant were infiltrated with the infiltration solutions in the abaxial side of the leaf until the whole leaf was infiltrated. The plants were covered with a hood and cultivated at RT and low light conditions (5 μM photons $\text{m}^{-2} \text{s}^{-1}$) for 2 days.



Figure 4: *N. benthamiana* plant used for infiltration.
Arrows indicate the leaves, which were infiltrated.

2.2.2 Molecular biological techniques

2.2.2.1 gDNA extraction of Arabidopsis

To determine plant genotypes, genomic DNA (gDNA) was extracted from 3-week-old Arabidopsis plants. A medium-sized leaf was placed in a 1.5 ml reaction tube containing 300 µl of gDNA extraction buffer. A pestle was used to manually disrupt the cells. After centrifugation at 12,000 x g for 10 min, the supernatant was transferred to a fresh 1.5 ml reaction tube and the pellet was discarded. To precipitate the gDNA, 300 µl of isopropanol was added to the new reaction tube and centrifuged again at 12,000 x g for 10 min. The supernatant was then discarded and washed with 500 µl of 70% EtOH. The pellet was then resuspended in 100 µl of distilled water and used for PCR (2.2.2.4).

2.2.2.2 RNA extraction of Arabidopsis

Plant material from Arabidopsis was placed together with 500 µl TRI Reagent® in liquid nitrogen. Afterward, it was ground with a pestle. After 5 min incubation at RT, 100 µl Chloroform was added and the sample was mixed carefully, followed by an incubation of 15 min at RT. The sample was centrifuged at 12,000 x g for 15 min at 4°C and the aqueous phase was placed in a new reaction tube and mixed with 125 µl Isopropanol and 125 µl High Salt Solution. After 10 min incubation at RT, the sample was centrifuged at 12,000 x g for 10 min at 4°C. The supernatant was discarded, and the pellet was washed with 700 µl 70% (v/v) EtOH by vortexing, followed by centrifugation at 7,500 x g for 5 min at 4°C. Afterward, the supernatant was removed and the pellet was dried in the air before resuspending it with 30 µl ddH₂O, followed by incubation at 55°C for 10 min.

The RNA extraction was followed by the DNase I digestion and was prepared as follows:

RNA	10 µg
10X Reaction Buffer with MgCl ₂	2 µl
DNase I, RNase-free	1.5 U
ddH ₂ O	ad 20 µl

The reaction mix was incubated at 37°C for 60 min, followed by the deactivation of the enzyme at 65°C for 10 min.

2.2.2.3 cDNA synthesis

For transcript analysis, the extracted RNA was reverse transcribed. Therefore, RevertAid Reverse Transcriptase was used as follows:

DNase treated RNA	10 µg
dNTPs [10 mM]	2 µl
Oligo dT primer [10 µM]	2 µl
5X Reaction Buffer	20 µl
RevertAid Reverse Transcriptase	100 U
ddH ₂ O	ad 100 µl

The cDNA synthesis reaction was incubated at 42°C for 60 min and the inactivation of the enzyme was done at 70°C for 10 min.

2.2.2.4 Polymerase chain reaction

Amplification of DNA fragments was achieved by polymerase chain reaction (PCR). If PCR was performed to check specific DNA sequences, the DreamTaq™ DNA polymerase was used. When performing a colony PCR, bacteria from a single colony were added as a template to the approach. The DNA sequences that were used for cloning, were amplified with Phusion™ HighFidelity DNA Polymerase. The standard approaches used are described below.

DreamTaq™ DNA Polymerase

DNA template [1 ng - 1 µg]	1 µl
dNTPs [10 mM]	1 µl
Forward primer [10 µM]	1 µl
Reverse primer [10 µM]	1 µl
10X DreamTaq™ Green Buffer	2 µl
DreamTaq DNA-Polymerase	0.25 U
ddH ₂ O	ad 20 µl

Run protocol for DreamTaq™ DNA Polymerase

Temperatur	Time	# passes
94°C	3 min	1
94°C	50 s	35
56°C	50 s	35
72°C	1 min/kb	35
72°C	10	1

Phusion™ High-Fidelity DNA Polymerase

DNA template [50 ng - 250 ng]	1 µl
dNTPs [10 mM]	0.4 µl
Forward primer [10 µM]	1 µl
Reverse primer [10 µM]	1 µl
5X DreamTaq™ Green Buffer	4 µl
Phusion™ High Fidelity DNA Polymerase	0.4 U
ddH ₂ O	ad 20 µl

Run protocol for Phusion™ High-Fidelity DNA Polymerase

Temperatur	Time	# passes
98°C	1 min	1
98°C	10 s	35
50-65°C	10 s	35
72°C	30 s/kb	35
72°C	7 min	1

The annealing temperature was set according to the oligomers, that were used in the PCR. All primers which were used in this work are listed in Appendix Table 5-10.

2.2.2.5 Quantitative real-time PCR

For quantitative expression analysis with real-time PCR, the Rotor-Gene SYBR® Green PCR Kit (QIAGEN GmbH) was used. All reactions were prepared in 2 technical replicates as follows:

cDNA	10 ng
Forward primer [100 µM]	0.105 µl
Reverse primer [100 µM]	0.105 µl
2X QuantiNova SYBR Green PCR Master Mix	7.5 µl
ddH ₂ O	ad 15 µl

The reaction was performed with the following run protocol:

Temperatur	Time	# passes
95°C	2 min	1
95°C	5 s	45
60°C	10 s	45

The values E (real-time PCR efficiency) and Ct (threshold cycle) required for the evaluation were taken from the Rotor-Gene® Q software (Version: 2.3.1) (QIAGEN GmbH). The calculation of the relative expression ratio R was calculated following the $\Delta\Delta Ct$ method. Therefore, the geometric mean of the two constitutively expressed genes *ACTIN 2* (*ACT2*, At3g18780) and *GLYCERALDEHYDE-3-PHOSPHATE DEHYDROGENASE C SUBUNIT* (*GAPC*, At3g04120) was used (Pfaffl, 2001; Vandesompele et al., 2002). For this purpose, the following formula was used:

$$R = \frac{E_{target}^{\Delta Ct}}{\sqrt{E_{ACT2}^{\Delta Ct} \times E_{GAPC}^{\Delta Ct}}}$$

(R : relative expression ratio, E : real-time PCR efficiency, Ct : threshold cycle).

2.2.2.6 Molecular cloning

DNA fragments intended for cloning were synthesized by PCR (2.2.2.4) using the Phusion High-Fidelity DNA Polymerase (Thermo Fisher Scientific Inc.). As a template cDNA of Col-0 *A. thaliana* plants was used. The desired fragment size was verified by horizontal agarose gel electrophoresis (2.2.2.7) and the corresponding fragments were extracted using the GeneJET™ Gel Extraction Kit (Thermo Fisher Scientific Inc.) according to the manufacturer's instructions. Afterward, a restriction was performed using conventional restriction endonucleases (Thermo Fisher Scientific Inc.) and for the ligation of DNA fragments, the T4 DNA ligase (Thermo Fisher Scientific Inc.) was used. All enzymes were used according to the manufacturer's instructions. The ligation mix was transformed into *E. coli* (2.2.3.2). On the next day, the plasmid was isolated with the GeneJET™ Plasmid-Miniprep-Kit (Thermo Fisher Scientific Inc.) according to the manufacturer's instructions. For further cloning in destination vectors, the Gateway™-technology (Thermo Fisher Scientific Inc.) was used. Therefore, the following reaction was prepared:

Entry vector	100-300 ng
Destination vector [150 ng]	150 ng
Gateway™ LR Clonase™ II enzyme mix	2 µl
1X TE-buffer	ad 8 µl

The reaction was incubated at 25°C for 1 h in a thermocycler. Subsequently, 1 µl Proteinase K was added, followed by incubation at 37°C for 10 min. The LR-reaction was transformed in *E. coli* (2.2.3.2) and afterward, plasmids were isolated with the GeneJET™ Plasmid-Miniprep-Kit (Thermo Fisher Scientific Inc.) according to the manufacturer's instructions. The DNA concentration was measured with the NanoDrop™2000 Spectrophotometer (Thermo Fisher Scientific Inc.) and all vectors were verified by sequencing (2.2.2.8) to ensure the correctness of the desired sequence.

2.2.2.7 Agarose gel electrophoresis

To separate DNA fragments in a size-dependent manner, an agarose gel electrophoresis was performed. Therefore, 0.4 g Agarose with 40 ml 1X TAE were melted and 2.7 µl ethidium bromide [5 mg/ml] was added. The agarose was poured into a gel tray with a comb. When the gel was solidified 1X TAE buffer was added. If necessary, the sample was mixed with 4X DNA loading dye. The DNA fragments were separated at 130 V for 30 min.

2.2.2.8 Sequencing

The sequencing of DNA samples was performed by Eurofins Genomics GmbH (Ebersberg, Germany), using the sanger sequencing method. Therefore, 450 ng of plasmid or 125 ng of PCR product in 7.5 µl of water were mixed with 2.5 µl of sequencing primer (10 µM) and sent to the company.

2.2.2.9 Molecular cloning of CRISPR/Cas9 constructs

The CRISPR/Cas9 system was used to generate knockout lines for the gene locus of *CNGC15*. Since the SAIL line *cngc16-2* has a BASTA resistance cassette, the available vector *CCPS1+2 CNGC15 pDeCAS9* with a BASTA resistance was used to change the resistance cassette to gentamycin with the restriction enzyme HindIII. The gentamycin resistance cassette was cut from the *pDeCAS9 GentR* vector. The restricted fragments were ligated and the new CRISPR/Cas9 vector was named *CCPS1+2 CNGC15 pDeCas9 GentR*.

2.2.2.10 Molecular cloning of Promoter:GUS constructs

For expression analysis, promoter sequences up to 1,500 bp upstream of the start codon were identified and amplified with PCR from genomic DNA. The PCR products were cloned in the entry vector pENTR1™A DS and later on with the Gateway™-technology in the destination vector *pBGWFS7*. All used primers are listed in Appendix Table 7 and the generated constructs are listed in Appendix Table 13.

2.2.2.11 Molecular cloning of reporter constructs

For Förster Resonance Energy Transfer (FRET) analysis N-terminal fusion constructs for *RBOHD* and *RBOHF* were generated with the cloning strategy described above. Therefore, the ORFs of the genes with stop codon were amplified with PCR, whereas Col-0 cDNA was used as a template. The primers which were used are listed in Appendix Table 8. The PCR products were restricted and ligated with the linearized entry vector *pENTR™1A DS*. Later on, a recombination reaction was performed to introduce the gene of interest in the destination vector pB7WGR2 or pB7WGF2 (Karimi et al., 2002). With this, the expression of the fusion protein was brought under the control of the ubiquitous 35S promoter. The constructs were named: *RFP-RBOHD*, *GFP-RBOHD*, *RFP-RBOHF*, *GFP-RBOHF*.

2.2.2.12 Molecular cloning of fusion proteins for protein expression

In this work MBP-6xHIS-fusion constructs of cytosolic protein parts of RBOHD, RBOHF and PIP2;1 were generated after the above-described cloning strategy. The primers which were used in this work are listed in Appendix Table 9. For the sequence of the N-terminus of *RBOHD*, the forward primer binds at the start codon and the reverse primer 1127 bp downstream of the start codon. The C-terminus of *RBOHD* was amplified with the forward primer binding 963 bp upstream of the stop codon and the reverse primer binding directly at the stop codon. The N-terminus of *RBOHF* was amplified with the forward primer binding the start codon and the reverse primer 1160 bp downstream of the start codon. The sequence of the cytosolic Loop2 of RBOHF was amplified with the forward primer binding 1836 bp downstream of the start codon and the reverse primer binding 2242 bp upstream of the stop codon. The C-terminus of RBOHF was amplified with the forward primer binding 2295 bp upstream of the stop codon and the reverse directly before the stop codon. For the sequence of the N-terminus of *PIP2;1*, the forward primer binds at the start codon and the reverse primer 138 bp downstream of the start codon. Due to their sizes, annealed oligomers were used for the sequence of Loop1 (position: 325-387 bp downstream of start codon) and C-terminus (position: 823-873 bp downstream of start codon) of *PIP2;1*. Subsequently, the amplifications were ligated in the expression vector pQE-60 with a C-terminal HIS-tag. According to better solubilization, the sequence was again amplified including the HIS-tag and was cloned in the pMAL-c5x vector with an N-terminal maltose-binding protein (MBP).

2.2.3 Microbiological techniques

2.2.3.1 Generation of chemically competent *Escherichia coli*

For the generation of chemically competent *E. coli* cells, an overnight culture at 37°C on solid LB-medium was prepared. Subsequently, a single colony was used to inoculate 5 ml of liquid LB-medium and let it grow at 37°C and 250 rpm. On the following day, 300 µl of the preculture was used to inoculate 100 ml of liquid LB-medium and kept under the same conditions until an optical density (OD600) of 0.3 was reached. All subsequent steps were performed at 4°C and the bacterial cells were kept on ice. First, the cells were pelleted for 5 min at 4°C and 1,000 x g. Afterward, the cells were resuspended in 80 ml of TF-buffer 1. After a 5 min incubation on ice, the cells were again pelleted for 5 min at 4°C and 1,000 x g and then resuspended in 4 ml of TF-buffer 2. The cells were aliquoted and subsequently placed in liquid nitrogen and stored at -80°C until further use.

2.2.3.2 Transformation of *Escherichia coli*

100 µl of chemically competent *E. coli* cells were thawed on ice and the ligation mixture or plasmid DNA was added, followed by incubation on ice for 30 min. Afterward, the suspension was heat shocked for 30 s at 42°C, followed by incubation on ice for 2 min. Subsequently, 200 µl of LB-medium was added and the cells were then regenerated for 1 h at 37°C and 650 rpm. Afterward, the bacterial suspension was spread on LB-medium with the corresponding antibiotics and incubated overnight at 37°C.

2.2.3.3 Generation of chemically competent *Agrobacterium tumefaciens*

For the generation of chemically competent *A. tumefaciens* cells, the bacteria were incubated on solid YEP-medium at 28°C and then a single colony was used to inoculate 2 ml of liquid YEP-medium. The culture was incubated overnight at 28°C and 250 rpm. On the next day, the preculture was used to inoculate 50 ml YEP-medium which was incubated at 28°C and 250 rpm until an optical density (OD₆₀₀) of 0.5. The cells were pelleted for 5 min at 4°C and 2,000 x g and resuspended in 10 ml 0.15 M NaCl. After another centrifugation of 5 min at 4°C and 1,000 x g, the cells were resuspended in 1 ml of 20 mM CaCl₂ and 15% (v/v) glycerol. Aliquots of 200 µl were prepared and subsequently placed in liquid nitrogen and stored at -80°C until further use.

2.2.3.4 Transformation of *Agrobacterium tumefaciens*

Chemically competent *A. tumefaciens* cells were thawed on ice and then 1 µg of plasmid was added. This was followed by a 30 min incubation on ice. Cells were then shock-frozen in liquid nitrogen for 1 min and thawed at 37°C. Subsequently, 1 ml of YEP-medium was added, and the cells were incubated at 28°C for 3 h. The cells were then centrifuged at 9,600 x g for 1 min. The supernatant was discarded, and the cells were resuspended in 100 µl of liquid YEP-medium. Subsequently, the cells were spread on YEP-medium with corresponding antibiotics and incubated at 28°C for 2 to 3 days.

2.2.3.5 Glycerol stock

Glycerol cultures were prepared to store transformed *E. coli* or *A. tumefaciens*. For this purpose, 200 µl glycerol was mixed with 800 µl overnight liquid culture and immediately frozen at -80°C.

2.2.4 Histochemical techniques

2.2.4.1 GUS analysis

The β -glucuronidase activity of stable transformed *Arabidopsis* plants was analyzed in plant material, which was incubated in X-Gluc solution for 8-24 h at 37°C. The substrate X-Gluc gets processed by β -glucuronidase to a blue precipitate (5,5'-dibrom-4,4'-dichlor-indigo). Subsequently, the plant material was placed in 70% (v/v) EtOH overnight, to remove the chlorophyll. For better visualization, the plant material was embedded in clearing solution and the pattern of the blue precipitate was imaged with a stereomicroscope and a brightfield microscope. Initial analyses of Promoter:GUS lines generated in this work included 10 independent lines. For further analysis, one line was chosen which was representative in the expression pattern.

2.2.4.2 Detection of reactive oxygen species

Plant material of *Arabidopsis* plants was incubated with DAB-staining solution for 8 h to detect hydrogen peroxide (H_2O_2) or with NBT-staining solution for 15 min to detect superoxide ($\text{O}_2^{\cdot-}$). DAB (3,3'-Diaminobenzidine) is oxidized by H_2O_2 and forms a brown precipitate, whereas nitro blue tetrazolium chloride (NBT) is reduced by $\text{O}_2^{\cdot-}$ to form a blue precipitate. The seedlings were placed in 70% (v/v) EtOH overnight to remove the chlorophyll. The plant material was embedded in clearing solution and the pattern of the brown and blue precipitate was imaged with a stereomicroscope. The ROS accumulation was quantified using ImageJ.

2.2.5 Plant physiological techniques

2.2.5.1 Stomatal closure assay

Epidermal peels of 3- to 4-week-old plants were prepared from the abaxial side of *Arabidopsis* leaves (Eisele et al., 2016). Three leaves of individual plants per treatment and genotype were used. Figure 5 shows the 7th leaf which was used in the assay. Subsequently, the leaves were floated on stomatal opening buffer under constant light ($70 \mu\text{M photons m}^{-2} \text{s}^{-1}$) for 2 h. Afterward, 100 μM ABA, 0.1 μM PSK or 0.5 mM H_2O_2 were added as indicated and the peels were incubated for 2 h. Stomata were visualized with a brightfield microscope (BX41, Olympus) and the width and length of minimum 25 stomatal pores per leaf were determined with ImageJ (Schindelin et al., 2012).

The stomata aperture index was calculated by dividing the width through the length for 3 leaves per experiment.



Figure 5: Seventh leaf of *A. thaliana* plant taken for stomatal closure assay.

2.2.5.2 Transpiration assay

To determine transpiration, leaves of 3- to 4-week-old plants were placed in reaction tubes (2 leaves per tube, 5 tubes per genotype and treatment) filled with H₂O and 100 μ M ABA or 50 mM mannitol as indicated and water loss per gram fresh weight was determined from the reduction in weight after 8 h incubation in a growth chamber (70 μ M photons m⁻² s⁻¹, 22°C, 60% relative humidity).

2.2.5.3 Protoplast expansion assay

Protoplasts were isolated from the hypocotyl of 5-day-old etiolated seedlings. The seedlings were harvested, and the cotyledons were cut off with a sharp scissor. Subsequently, the hypocotyls were collected in a drop of enzyme solution to prevent loss of moisture and cut into small pieces (≤ 0.5 mm) with a sharp razor blade. The pieces of the hypocotyl were placed in 1 ml enzyme solution. The maceration of cell walls and the middle lamella were taken place at 22°C for 3 hours in the dark. Afterward, the enzyme solution was washed through nylon meshes (100 μ m, 50 μ m and 30 μ m) with 1 ml washing solution. Protoplasts were placed in 500 μ l washing solution with 2% (w/v) Neutral red to determine the viability because the stain permeates the plasma membrane of vital protoplasts. 19 μ l of the protoplast solution were placed in 60 well Nunc[®] MicroWell[®] with low profile and lid (ThermoScientific) per well. The remaining wells were filled with 20 μ l of washing solution each. This ensures a high humidity in the plate and a decreased evaporation of the sample solution. The plate was let stand for 30 min for sedimentation of protoplasts. To take photographs during the assay an inverted microscope was used with a 40x objective for magnification. At least one protoplast per genotype and treatment per well was chosen. One protoplast was focused two times for technical replicates, afterwards, the next protoplast was focused and monitored. These steps were reiterated every 5 minutes in the

same order. The protoplast circumference was monitored at 5 min intervals and net volume changes were calculated from the circumference at each time point. After 35 min, 1 µl of 20 nM PSK or the washing solution as mock was added. It was continued to take pictures every 5 min for at least 30 min. With the software ImageJ (Schindelin et al., 2012) the area (A) of the protoplast by drawing the circumference was measured. The average of both areas (A_{mean}) of the technical replicates from each protoplast at each time point was calculated. Based on the assumption that the protoplast is spherical, the radius (r) was calculated:

$$r = \sqrt{\frac{A_{mean}}{\pi}}$$

and from r the respective volume (V):

$$V = \frac{4}{3} \cdot \pi \cdot r^3$$

Afterward, the relative volumes (V_{rel}) of protoplasts at each time point ($V_{t=x}$) relative to the protoplast volume of 100% at time point 0 ($V_{t=0}$) was evaluated.

$$V_{rel} = \frac{V_{t=x}}{V_{t=0}} \cdot 100$$

The data points (V_{rel} on Y-axis and time on X-axis) before the addition of the effector or mock treatment were put in a graph to perform a linear regression and use the linear equation to calculate the extrapolated volume (V_{extr}) given that shrinkage proceeded at the same rate as before effector addition.

$$V_{extr} = m \cdot x + b$$

In the end, V_{extr} was extracted from V_{rel} to obtain the net volume change (V_{change}) over time:

$$V_{change} = V_{rel} - V_{extr}$$

2.2.6 Protein analysis techniques

2.2.6.1 Heterologous protein expression

The plasmids used for heterologous protein expression were transformed into *E. coli* BL21 (DE3). Prior protein expression, 3 ml LB-medium with 0.2% (w/v) Glucose and corresponding antibiotics was inoculated with glycerol stocks and incubated at 37°C while shaking overnight. On the next day, 50 ml or 200 ml LB-medium with 0.2% (w/v) Glucose and corresponding antibiotics were inoculated with the overnight liquid culture and kept shaking at 37°C until an OD600 of 0.5 was reached. Protein expression was induced with 0.3 mM IPTG for MBP-fusion proteins and incubated for 4 h at 28°C. The PSKR1 kinase expression was induced with 1 mM IPTG and incubated overnight at 20°C. Cells were harvested by centrifugation at 2,500 x g for 5 min and the pellet was directly frozen at -20°C.

2.2.6.2 Protein purification

The cell pellet of the heterologous protein expression was resuspended in 3 ml extraction buffer for HIS-tagged proteins on ice. Subsequently, the cells were disrupted using French Press with 1,000 PSIG, followed by sonication of 3x 10 s. The crude extract was centrifuged for 30 min at 20,000 x g at 4°C. Subsequently, the supernatant was incubated with 50 µl prewashed TALON® Metal Affinity Resin or Amylose on a rotator for 1 h at RT. Afterward, the TALON or Amylose protein solution was washed three times with 500 µl washing buffer for HIS-tagged proteins or column buffer for MBP-tagged proteins on a Pierce® Spin Column (Thermo Fisher Scientific Inc.). Followed by the elution of the proteins in 50 µl with the corresponding elution buffer, which was incubated for 10 min at RT. The concentration of the proteins was measured with the NanoDrop™2000 and analyzed on a polyacrylamide gel by SDS PAGE (2.2.6.3).

2.2.6.3 SDS PAGE

The separation of proteins according to molecular weight was carried out by discontinuous sodium dodecyl sulfate-polyacrylamide-gel electrophoresis (SDS-PAGE) according to Laemmli (Laemmli, 1970). Therefore, polyacrylamide gels were prepared as follows:

12.5% Separating gel

1.5 M TRIS/HCl, pH 8.8	1.25 ml
30% Acrylamid/Bisacrylamid	2.1 ml
10% APS	20 µl
TEMED	6.1 µl
ddH ₂ O	1.67 ml

5% Stacking gel

0.5 M TRIS/HCl, pH 6.8	625 µl
30% Acrylamid/Bisacrylamid	400 µl
10% APS	37.5 µl
TEMED	3.75 µl
ddH ₂ O	1.45 ml

All proteins were denatured with the addition of 4X SDS sample buffer and incubation of 5 min at 95°C. The samples, as well as 5 µl of the protein marker, were separated in the polyacrylamide gel with a voltage of 15 mA in 1X Laemmli buffer and successively increased to 30 mA. Subsequently, the polyacrylamide gel was stained in Coomassie staining solution for 15 min and prewashed with water until it was destained with Destain solution.

2.2.6.4 Kinase assay

The analysis of *in vitro* phosphorylation of different fusion proteins by the PSKR1 kinase was performed in the isotope lab. Therefore, 0.25 µg kinase and 1 µg of the fusion protein were prepared in a reaction volume of 7 µl with kinase buffer. Subsequently, 5 µCi γ -³²P-ATP was added to the reaction and incubated for 1 h at 25°C. The reaction was stopped by adding 3 µl 4X SDS sample buffer, followed by the denaturation at 95°C for 3 min. Afterward, the proteins were separated in a 12.5% polyacrylamide gel by SDS PAGE (2.2.6.3) and stained for 15 min in Coomassie staining solution. After destaining overnight, the gels were dried and exposed to an X-ray film.

2.2.7 Microscopy techniques

2.2.7.1 Fluorescence resonance energy transfer

For FRET-acceptor photobleaching (FRET-AB) analysis, the coding sequences of *BRI1*, *RLP44*, *PSKR1* (Ladwig et al., 2015; Wolf et al., 2014), *RBOHD* (provided by C. Kaufmann) and *RBOHF* were expressed as C-terminal fluorophore fusions in pH7FWG2 (eGFP), pK7RWG2 and pB7RWG2 (mRFP1.2) (Karimi et al., 2002) and N-terminal fluorophore fusions in pH7WGF2 (eGFP) and pB7WGR2 (mRFP1.2) (Karimi et al., 2002). The fusion constructs of *PSKR1*, *BRI1*, *RLP44*, *RBOHD* and *RBOHF* were transformed in *Agrobacterium tumefaciens* strain *EHA105*, whereas the gene silencing suppressor P19 was present in GV3101. The vector combinations together with the gene silencing suppressor were infiltrated into *N. benthamiana* leaves (2.2.1.5). Measurements were performed 2 days after infiltration using a confocal laser scanning microscope. The presence of both fluorophores was verified using 488 and 561 nm lasers for eGFP and mRFP1.2 excitation, respectively. Emission signals were detected at 490-530 nm and 588-633 nm. Dequenching of the donor eGFP by photobleaching of the acceptor mRFP1.2 was obtained by setting the laser power to 100% for 30 iterations. Due to instability of the fluorophore, 5 pictures before (D_{pre}) and after bleaching (D_{post}) were taken and the average of the intensities was used for further calculations. The FRET efficiency ($FRET_{eff}$) was calculated from the fluorescence intensities of the donor before and after bleaching. Therefore, the following formula was used:

$$FRET_{eff} = \frac{(D_{post} - D_{pre})}{D_{post}}$$

2.2.7.2 ROS measurement in guard cells

To detect H_2O_2 in guard cells, epidermal peels of 3- to 4-week-old plants were prepared with forceps from the abaxial side of leaves and were floated on stomatal opening buffer under constant light in the climate chamber for 2 h. Subsequently, ABA was added to the buffer at the concentrations indicated, peels were floated for 2 h and then stained with 50 μM 2',7''-dichlorodihydrofluorescein diacetate (H_2DCF -DA) for 30 min. The peels were washed three times with stomatal opening buffer. The H_2O_2 -dependent fluorescence was detected at 490-530 nm after excitation at 488 nm with a confocal laser scanning microscope and quantified with ImageJ (Schindelin et al., 2012).

3 RESULTS

3.1 Phytosulfokine signaling is required for stomatal closure

3.1.1 Expression analysis of PSK precursor and receptor genes

Previous results indicated the importance of phytosulfokine (PSK) signaling during osmotic stress and drought (Rajamanickam et al., 2021; Reichardt et al., 2020; Stührwohltd et al., 2021) but the physiological and molecular mechanisms have not been fully elucidated. One of the first responses of plants to water shortage is stoma closure. To examine the potential role of PSK signaling genes in stoma regulation we analyzed the expression of PSK precursor and PSK receptor genes. Bioinformatic tools using RNA sequencing data deposited in the eFP-seq browser database (Sullivan et al., 2019) were analyzed (Figure 6).

gene	root	root apical meristem	aerial	leaf	carpel	receptacle	st. 12 inflorescence	mature pollen
<i>PSK1</i> (At1g13590)	27.7	28.7	0.0	0.0	0.0	0.0	0.0	0.0
<i>PSK2</i> (At2g22860)	3.7	30.3	3.6	6.8	0.2	113.4	43.3	28.6
<i>PSK3</i> (At3g44735)	27.0	20.8	82.2	43.3	114.5	75.6	65.0	0.0
<i>PSK4</i> (At3g49780)	44.2	10.9	17.2	7.6	0.9	40.1	1.9	0.0
<i>PSK5</i> (At5g65870)	11.7	4.6	19.7	12.1	3.2	94.2	93.9	0.0
<i>PSKR1</i> (At2g02220)	14.1	18.3	5.5	8.0	9.3	13.2	7.6	0.0
<i>PSKR2</i> (At5g53890)	7.8	1.7	4.5	5.6	8.0	40.2	5.8	0.0

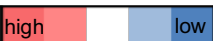
TPM  high low

Figure 6: Expression of PSK precursor and receptor genes throughout organs in Arabidopsis. Transcript levels per million (TPM) of PSK precursor and receptor genes in different organs are provided in numbers and as heat map (eFP-seq Browser) (Sullivan et al., 2019). The numbers are a mean of individual experiments. The RNA sequencing experiment numbers can be seen in Appendix Table 14.

Arabidopsis has five precursor genes of which *PSK1* was predominantly expressed in roots. Higher transcript levels in the inflorescence and receptacle were observed for *PSK2*, *PSK3* and *PSK5*. *PSK3* and *PSK4* were expressed throughout the plant. The known pseudogene *PSK6* was expressed in mature pollen (data not shown). Both PSK receptor genes, *PSKR1* and *PSKR2*, present in the Arabidopsis genome were expressed at an overall low level with *PSKR2* being expressed stronger in the receptacle.

To specifically look at gene expression in guard cells in comparison to mesophyll cells we used microarray data from the eFP browser (Winter et al., 2007) (Figure 7).

PSK4 showed the highest expression value in transcripts per million (TPM) in guard cells. The *PSK4* transcript level was ~10 times higher than that of other PSK precursor genes. While *PSK2*, *PSK3* and *PSK5* showed almost the same expression, *PSK1* had the lowest expression. Compared with mesophyll cells, the expression of *PSK4* was twice as high in guard cells. This was also seen with *PSK2* and *PSK5*. No expression data were available for the pseudogene *PSK6*. Both PSK receptor genes showed higher expression in guard cells than in mesophyll cells. In summary, the results revealed higher expression of *PSK2*, *PSK4*, *PSK5*, and the PSK receptor genes in guard cells compared to mesophyll cells possibly indicating a specific function in stomata.

gene	guard cell	mesophyll cell
<i>PSK1 (At1g13590)</i>	20.6	26.3
<i>PSK2 (At2g22860)</i>	440.3	184.9
<i>PSK3 (At3g44735)</i>	438.9	516.1
<i>PSK4 (At3g49780)</i>	3857.2	1955.5
<i>PSK5 (At5g65870)</i>	400.9	138.4
<i>PSKR1 (At2g02220)</i>	421.3	227.3
<i>PSKR2 (At5g53890)</i>	906.9	11.2


TPM  high low

Figure 7: PSK precursor and receptor genes are expressed in guard cells.

Transcript levels per million (TPM) of PSK precursor and PSK receptor genes in guard cells and mesophyll cells are provided in numbers and as a heat map (eFP Browser) (Winter et al., 2007).

To independently verify expression in guard cells, *Promoter:GUS* reporter lines for those genes were used that showed a higher transcript level in guard cells compared with mesophyll cells. Promoter activities were analyzed in 8-day-old seedlings using the GUS reporter lines *PSK2:GUS2*, *PSK4:GUS2*, *PSK5:GUS1*, *PSKR1:GUS4* and *PSKR2:GUS3*. The *PSK4* promoter was active specifically in guard cells of true leaves and cotyledons (Figure 8A-C). The *PSKR1* promoter was active in guard cells, as well as in the surrounding epidermal cells of the first true leaves (Figure 8D-F). This could not be observed in the cotyledons. All promoters of *PSK2*, *PSK4*, *PSK5*, *PSKR1* and *PSKR2* were active in veins of cotyledons. Whereas no promoter activity in guard cells of 8-day-old seedlings was observed for *PSK2*, *PSK5* and *PSKR2* (Figure 8G-O).

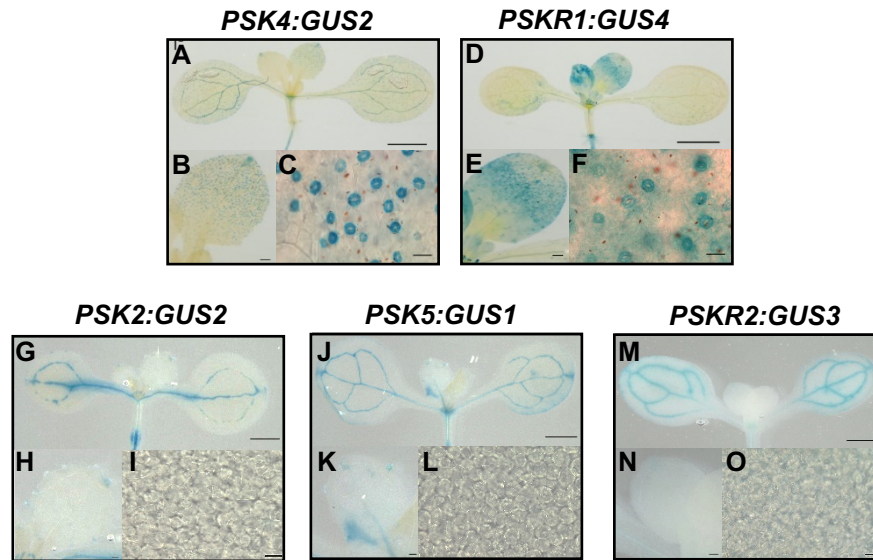


Figure 8: *PSK4* and *PSKR1* are specifically expressed in guard cells.

A-C, Expression of *PSK4* in leaves of 8-day-old seedlings was analyzed using the GUS reporter *PSK4:GUS2*.

D-F, Expression of *PSKR1:GUS4* in the seedling shoot.

G-I, Expression of *PSK2:GUS2* in the seedling shoot.

J-L, Expression of *PSK5:GUS1* in the seedling shoot.

M-O, Expression of *PSKR2:GUS3* in the seedling shoot.

Scale bars = 1 mm (A,D,G,J,M), = 0.1 mm (B,E,H,K,N) and = 0.05 mm (C,F,I,L,O).

3.1.2 Protein expression of PSKR1 and PSKR2

We next analyzed protein expression of PSKR1 and PSKR2 using the 7th leaf of 3- to 4-week-old *PSKR1:PSKR1-GFP1.2*, 3.1, 4.5 and *PSKR2:PSKR2-GFP1.3*, 3.2, 4.1 reporter lines in the *pskr1-3 pskr2-1* background. All independent lines showed similar results and one of each is shown as a representative picture (Figure 9). PSKR1 and PSKR2 expression were both present in epidermal cells as well as in guard cells.

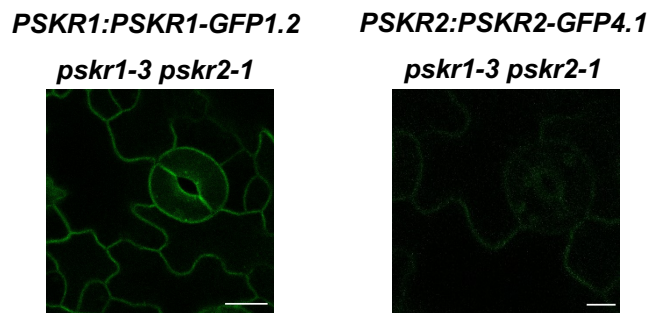


Figure 9: PSKRs are expressed in guard cells.

The *PSKR1:PSKR1-GFP1.2* and *PSKR2:PSKR2-GFP4.1* reporter constructs in the *pskr1-3 pskr2-1* background demonstrate PSKR1 and PSKR2 expression at the plasma membrane of guard cells and epidermal cells. Scale bar = 10 μm.

3.1.3 The knockout of *PSKR1* and *PSKR2* results in higher leaf transpiration

Gene expression and protein localization analysis suggested that PSK signaling might play a role in guard cell function. To look into such a role, a transpiration assay was performed with wild-type and *pskr1-3 pskr2-1* plants. The 7th leaf of 3- to 4-week-old plants was incubated either with water as a control, 100 μ M ABA or 50 mM mannitol for 8 h and water loss was determined at the end of the incubation period. Mannitol was used as an osmolyte that leads to hyperosmotic conditions. In the presence of ABA or mannitol, lower transpiration rates compared to control conditions were observed in the wild type, indicating closure of the stomata (Figure 10). Transpiration was also reduced by ABA and mannitol in *pskr1-3 pskr2-1* leaves, but transpiration rates remained higher in *pskr1-3 pskr2-1* compared to wild type.

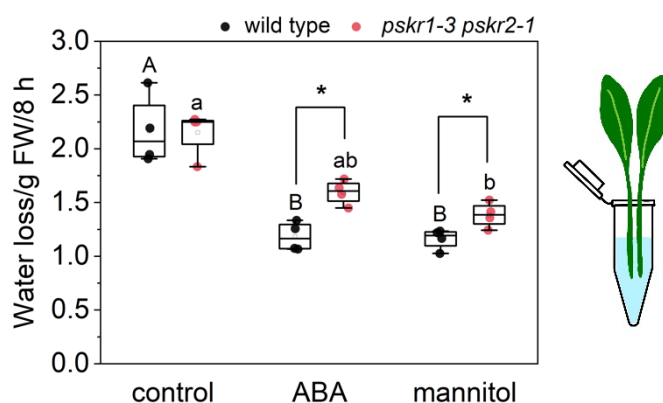


Figure 10: PSKR signaling is required to avoid increased leaf transpiration under water stress conditions.

Water loss was analyzed in the 7th leaf of 3-4-week-old wild-type and *pskr1-3 pskr2-1* plants incubated with water, 100 μ M ABA or 50 mM mannitol for 8 h. Mean \pm SE were obtained from 4 independent experiments each analyzing 10 leaves per genotype and treatment. Letters and asterisks indicate significant differences at $p < 0.05$, evaluated with Kruskal-Wallis and Mann-Whitney-U test.

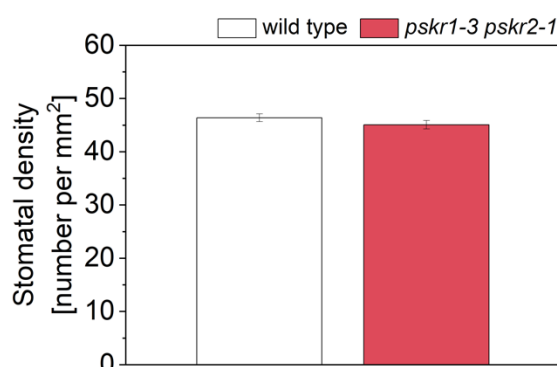


Figure 11: No developmental defects of guard cells in *pskr1-3 pskr2-1*.

The stomatal density was examined for 1 mm² from the abaxial side of the 7th leaf of 3-4-week-old wild-type and *pskr1-3 pskr2-1* plants. 16 leaves per genotype were evaluated that included at least 4 regions on the leaf (n=16). No significant difference was evaluated with two-sample *t*-test.

The results showed that knockout of PSK receptors results in higher transpiration under water stress conditions mimicked by the stress hormone ABA or by the osmolyte mannitol. Elevated transpiration rates could be a result of altered stoma numbers or altered stoma regulation. To differentiate between the two, the stomata density of the 7th leaf of 3- to 4-week-old wild-type and *pskr1-3 pskr2-1* plants was determined. The results showed no difference in stomatal density between *pskr1-3 pskr2-1* and wild type (Figure 11). This suggested that the higher transpiration rate observed in stressed *pskr1-3 pskr2-1* leaves could result from impaired closure of stomata.

3.1.4 PSK receptor signaling is required for ABA-mediated stomatal closure

After showing that PSK receptor signaling regulates transpiration in water stress conditions, we analyzed whether stomatal closure is a target of the PSK receptor pathway using the stomatal aperture index (SAI) as an indicator. To study stomatal closure, we established an assay using ABA to induce stoma closure in epidermal peels of the 7th leaf of 3- to 4-week-old wild-type and *pskr1-3 pskr2-1* plants that were floated on stomatal opening buffer for 2 h under constant light conditions. Subsequently, 10, 50 or 100 μ M ABA was added, to test for dose-dependence. Increasing ABA concentration led to increasing stoma closure in wild type whereas stomata of *pskr1-3 pskr2-1* partially closed at 10 μ M ABA (Figure 12). At 50 and 100 μ M ABA, the closure of *pskr1-3 pskr2-1* stomata stayed the same as with 10 μ M ABA resulting in significant differences in SAI between wild type and *pskr1-3 pskr2-1*. Significant differences at higher ABA concentrations indicate that PSKR signaling is required for full stoma closure. The findings support a role of PSKRs in regulating stomatal closure.

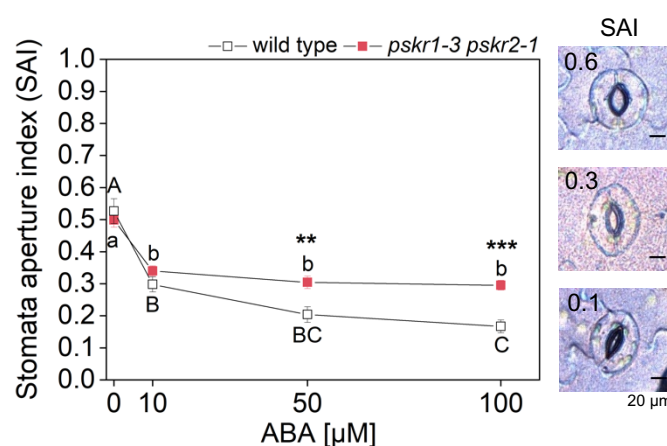


Figure 12: PSKR signaling is required for stomatal closure in response to ABA.

Epidermal peels from 3- to 4-week-old wild-type and *pskr1-3 pskr2-1* plants were treated with ABA for 2 h to induce stoma closure. Results are means \pm SE from 2-3 leaves analyzed in each of 4 independent biological experiments ($n = 11$). The average SAI per leaf was obtained from ≥ 25 stomata. Letters ($p < 0.05$) and asterisks (** $p < 0.01$, *** $p < 0.001$) indicate significant differences, evaluated with one-way ANOVA with Tukey-Kramer and two-sample t -test.

To validate that PSKR signaling is responsible for impaired ABA-sensitivity, stomata closure was analyzed in overexpression lines, as well as a complementation line (Figure 13A,B). Complementation of *pskr1-3 pskr2-1* was verified with RT-PCR (Figure 13C). Overexpression, as well as complementation, led to restoration of stomatal closure to the wild-type level, showing that stomata closure is indeed controlled by PSKR. The results also revealed that receptor overexpression did not enhance closure.

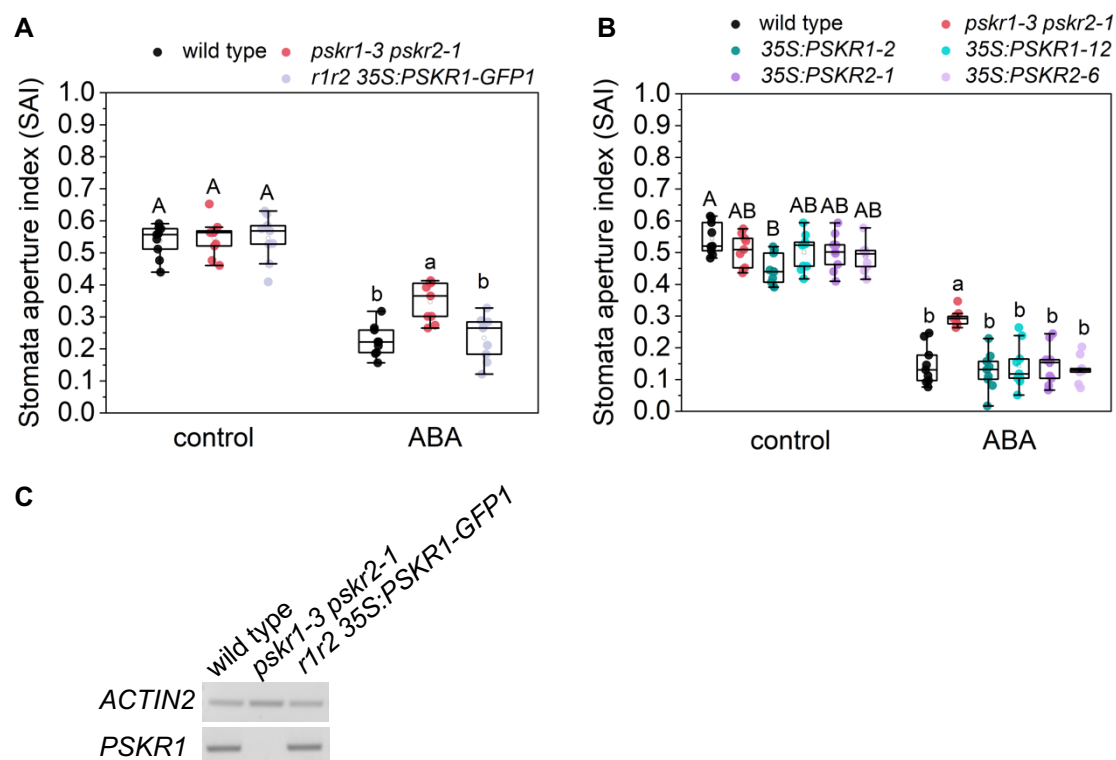


Figure 13: Complementation and overexpression constructs of *PSKR1* and *PSKR2* rescue the *pskr1-3 pskr2-1* phenotype.

A, Stomatal aperture index in leaves of wild type, *pskr1-3 pskr2-1* (*r1r2*) and the complementation line *r1r2 35S:PSKR1-GFP1*. Values are means \pm SE of SAI-means of $n = 9$ leaves analyzed. Capital and minor letters indicate significant differences within treatments at $p < 0.05$, evaluated with one-way ANOVA with Tukey-Kramer test. Significant differences were found between control and treatment in all genotypes, evaluated with two-sample t -test ($p < 0.05$).

B, Mean (\pm SE) SAI values of $n = 9$ leaves of wild-type, *pskr1-3 pskr2-1*, *35S:PSKR1-2* and *-12*, *35S:PSKR2-1* and *-6* plants. Capital and minor letters indicate significant differences within treatments at $p < 0.05$, evaluated with one-way ANOVA and Tukey-Kramer test. Significant differences were found between control and treatment in all genotypes, evaluated with two-sample t -test ($p < 0.05$).

C, Expression of *PSKR1* reaches wild type level in *35S:PSKR1-GFP1* in *pskr1-3 pskr2-1* (*r1r2*) background, validated with RT-PCR. *ACTIN2* was used as a control gene.

To investigate the contribution of the individual PSKRs, the stomatal closure of *pskr1-3* and *pskr2-1* were analyzed in response to ABA. Knockout of single receptors impaired stomatal closure in response to ABA to a similar degree as observed for the PSK receptor double knockout (Figure 14).

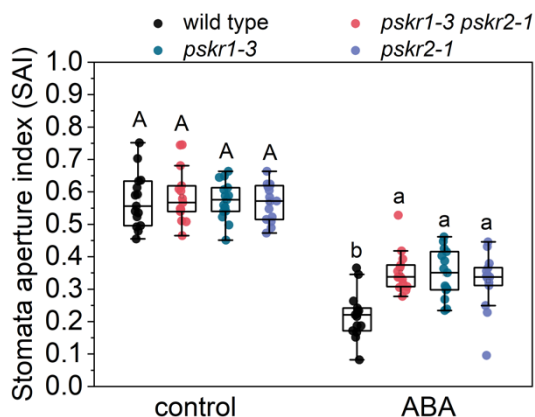


Figure 14: Both PSK receptors are individually important for ABA-mediated stomatal closure. ABA-induced stomatal closure in wild type, *pskr1-3 pskr2-1* and the single knockouts *pskr1-3* and *pskr2-1* in epidermal peels from 3-4-week-old plants treated with 100 μ M ABA for 2 h. Values are means \pm SE of 3 independent biological repeats analyzing 3 leaves with ≥ 25 stomata per leaf. Capital and minor letters indicate significant differences within treatments at $p < 0.05$, evaluated with Kruskal Wallis test. Significant differences were found between control and treatment in all genotypes, evaluated with Mann-Whitney-U test ($p < 0.05$).

3.1.5 The PSK peptide can restore impaired stomatal closure in *tpst-1*

The pre-pro-proteins of PSK undergo post-translational processing to generate the fully active peptide. An essential modification of the pro-protein is the post-translational sulfation of two tyrosine residues within the PSK domain that is catalyzed by the enzyme tyrosyl protein sulfotransferase (TPST) located in the *cis*-Golgi network. To investigate PSK signaling in stoma closure the loss-of-function mutant *tpst-1* was analyzed. ABA-induced stomatal closure was impaired in *tpst-1* compared to wild type and also impaired compared to *pskr1-3 pskr2-1* indicating that sulfated peptide signaling controls ABA-induced stoma closure (Figure 15A).

To study the contribution of the PSK peptide, wild type and *tpst-1* were supplemented with 100 μ M ABA, 0.1 μ M PSK or both hormones. In the absence of ABA, PSK did not alter stoma aperture in either wild type or *tpst-1* (Figure 15B). In the presence of ABA, PSK induced stoma closure in *tpst-1* to the same degree as in wild type indicating that both, PSK ligand and PSKRs are important for ABA-mediated stoma closure.

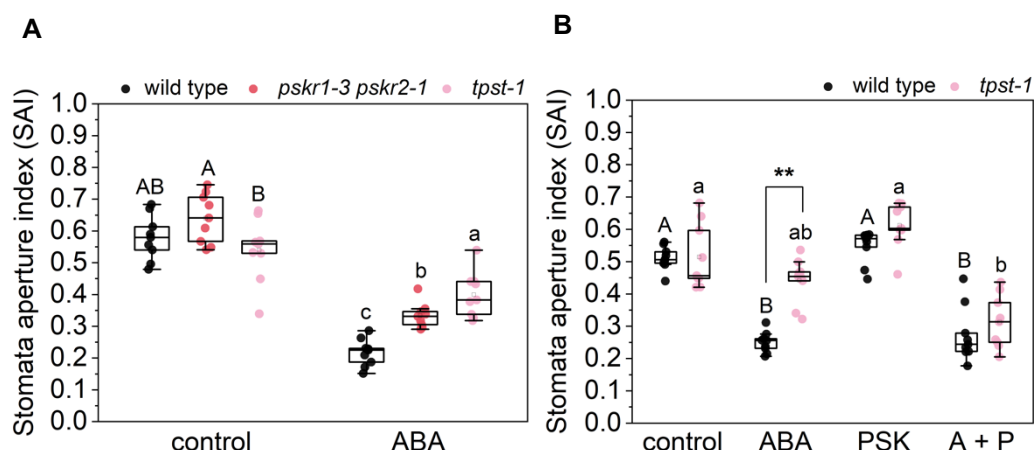


Figure 15: ABA-mediated stomatal closure is impaired in *tpst-1* and restored by PSK.

A, ABA-induced stomatal closure in wild type, *pskr1-3 pskr2-1* and *tpst-1* in epidermal peels from 3-4-week-old plants treated with 100 μ M ABA for 2 h. Values are means \pm SE of 3 independent biological repeats each analyzing 3 leaves with ≥ 25 stomata per leaf. Capital and minor letters indicate significant differences within treatments at $p < 0.05$, evaluated with one-way ANOVA with Tukey-Kramer. Significant differences were found between control and treatment in all genotypes, evaluated with two-sample t -test ($p < 0.05$).

B, ABA and PSK-dependent stomatal closure was compared in wild type and *tpst-1*. Epidermal peels were treated with either 100 μ M ABA, 0.1 μ M PSK or both together. Values are means \pm SE of leaves ($n = 9$) analyzed in 3 independent experiments. Capital and minor letters indicate significant differences within genotypes at $p < 0.05$, evaluated with Kruskal Wallis test. Asterisks ($p < 0.01$) indicate significant differences within treatments, evaluated Mann-Whitney-U test.

3.2 PSKR signaling is required for the accumulation of ROS in guard cells in response to ABA likely via regulation of RBOH

Results described above revealed a role for PSKR signaling in ABA-induced stomatal closure. We next set out to analyze the mechanistics of how the regulation is achieved through the PSKRs. Stomatal closure is tightly regulated by different stimuli, such as water status, light and CO_2 , as well as, ABA, Ca^{2+} and ROS. A series of ABA-induced signaling cascades promote an increase of ROS in guard cells that is activating Ca^{2+} signaling, which is required for the regulation of stomatal closure (Postiglione and Muday, 2020).

3.2.1 PSKR signaling maintains ROS levels in ABA- or mannitol-stressed leaves

To analyze the requirement of PSKR signaling in ROS accumulation, 7-day-old seedlings of wild type and *pskr1-3 pskr2-1* were treated with 100 μ M ABA or 50 mM mannitol for 2 h. To visualize O_2^- , the seedlings were subsequently stained with nitro tetrazolium blue chloride (NBT). To detect H_2O_2 , the seedlings were stained with 3,3'-diaminobenzidine (DAB). The histological staining assays revealed that wild-type leaves accumulated comparable amounts of ROS in control and treatment conditions.

In *pskr1-3 pskr2-1* seedlings $O_2^{\cdot-}$ accumulation was not significantly altered when treated with ABA or mannitol (Figure 16A,B) whereas H_2O_2 levels decreased in response to ABA and mannitol (Figure 16C,D). When genotypes were compared, ROS levels were significantly lower in *pskr1-3 pskr2-1* than in wild type under stress conditions (Figure 16B,D). The results revealed that PSKRs are required for ROS formation in response to osmotic stress or ABA.

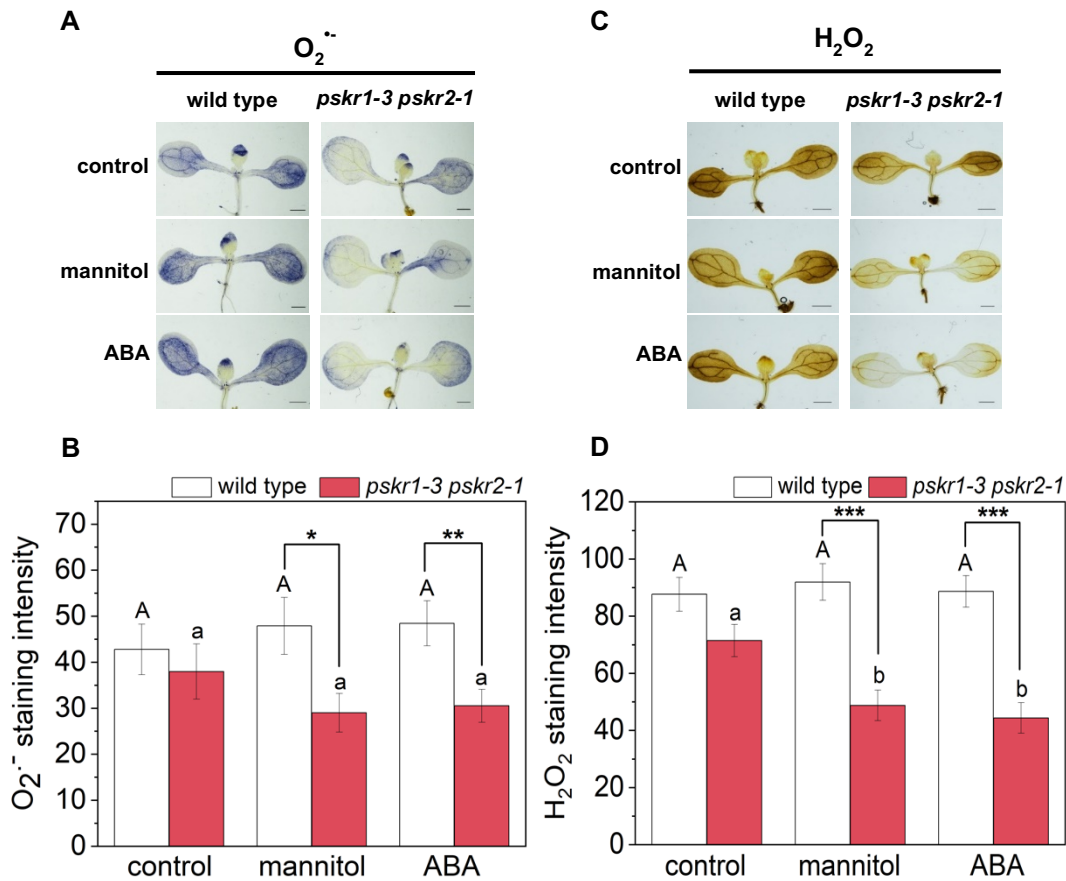


Figure 16: PSKR signaling maintains ROS levels after treatment with ABA or mannitol.

A, ROS levels were compared in wild-type and *pskr1-3 pskr2-1* shoots of 7-day-old seedlings after treatment with 1 μ M ABA and 50 mM mannitol for 2 h. The representative pictures of the seedlings show the $O_2^{\cdot-}$ -dependent nitro tetrazolium blue chloride (NBT) staining. Scale bar = 1 mm.

B, The $O_2^{\cdot-}$ staining intensity of wild-type and *pskr1-3 pskr2-1* shoots were analyzed. Results are means \pm SE of shoots (n= 30) analyzed. Capital and minor letters indicate significant differences within genotypes at $p < 0.05$, evaluated with Kruskal Wallis test. Asterisks (* $p < 0.05$, ** $p < 0.01$) indicate significant differences within treatments, evaluated with Mann-Whitney-U test.

C, H_2O_2 -dependent DAB staining of wild-type and *pskr1-3 pskr2-1* shoots was compared after 2 h of ABA and mannitol treatment. Scale bar = 1 mm.

D, The H_2O_2 staining intensity of wild-type and *pskr1-3 pskr2-1* shoots were analyzed. Values are means \pm SE of shoots (n = 30). Capital and minor letters indicate significant differences within genotypes at $p < 0.05$, evaluated with Kruskal Wallis test. Asterisks (***) $p < 0.001$ indicate significant differences within treatments, evaluated with Mann-Whitney-U test.

ABA-dependent ROS formation is catalyzed by RBOH at the plasma membrane. To identify the source of PSKR-dependent ROS production, 7-day-old seedlings of wild type, *pskr1-3 pskr2-1*, *35S:PSKR1-2* and *-12*, *35S:PSKR1-GFP-1*, *35S:PSKR2-1* and *-6* were treated with diphenyleneiodonium (DPI) which inhibits superoxide production at the plasma membrane by binding to flavoenzymes. The $O_2^{\cdot -}$ accumulation was examined by staining with NBT (Figure 17A). Superoxide accumulation was reduced in, both, wild-type and *pskr1-3 pskr2-1* seedlings when treated with DPI. Overexpression of *PSKR1* and *PSKR2* elevated ROS levels under control conditions compared with wild type (Figure 17B) whereas no differences in ROS levels were observed between genotypes in the presence of DPI, indicating that PSK receptors promote ROS formation in leaves via RBOH.

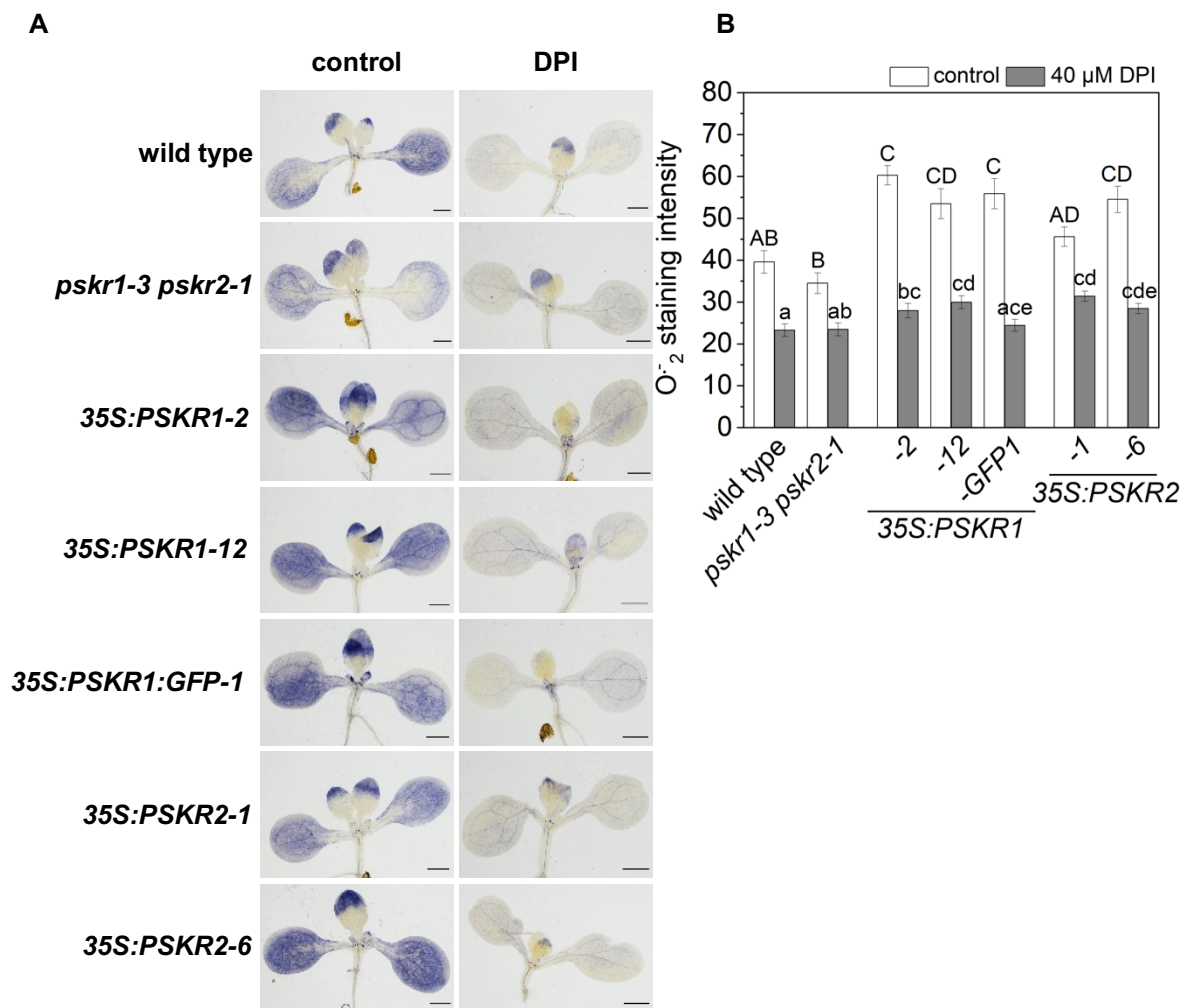


Figure 17: Overexpression of PSK receptors *PSKR1* or *PSKR2* promotes $O_2^{\cdot -}$ formation.

A, DPI-dependent reduction of ROS levels was analyzed in 7-day-old wild-type, *pskr1-3 pskr2-1*, *35S:PSKR1-2* and *-12*, *35S:PSKR1-GFP-1*, *35S:PSKR2-1* and *-6* shoots with the $O_2^{\cdot -}$ sensitive nitro blue tetrazolium chloride (NBT) staining. Scale bar = 1 mm.

B, The $O_2^{\cdot -}$ -dependent NBT staining was quantified from wild-type, *pskr1-3 pskr2-1*, *35S:PSKR1-2* and *-12*, *35S:PSKR1-GFP*, *35S:PSKR2-1* and *-6* shoots. Results are means \pm SE of shoots $n=30$ shoots analyzed. Capital and minor letters indicate significant differences within treatments at $p < 0.05$, evaluated with Kruskal Wallis test. Significant differences were found between control and treatment in all genotypes, evaluated with Mann-Whitney-U test ($p < 0.001$).

3.2.2 PSKR signaling is required for ABA-induced H₂O₂ accumulation in guard cells

Results described in chapter 3.2.1 suggested a role for PSKR signaling in ROS accumulation in water-stressed leaves. Since ROS are important to promote stomatal closure, we next examined H₂O₂ accumulation specifically in guard cells with high-resolution microscopy using the H₂O₂-sensitive dye 2',7'-dichlorofluorescein (H₂DCF-DA). The sensitive methodology used for the measurement only allows the investigation of the H₂O₂-dependent fluorescence of one genotype to the respective control. Guard cells of wild type treated with 100 μ M ABA for 2 h had a two times higher H₂O₂-dependent fluorescence compared with control guard cells (Figure 18A,B). No increase of H₂O₂-dependent fluorescence was observed in *pskr1-3 pskr2-1* in response to ABA suggesting that PSKR signaling controls H₂O₂ formation in guard cells during ABA-induced stomatal closure.

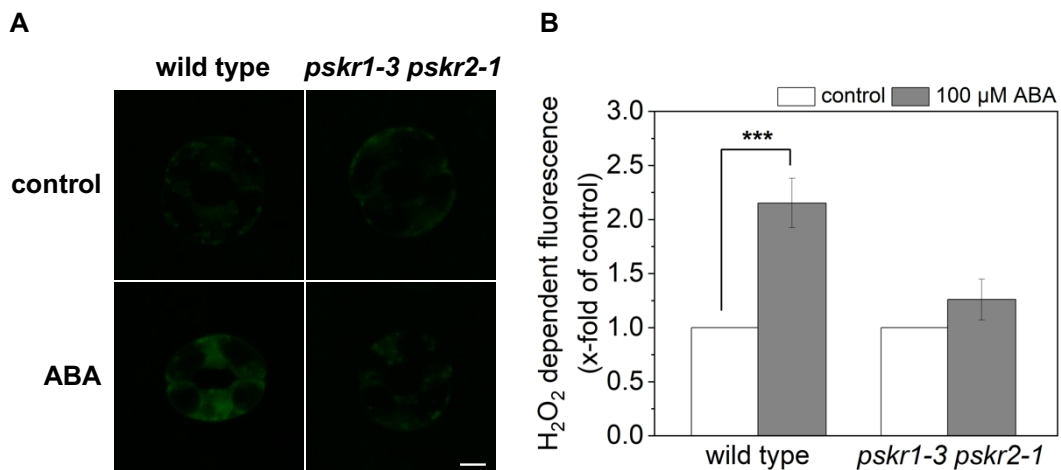


Figure 18: ABA-induced H₂O₂ accumulation in guard cells is impaired in *pskr1-3 pskr2-1*.

A, ABA-dependent ROS accumulation in guard cells was analyzed in epidermal peels of 3-4-week-old wild-type and *pskr1-3 pskr2-1* plants. Staining with the H₂O₂-selective dye 2',7'-dichlorofluorescein (H₂DCF-DA) was performed after treatment with ABA for 2 h. Scale bar = 5 μ m. B, The change in H₂O₂-dependent fluorescence after treatment with ABA was analyzed in wild type and *pskr1-3 pskr2-1*. Results are means \pm SE of H₂O₂ staining intensity compared to the control of the respective genotype, wild type (n = 15) *pskr1-3 pskr2-1* (n = 7). Asterisks indicate a significant difference at $p < 0.001$ to the control, evaluated with Mann-Whitney-U test.

Analysis of the overexpression lines *35S:PSKR1-2* and *-12*, *35S:PSKR2-1* and *-6* revealed H_2O_2 accumulation in guard cells after ABA treatment (Figure 19) that was comparable to the two-fold increase in wild type. The used technique is too sensitive to perform all genotypes in one experiment, the fluorescence intensities were compared to the control of the respective genotype. Comparisons among genotypes cannot be made.

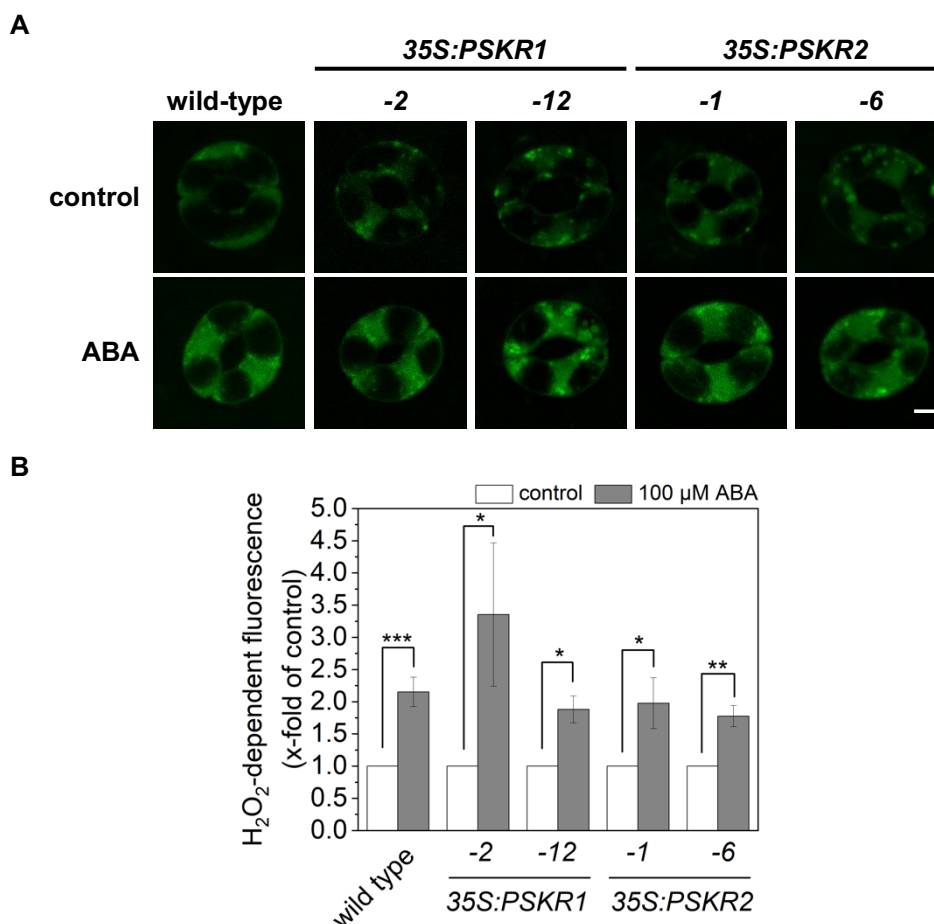


Figure 19: Overexpression of *PSKR1* or *PSKR2* does not further promote ABA-induced ROS accumulation in guard cells.

A, ABA-dependent ROS accumulation in guard cells was analyzed in wild type and *pskr1-3 pskr2-1* and the overexpression lines *35S:PSKR1-2* and *-12*, *35S:PSKR2-1* and *-6*. The epidermal peels of the 7th leaf of 3-4-week-old plants were stained with the H_2O_2 -selective dye 2',7'-dichlorofluorescein (H2DCF-DA) after treatment with ABA for 2h. Scale bar = 5 μ m.

B, Quantification of H_2O_2 -dependent fluorescence. Results are means \pm SE of H_2O_2 staining intensity compared to the control of the respective genotype, wild type (n = 15), *35S:PSKR1-2* (n = 4), *-12* (n = 3), *35S:PSKR2-1* (n = 4), *-6* (n = 5). Asterisks (* $p < 0.05$, ** $p < 0.01$, *** $p < 0.001$) indicate significant differences, evaluated with Mann-Whitney-U test.

These results indicated that PSKR signaling is required for ROS accumulation in guard cells in response to ABA. To examine if the impaired closure of stomata in *pskr1-3 pskr2-1* is due to lack of ROS accumulation, epidermal peels of the 7th leaf of 3- to 4-week-old wild-type and *pskr1-3 pskr2-1* plants were treated with 100 μ M ABA, 0.5 mM H₂O₂ or both together. While ABA-induced stoma closure was impaired in *pskr1-3 pskr2-1*, stomatal closure of *pskr1-3 pskr2-1* was recovered to the wild type level by H₂O₂. Similarly, when exposed to ABA and H₂O₂ at the same time closure of *pskr1-3 pskr2-1* stomata was comparable to that of wild type (Figure 20). The results support a role of PSKR signaling in ROS regulation that is essential for full ABA-induced stomatal closure.

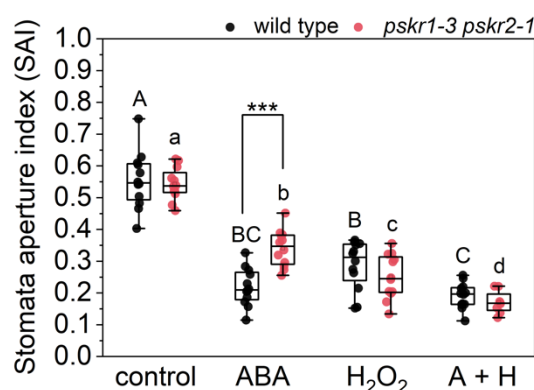


Figure 20: ABA-mediated stomatal closure is impaired in *pskr1-3 pskr2-1* and restored by H₂O₂.

Stomatal closure in response to 100 μ M ABA and 0.5 mM H₂O₂ was analyzed in 3-4-week-old plants of wild type and *pskr1-3 pskr2-1*. Results are means \pm SE from 2-3 leaves analyzed in each of 4 independent biological experiments. The average SAI per leaf was obtained from ≥ 25 stomata. Capital and minor letters indicate significant differences within genotypes at $p < 0.05$, evaluated with one-way ANOVA. Asterisks (***) $p < 0.001$ indicate significant differences, evaluated with two-sample t -test.

3.2.3 *RBOHD* and *RBOHF* are not transcriptional regulated by PSKRs in response to osmotic stress or ABA

After showing that PSK receptor signaling is required for ABA-induced ROS accumulation possibly via RBOH, we analyzed whether RBOH regulation occurred at the level of gene expression. The Arabidopsis genome encodes 10 genes of the RBOH family, whereas *RBOHD* and *RBOHF* are responsible for ABA-induced ROS elevation in guard cells (Kwak et al., 2003). We specifically analyzed transcripts of *RBOHD* and *RBOHF* in the 7th leaf of 3- to 4-week-old wild-type and *pskr1-3 pskr2-1* plants treated with or without 100 μ M ABA or 50 mM mannitol, using RT-qPCR. *RBOHD* expression was not significantly altered by ABA or mannitol in either wild type or *pskr1-3 pskr2-1* (Figure 21A). *RBOHF* transcript levels were elevated in response to ABA with no significant difference between genotypes (Figure 21B) while mannitol did not alter *RBOHF* expression. The results revealed that PSKRs do not target *RBOHD* and *RBOHF* activity at the transcriptional level.

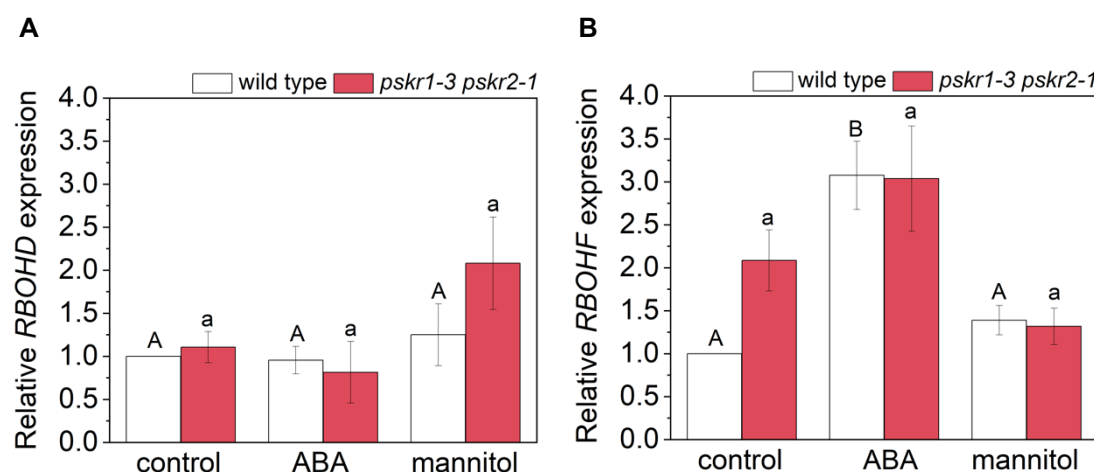


Figure 21: PSKR signaling does not regulate the expression of *RBOHD* and *RBOHF* in response to osmotic stress or ABA.

A, Relative expression of *RBOHD* in the 7th leaf of 3-4-week-old wild type and *pskr1-3 pskr2-1* after treatment with 50 mM mannitol and 100 μ M ABA for 2 h. Bars are means \pm SE of relative expression obtained from 3 independent experiments with 2 technical replicates ($n = 3$). Letters indicate the significant differences at $p < 0.05$, evaluated with one-way ANOVA and two-sample *t*-test.

B, ABA- and mannitol-dependent relative expression of *RBOHF* was compared in 3- to 4-week-old leaves of wild type and *pskr1-3 pskr2-1*. Values are means \pm SE of relative expression obtained from 3 independent experiments with 2 technical replicates ($n = 3$). Capital and minor letters indicate significant differences within genotypes at $p < 0.05$, evaluated with one-way ANOVA. No significant differences were found between genotypes at any given treatment, evaluated with two-sample *t*-test.

3.2.4 RBOHD/F and PSKR1 proteins exist in proximity in the plasma membrane

Previous results showed that guard cells of *pskr1-3 pskr2-1* plants cannot accumulate ROS in response to ABA and are impaired in stoma closure as a result. Since ROS accumulation is dependent on RBOH activity and PSKR signaling did not alter *RBOHD* and *RBOHF* transcript levels in response to osmotic stress or ABA, we hypothesized that regulation may occur at the protein level. To examine a possible PSKR-RBOH interaction *in planta*, FRET was used. The method is based on an energy transfer, where the emitted energy of a donor fluorophore is transferred to an acceptor fluorophore, which results in the emission of the acceptor. This can only take place if the two fluorophores are at a distance of less than 10 nm (Piston and Kremers, 2007). One way of measuring FRET efficiency is acceptor photobleaching. Due to the energy transfer from donor to acceptor, the fluorescence of the donor is quenched. If the acceptor is photobleached rapidly, the quenching process is prevented and the fluorescence of the donor increases. The fluorescence intensity of the donor before and after photobleaching is an indicator of FRET efficiency. To test if PSKR1 is in proximity to RBOHD or RBOHF, available constructs were taken where PSKR1 was fused C-terminally to GFP or RFP and RBOHD was fused C-terminally to GFP or RFP. New constructs were generated for RBOHD and RBOHF where the coding sequence was fused N-terminally to GFP. As a positive control, RLP44-RFP was used, which is known to directly interact with PSKR1-GFP (Holzwardt et al., 2018). BRI1-RFP was used as a negative control because PSKR1 and BRI1 were shown to not interact (Ladwig et al., 2015). The constructs were infiltrated in leaves of 4- to 5-week-old tobacco plants and the analysis was performed 2 days after infiltration. RLP44-RFP with PSKR1-GFP showed a FRET efficiency of ~11%, RBOHD-RFP with PSKR1-GFP of 3% and BRI1-RFP with PSKR1-GFP of ~0.15% (Figure 22A). The FRET efficiency of RBOHD-RFP with PSKR1-GFP was between the positive and negative control, showing that RBOHD is in proximity to PSKR1 but not as close as RLP44. When the experiment was repeated with permuted fluorophores the ratios stayed the same (Figure 22B). Co-immunoprecipitation identified RBOHD as a possible interaction partner of PSKR1 (AG Sauter, personal communication).

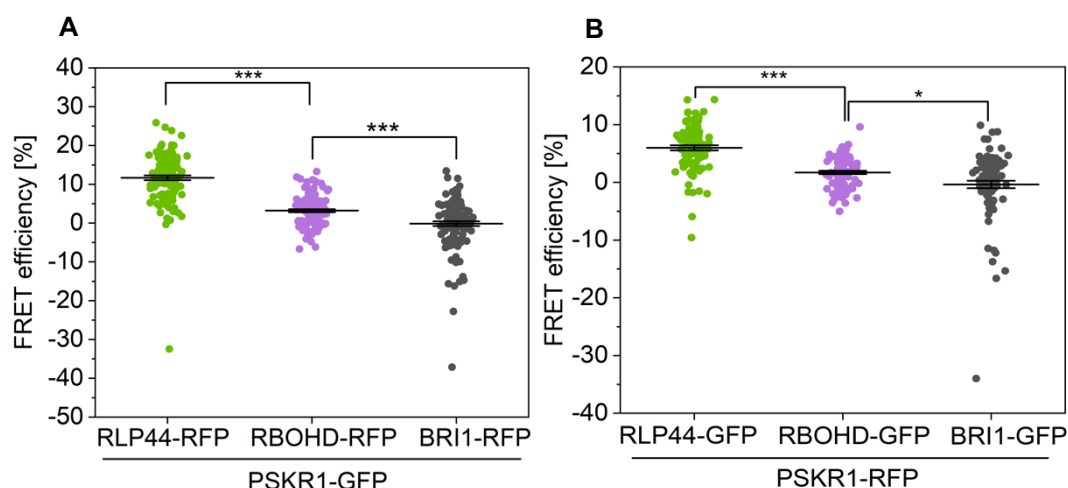


Figure 22: RBOHD is in proximity to PSKR1 in the plasma membrane.

A, Analyzing the distance of PSKR1-GFP to RLP44-RFP, RBOHD-RFP and BRI1-RFP with FRET-AB in *Agrobacterium* infiltrated *N. benthamiana* leaves. Data of the FRET efficiency analysis (n = 115-120) are shown as dots and the mean as a bar \pm SE. Asterisks (***) indicate significant differences, evaluated with Mann-Whitney-U test.

B, Analyzing the distance of PSKR1-RFP to RLP44-GFP, RBOHD-GFP and BRI1-GFP with FRET-AB in *Agrobacterium* infiltrated *N. benthamiana* leaves. Data of the FRET efficiency (n = 88-89) is shown as dots and the mean as a bar \pm SE. Asterisks (* p < 0.05, *** p < 0.001) indicate significant differences, evaluated with Mann-Whitney-U test.

The FRET efficiency of GFP-RBOHF with PSKR1-RFP was ~4.5%, RLP44-GFP and PSKR1-RFP was ~4%, and BRI1-GFP with PSKR1-RFP ~0.3% (Figure 23). The FRET efficiencies of PSKR1-RFP and the positive control RLP44-GFP and PSKR1-RFP with GFP-RBOHF were similarly high, indicating that RBOHF is in proximity to PSKR1. Taken together, the data revealed that RBOHD and RBOHF exist proximal to PSKR1 in the plasma membrane.

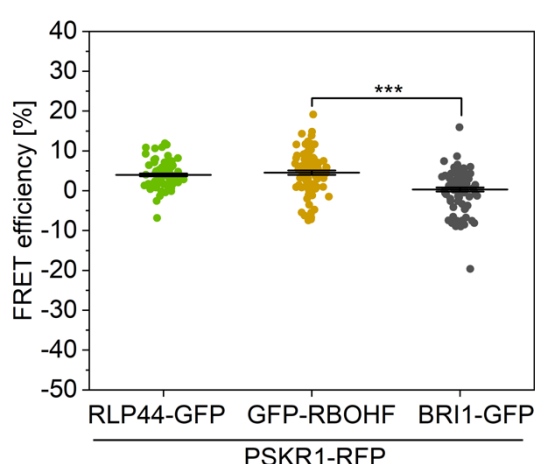


Figure 23: RBOHF is in proximity to PSKR1 in the plasma membrane.

Analyzing the distance of PSKR1-RFP to RLP44-GFP, GFP-RBOHF and BRI1-GFP with FRET-AB in *Agrobacterium* infiltrated *N. benthamiana* leaves. Data of the FRET efficiency analysis (n = 86-90) are shown as dots and the mean as a bar \pm SE. Asterisks (***) indicate significant differences, evaluated with Mann-Whitney-U test.

3.2.5 PSKR1 phosphorylates RBOHD and RBOHF *in vitro*

The FRET analyses suggested that RBOHD and RBOHF are in proximity to PSKR1, supporting regulation of the ROS accumulation through direct PSKR-RBOH interaction. PSKR1 is an active serine/threonine kinase that could phosphorylate RBOHD and RBOHF as substrates. Previous research on RBOHD revealed that the N-terminus and C-terminus of RBOHD are located in the cytosol (Figure 24A) (Kimura et al., 2020; Torres et al., 1998). Both cytosolic protein domains were each fused to an N-terminal MBP and a C-terminal 6xHIS tag (Figure 24B). The cytosolic N- and C-termini of RBOHD were ectopically expressed (Figure 24C) in *E.coli* and the recombinant proteins were used together with the ectopically expressed kinase domain of PSKR1 (PSKR1-KD) in an *in vitro* phosphorylation assay.

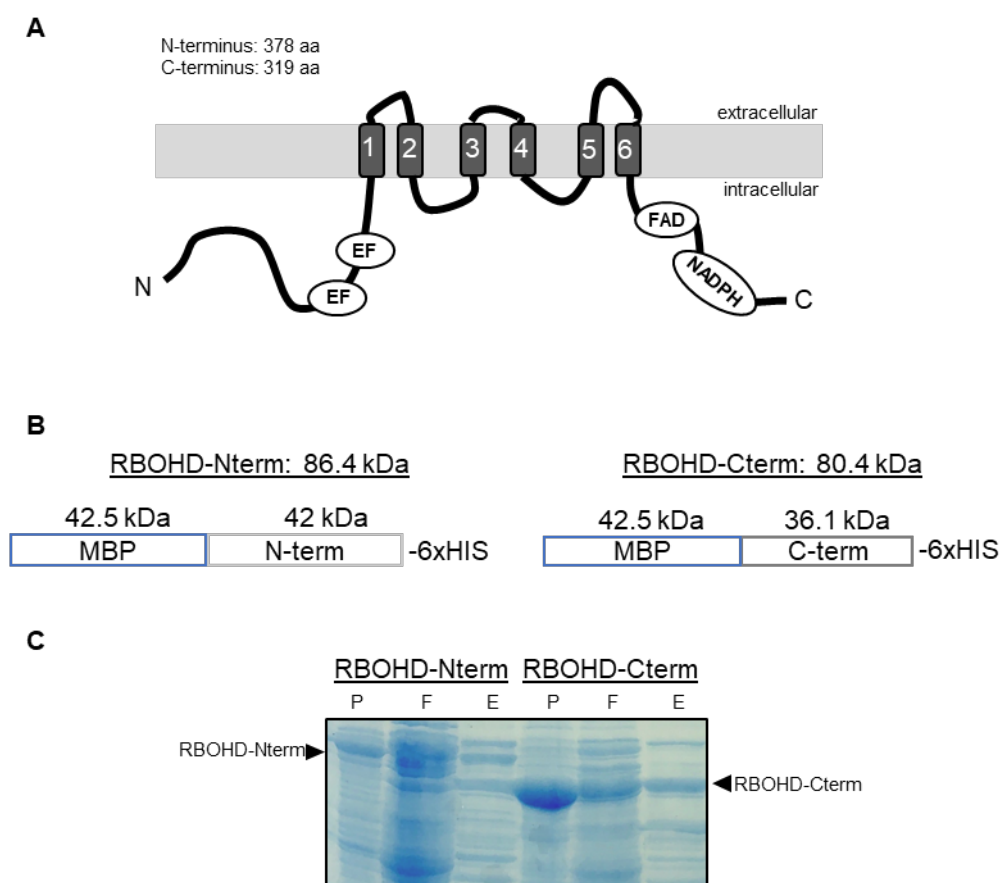


Figure 24: Expression of cytosolic protein domains of RBOHD.

A, Schematic figure showing membrane topology of RBOHD at the plasma membrane (based on Kimura et al., 2020; Torres et al., 1998). The protein contains cytosolic N-terminus (376 aa) and C-terminus (319 aa) as well as 6 transmembrane domains. The N-terminus harbors 2 EF-hands (EF) and the C-terminus has a FAD-binding domain (FAD) and an NADPH binding domain (NADPH). B, Schematic scheme of fusion proteins of N-terminus and C-terminus of RBOHD with the corresponding sizes. Both protein constructs contain an N-terminal MBP tag and a C-terminal 6xHIS tag. C, Exemplary SDS polyacrylamide gel of protein expression of RBOHD-Nterm and RBOHD-Cterm. The cell pellet (P), the crude extract (F) and the purified protein (E) are shown. RBOHD-Nterm is seen at a size of 86.4 kDa and RBOHD-C-term at 80.4 kDa.

As a control, MBP without fusion was analyzed and only autophosphorylation of PSKR1-KD was detected (Figure 25A). The kinase assay for RBOHD showed transphosphorylation of the N-terminus (RBOHD-Nterm) and the C-terminus (RBOHD-Cterm) as well as autophosphorylation of PSKR1-KD (Figure 25B).

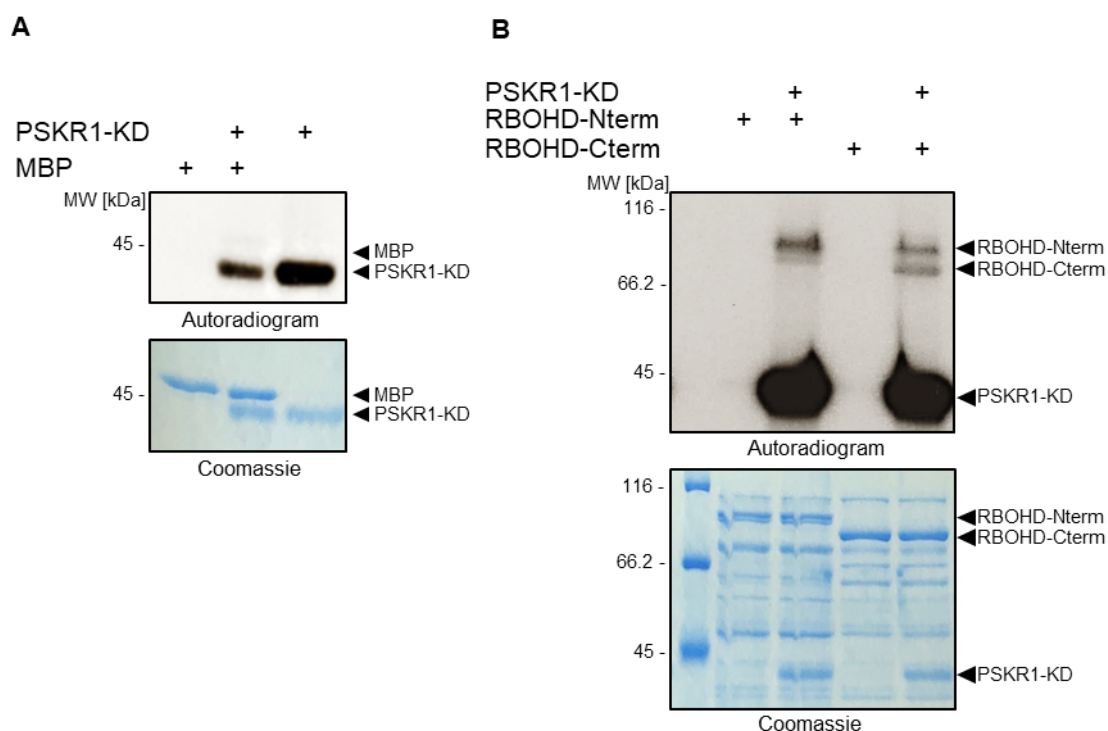


Figure 25: *In vitro* phosphorylation of RBOHD N- and C-terminus by PSKR1 kinase.

A, PSKR1 kinase (PSKR1-KD) (0.25 μ g) were incubated with γ - 32 P-ATP and 1 μ g of purified MBP. The autoradiogram shows autophosphorylation activity of PSKR1-KD. Input proteins were stained with Coomassie to visualize the loading of samples.

B, PSKR1 kinase domain (PSKR1-KD) (0.25 μ g) were incubated with γ - 32 P-ATP and 1 μ g of purified N- and C-terminus of RBOHD. The autoradiogram shows transphosphorylation of RBOHD-Nterm (86.4 kDa) and RBOHD-Cterm (80.4 kDa) and autophosphorylation activity of PSKR1-KD (39.2 kDa). Input proteins were stained with Coomassie to visualize the loading of samples.

Topology prediction analysis of a previous publication (Keller et al., 1998) and online prediction software like Protter-visualize proteoforms (Omasits et al., 2014) and TOPCONS (Tsirigos et al., 2015) provided different results for RBOHF. All sequence predictions had in common that the N-terminus of RBOHF is in the cytosol, whereas the number of transmembrane domains was changing, resulting in a not defined location of the C-terminus (Figure 26A,B). Since the analysis did not show a clear result for the C-terminus of RBOHF, we decided to generate fusion constructs of Loop2 of one prediction (Figure 26A), harboring a FAD-binding domain and the C-terminus of the other sequence analysis (Figure 26B), harboring an NADPH-binding site. In addition, a fusion construct for the N-terminus of RBOHF was generated.

All proteins were fused to an N-terminal MBP and a C-terminal 6xHIS tag (Figure 26C). The N-terminus of RBOHF could not be expressed, although several temperatures, time points and tags were tried to achieve a better expression (Figure 26D).

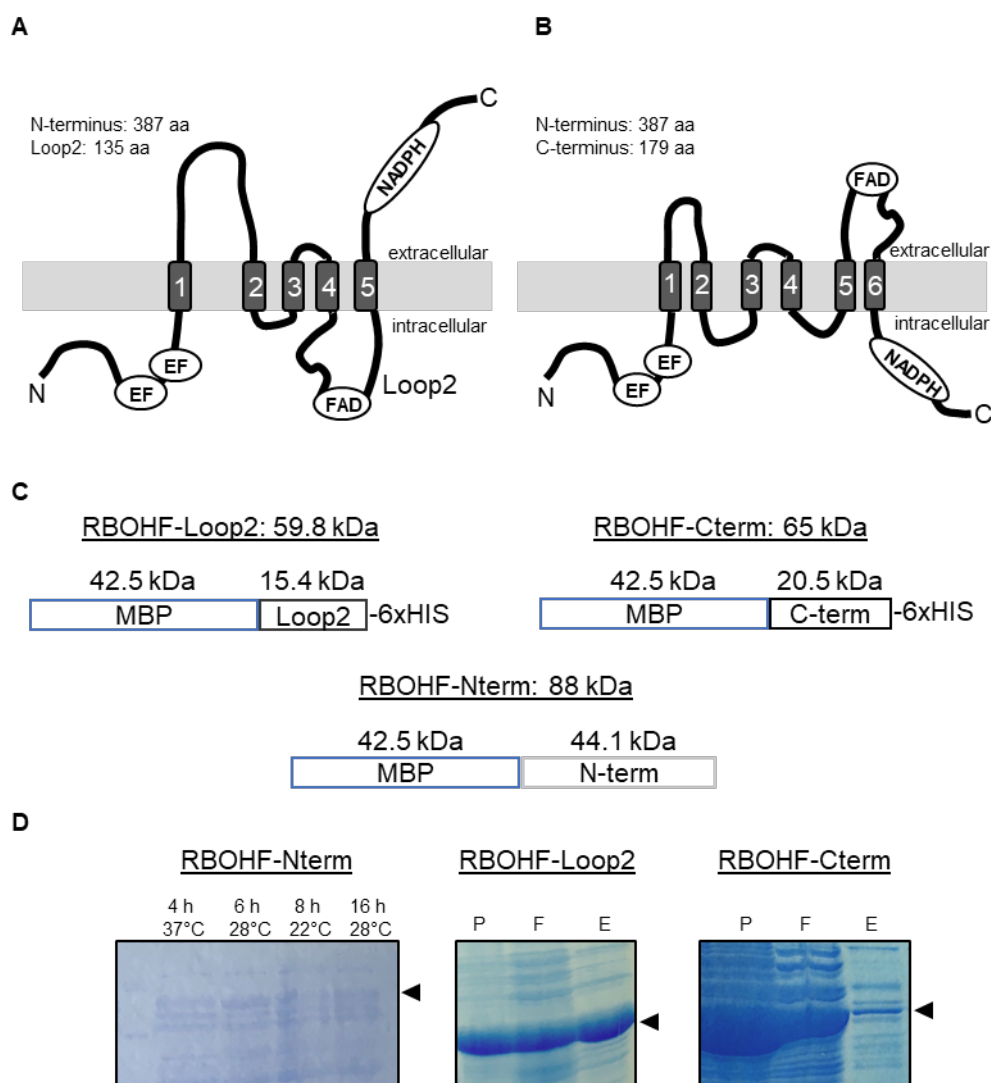


Figure 26: Expression of protein domains of RBOHF.

A, Schematic figure showing membrane topology of RBOHF at the plasma membrane. Sequence analysis was performed with Protter-visualize proteoforms (Omasits et al., 2014). The prediction revealed a cytosolic 387 aa N-terminus, a 20 aa intracellular loop1 and a 135 aa intracellular Loop2. It was predicted that the protein consists of 5 transmembrane domains.

B, The schematic structure of RBOHF is based on topological data from UniProt (Keller et al., 1998). The prediction revealed a cytosolic 387 aa N-terminus, a 20 aa intracellular Loop1, a 8 aa intracellular Loop2 and a 179 aa C-terminus. It was predicted that the protein consists of 6 transmembrane domains.

C, Schematic scheme of fusion proteins of N-terminus, Loop2 and C-terminus of RBOHF with the corresponding sizes. Protein constructs contain an N-terminal MBP tag and the Loop2 and the C-terminus a C-terminal 6xHIS tag.

D, Exemplary SDS polyacrylamide gel of protein expression of RBOHF-Nterm, RBOHF-Loop2 and RBOHF-Cterm. Cell pellets from different time points and temperatures are shown for RBOHF-Nterm (expected size 88 kDa). The cell pellet (P), the crude extract (F) and the purified protein (E) were separated due to their molecular weight for RBOHF-Loop2 (59.8 kDa) and RBOHF-Cterm (65 kDa).

The protein domain with a FAD-binding site (RBOHF-Loop2) and the protein domain with an NADPH-binding site (RBOHF-Cterm) of RBOHF (Figure 26D) were successfully expressed and the resulting recombinant protein was further used together with the kinase domain of PSKR1 (PSKR1-KD) in a phosphorylation assay. The results showed transphosphorylation of RBOHF-Loop2 as well as autophosphorylation of PSKR1-KD (Figure 27). After a long exposure time, a weak signal for the C-terminus of RBOHF was detectable, but negligible due to the very low intensity, revealing that the C-terminus of RBOHF (RBOHF-Cterm) was not transphosphorylated by the PSKR1 kinase. This result reveals the specific phosphorylation of the RBOHF protein in the region of the FAD-binding domain (RBOHF-Loop2) *in vitro*.

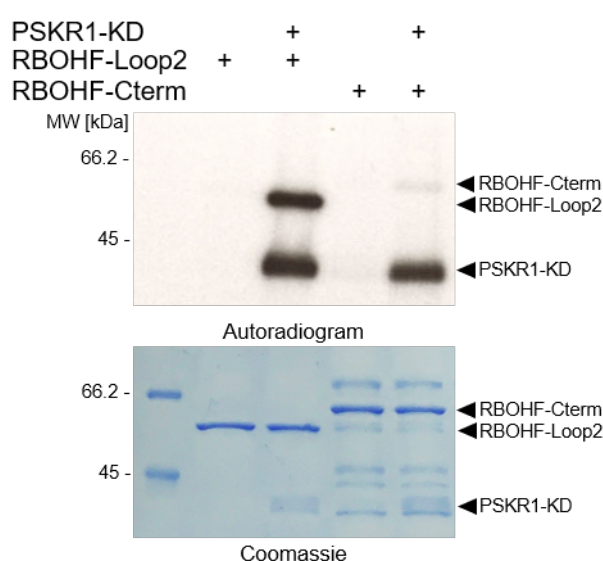


Figure 27: *In vitro* phosphorylation of RBOHF protein domain with FAD-binding site by PSKR1 kinase.

PSKR1 kinase domain (PSKR1-KD) (0.25 μ g) were incubated with γ - 32 P-ATP and 1 μ g of purified Loop2 and C-terminus of RBOHF. The autoradiogram shows transphosphorylation of RBOHF-Loop2 (59.8 kDa) and autophosphorylation activity of PSKR1-KD (39.2 kDa). Weak signal was detected for C-terminus RBOHF (65 kDa) after long exposure (16 h). Input proteins were stained with Coomassie to visualize the loading of samples.

Since PSKR1-KD phosphorylated the N- and C-terminus of RBOHD and the Loop2 of RBOHF *in vitro* it is conceivable that PSKR1 regulates RBOH at the plasma membrane at the protein level in guard cells thereby promoting ROS production and consequently stomatal closure. Future analysis, using mass spectrometry will analyze the specific phosphorylation sites.

3.3 The aquaporin PIP2;1 as a possible target of PSKR signaling

We showed that ABA-induced stomatal closure requires PSKR signaling to elevate ROS levels in guard cells possibly by activating RBOHD and RBOHF. RBOH generates ROS in the apoplast, but to act as a stimulus for ion channels, ROS are required inside the cell (Pei et al., 2000; Mori and Schroeder, 2004). The aquaporin PIP2;1 is known to facilitate uptake of H_2O_2 in the guard cells during ABA-induced stomatal closure (Rodrigues et al., 2017).

3.3.1 The aquaporin PIP2;1 contributes to PSK-induced protoplast expansion

Cell expansion is based on accumulation and release of solutes, the influx of water into the cell and cell wall yielding. Despite the irreversible volume change, guard cells are a well-studied example for reversible volume change which is obtained by the variation of the turgor pressure. PSKR signaling is required for stomatal closure (3.1.4) and is known to promote cell expansion (Kutschmar et al., 2009; Stührwohltd et al., 2011) but it remains unresolved whether an aquaporin contributes to it. A previous co-immunoprecipitation indicated an interaction of PSKR1 and PIP2;1 (AG Sauter, personal communication). To test if the aquaporin PIP2;1 is required for PSK-induced cell expansion, root length of 5-day-old wild-type, *pskr1-3 pskr2-1* and *pip2;1* seedlings grown with or without exogenous PSK were analyzed (Figure 28 A).

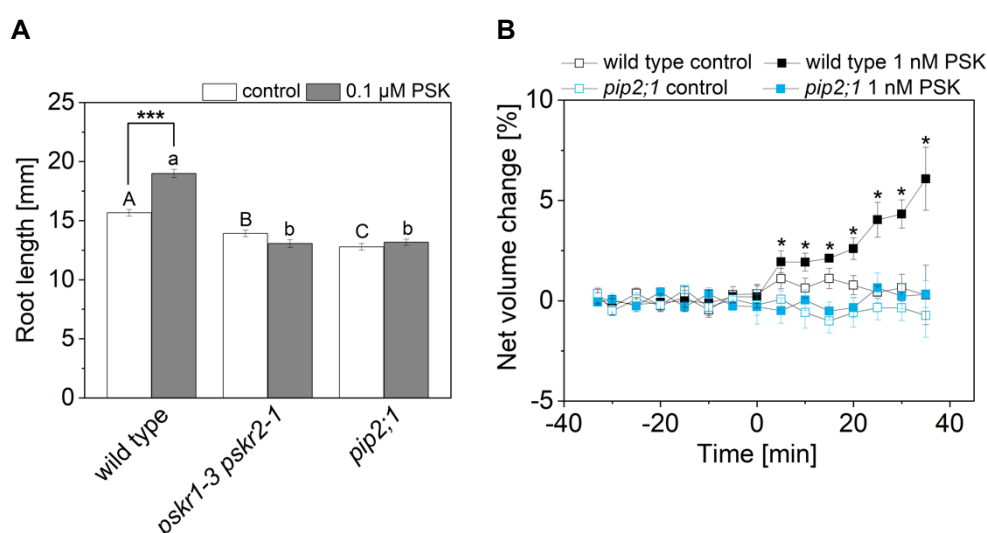


Figure 28: PIP2;1 maintains the PSK-dependent cell expansion.

A, Root length of 5-day-old wild-type, *pskr1-3 pskr2-1* and *pip2;1* seedlings in response to 0.1 μM PSK. Values are means ± SE (n = 85-115). Letters ($p < 0.05$) and asterisks (***) indicate significant differences between and within genotypes, respectively, evaluated with Kruskal-Wallis and Mann-Whitney-U test (Faroux, 2021).

B, Protoplast expansion in response to 1 nM PSK was analyzed in wild type and *pip2;1*. Results are means ± SE of the net volume change (n ≤ 9). Asterisks indicate significant differences between wild-type and *pip2;1* protoplasts when treated with PSK ($p < 0.05$, two-sample *t*-test).

The results revealed that PSK promoted root elongation in wild type but not in *pskr1-3 pskr2-1* and *pip2;1* (Figure 28A), showing the importance of *PIP2;1* in PSK-dependent root elongation. To independently verify that *PIP2;1* is required for PSK-dependent growth, protoplasts were used as an experimental system (Jiang et al., 2013). Protoplasts isolated from the hypocotyl of 5-day-old wild-type and *pip2;1* seedlings were treated with 1 nM PSK, a concentration previously shown to promote protoplast expansion (Stührwohldt et al., 2011). The net volume change was continuously recorded for up to 40 min. PSK-dependent expansion was observed in wild-type protoplasts with a ~5% higher net volume compared to control conditions (Figure 28B). The net volume of *pip2;1* protoplasts remained at the control level even after addition of PSK, suggesting that water uptake through *PIP2;1* is crucial for PSK-dependent protoplast expansion. This observation raised the possibility that *PIP2;1* might be a target of PSKR signaling.

3.3.2 Transcripts of *PIP2;1* are not regulated by *PSKR*s

After displaying that *PIP2;1* is required for a PSK-dependent cell expansion, a possible regulation on *PIP2;1* expression by the PSKR signaling was analyzed with RT-qPCR. The expression was analyzed in the 7th leaf of 3- to 4-week-old plants that were treated with 100 μ M ABA or 50 mM mannitol. The results showed that the expression of *PIP2;1* was slightly induced with the treatment of ABA in wild type and *pskr1-3 pskr2-1* (Figure 29). No differences were observed when wild type and *pskr1-3 pskr2-1* were compared, showing that there is no regulation on transcript level via PSKR signaling.

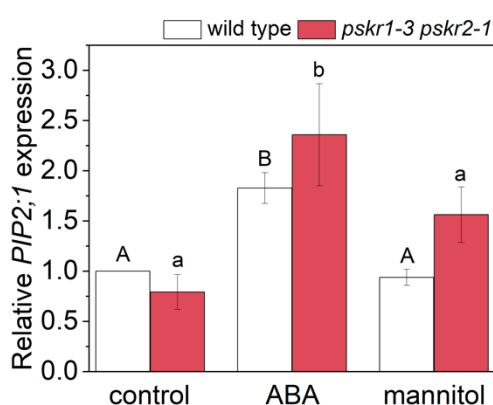


Figure 29: *PIP2;1* transcript level is not regulated by PSKR signaling.

Relative expression of the aquaporin *PIP2;1* in the 7th leaf of 3-4-week-old wild-type and *pskr1-3 pskr2-1* plants after treatment with 50 mM mannitol or 100 μ M ABA for 2 h. Bars are means \pm SE of relative expression ($n = 3$) obtained from 3 independent experiments with 2 technical replicates. Capital and minor letters indicate significant differences within genotypes at $p < 0.05$, evaluated with Kruskal Wallis test. No significant differences were found between genotypes at any given treatment, evaluated with Mann-Whitney-U test (Faroux, 2021).

3.3.3 Phosphorylation of S280/S283 at the C-terminus of PIP2;1 is not of importance for stomatal closure

Results in Chapter 3.1.4 have shown that the PSK signaling pathway is required for full ABA-induced stomatal closure. PIP2;1 was previously demonstrated to be required in stomatal closure (Grondin et al., 2015), not only through its ability to facilitate the entry of water into the cells but also through its ability to direct H₂O₂ into the cell (Rodrigues et al., 2017). Phosphorylation of PIP2;1 plays an important regulatory role in channel opening (Qiu et al., 2020) that remains to be characterized in the context of PSKR signaling during stomatal closure. To do so, we used the knock-out line *pip2;1* and lines complemented with PIP2;1 harboring site-directed mutations at S280 and S283 under the control of the endogenous promoter of *PIP2;1* in the *pip2;1* background. The 7th leaf of 3- to 4-week-old plants of wild type, *pskr1-3 pskr2-1*, *pip2;1*, and the complementation lines in the *pip2;1* background *PIP2;1-AA*, mimicking a constitutive phosphorylation deficiency at S280A/S283A, *PIP2;1-DD* with the constitutive phosphomimetic mutations S280D/S283D, and *PIP2;1-SS* mimicking wild type, were analyzed for stomatal closure in response to ABA. The results showed a requirement for PIP2;1 in stoma closure. However, plants expressing *PIP2;1-AA*, *PIP2;1-DD* or *PIP2;1-SS* showed similar stoma closure as wild type (Figure 30) indicating that phosphorylation of S280 and S283 at the C-terminus of PIP2;1 is not a regulatory mechanism for ABA-mediated stomatal closure.

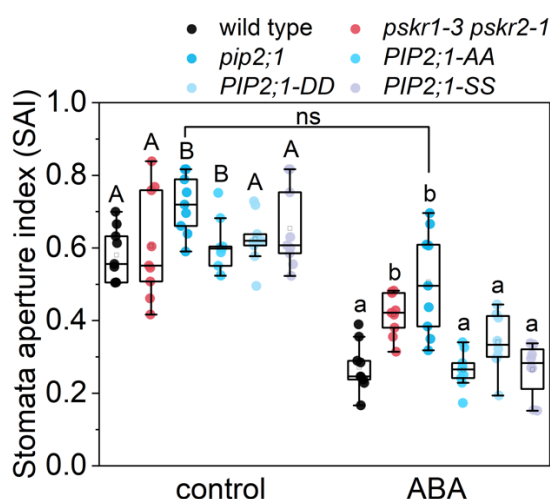


Figure 30: Phosphorylation of PIP2;1 is required for ABA-induced stomatal closure, whereas its phosphorylation at S280 and S283 is not.

Stomatal closure was analyzed in wild type, *pskr1-3 pskr2-1*, *pip2;1* and in the *PIP2;1* lines with point mutations at S280 and S283, *PIP2;1-AA*, *PIP2;1-DD* and *PIP2;1-SS*. Epidermal peels from 3-4-week-old plants treated with 100 μ M ABA for 2 h were examined. Values are means \pm SE of 3 independent biological repeats, each analyzing 3 leaves with ≥ 25 stomata per leaf ($n = 9$). Capital and minor letters indicate significant differences within treatments at $p < 0.05$, evaluated with Kruskal Wallis test. Significant differences between control and treatment were evaluated with Mann-Whitney-U test ($p < 0.05$), whereas *pip2;1* was not significantly different from its control.

3.3.4 PSKR1 kinase regulates PIP2;1 through phosphorylation

PIP2;1 expression was not dependent on PSKR1 and the phosphorylation status of S280/S283 was not crucial for ABA-mediated stoma closure, suggesting that *PIP2;1* regulation occurred at the protein level possibly at other phosphorylation sites. *PIP2;1* was previously detected in two independent co-immunoprecipitations with PSKR1 as a bait (AG Sauter, personal communication). Taken these findings together, they suggest that PSKR1 may phosphorylate *PIP2;1* at sites other than S280/S283. To test this hypothesis, a kinase assay was performed. The sequence prediction software Protter-visualize proteoforms (Omasits et al., 2014) and a previous publication (Yoo et al. 2016) revealed 6 transmembrane domains, a cytosolic N- and C-terminus, as well as 2 intracellular loops (Figure 31A).

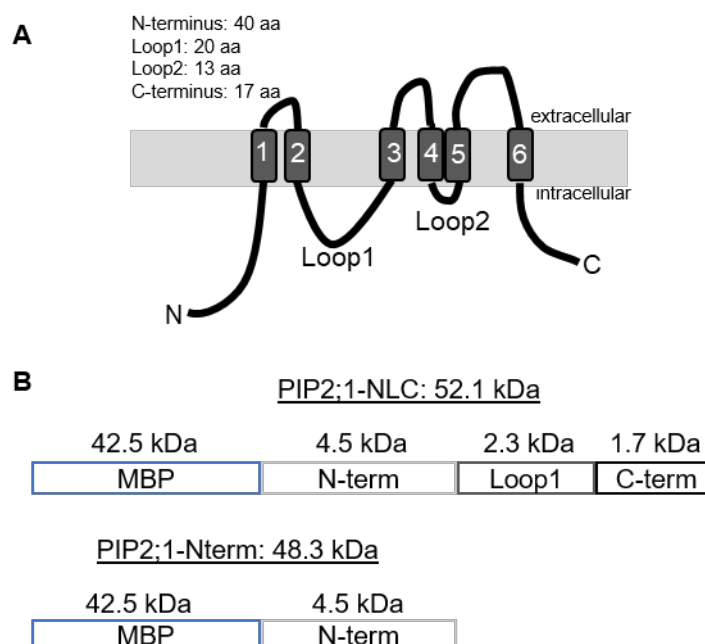


Figure 31: Membrane topology of *PIP2;1* at the plasma membrane.

A, Topology prediction by Protter-visualize proteoforms (Omasits et al., 2014) and a previous publication (Yoo et al., 2016). The sequence prediction revealed a cytosolic 40 aa N-terminus, a 20 aa intracellular loop1, a 13 aa loop2 and a 17 aa C-terminus in the cytosol. It was predicted that the protein consists of 6 transmembrane domains.

B, Scheme of the fusion proteins of the N-terminus (*PIP2;1*-Nterm) and a combination of N-terminus, Loop1 and C-terminus of *PIP2;1* (*PIP2;1*-NLC) with the corresponding sizes. Both protein constructs contain an N-terminal MBP tag.

To identify possible phosphorylation sites we cloned the cytosolic protein domains of *PIP2;1* except for loop2 which has a very low molecular weight of 13 aa, and further generated a construct generating a chimeric protein consisting of N-terminus, loop1 and C-terminus (*PIP2;1*-NLC), for ectopic expression in *E.coli*. The cytosolic N-terminus of *PIP2;1* (*PIP2;1*-Nterm) was also expressed alone (Figure 31B). For better solubilization, the proteins were tagged with an N-terminal MBP.

To analyze phosphorylation of PIP2;1 by PSKR1, an *in vitro* kinase assay with 1 μ g recombinant PIP2;1 protein and 0.25 μ g kinase domain of PSKR1 (PSKR1-KD) was performed with γ - 32 P-ATP used for radiolabeling. As a control, MBP without fusion was analyzed and only autophosphorylation of PSKR1-KD was detected (Figure 32A). Kinase assay for PIP2;1 showed transphosphorylation of the PIP2;1-Nterm at a size of 48.3 kDa and of the chimeric protein PIP2;1-NLC at 52.1 kDa (Figure 32B). Autophosphorylation of the PSKR1-KD was identified at 39.2 kDa. The results showed *in vitro* phosphorylation of PIP2;1 by PSKR1-KD, supporting the possibility that PSKR1 may phosphorylate PIP2;1 as a direct substrate in guard cells. The ectopically expressed proteins can be used in future to identify specific phosphorylation sites with mass spectrometry.

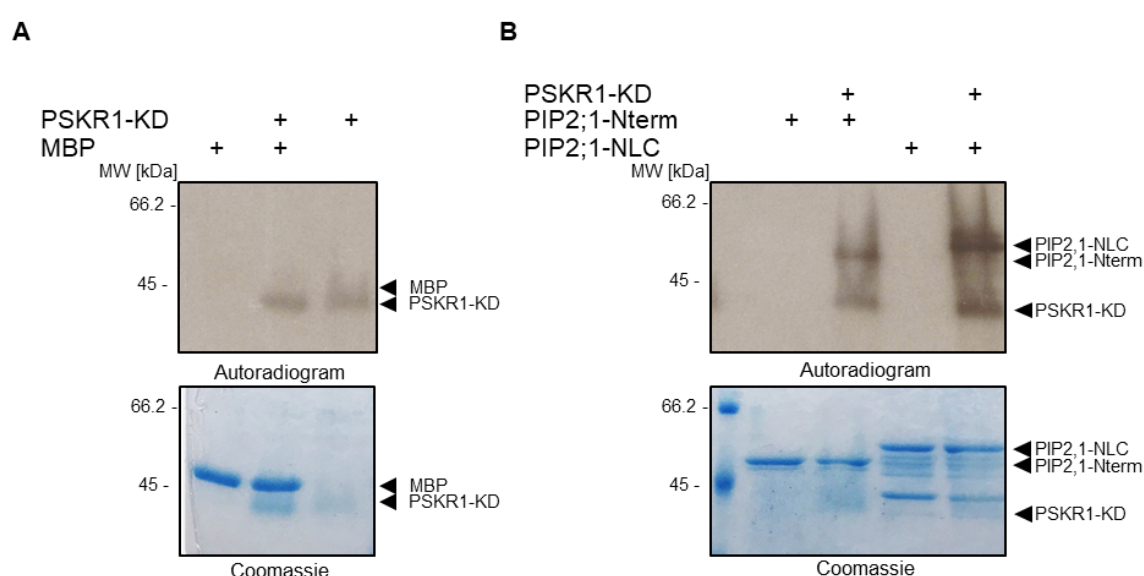


Figure 32: *In vitro* phosphorylation of cytosolic domains of PIP2;1.

A, PSKR1 kinase (PSKR1-KD) (0.25 μ g) were incubated with γ - 32 P-ATP and 1 μ g of purified MBP. The autoradiogram shows autophosphorylation activity of PSKR1-KD. No transphosphorylation of MBP was detected. Input proteins were stained with Coomassie to visualize the loading of samples. B, The PSKR1 kinase domain (PSKR1-KD) (0.25 μ g) was incubated with γ - 32 P-ATP and 1 μ g of the purified N-terminus (PIP2;1-Nterm) or a combination of N-terminus, loop1 and C-terminus (PIP2;1-NLC) of PIP2;1. The autoradiogram shows transphosphorylation of PIP2;1-Nterm (48.3 kDa) and PIP2;1-NLC (52.1 kDa) and autophosphorylation activity of PSKR1-KD (39.2 kDa). Proteins were stained with Coomassie to visualize the loading of samples (Faroux, 2021).

3.4 Expression analysis of CNGCs in guard cells

As described, PSKR signaling is required for ABA-mediated stomatal closure by elevating ROS levels in the guard cells. We have tested the hypothesis that PSKRs regulate ROS accumulation through interaction with RBOHD/F that generates ROS in the apoplast or with PIP2;1 that imports H₂O₂ from the apoplast into the guard cell. Another level of regulation of ROS levels by PSKR1 could occur through plasma membrane-localized cation channels of the CNGC family. PSKR1 was shown to exist in a nanocluster together with CNGC17 (Ladwig et al., 2015), one of 20 members of the CNGC family which are known to mediate the influx of cations. Previous analysis identified CNGC2, CNGC5-10, CNGC14, CNGC16 and CNGC18 to permeate Ca²⁺ (Wang et al., 2017; Zhang et al., 2017; Wang et al., 2013; Gao et al., 2016). Calcium functions as a second messenger in stomatal closure by binding to the calcium activation domain of calcium-dependent protein kinases (CPKs) (Bender et al., 2018). CPK4-6 and CPK11 were shown to phosphorylate and activate RBOHD resulting in ROS production (Sierla et al., 2016). An increase in Ca²⁺ in guard cells is promoted by CNGC5 and CNGC6 but they are not solely responsible for it (Wang et al., 2013). The other channels mediating Ca²⁺ influx into guard cells in response to ROS, to activate CPKs, have not yet been elucidated. Despite the indirect regulation of RBOH by CPKs, direct regulation of ROS production could be mediated by the binding of Ca²⁺ to EF-hand motifs of RBOHs (Sierla et al., 2016).

3.4.1 Specific expressions of CNGCs in Arabidopsis

To explore the possibility that PSKR may promote stoma closure via CNGCs, we looked into *CNGC* gene expression. The CNGC protein family includes 20 members, which cluster into five groups (Figure 33). CNGC17, which is known to exist in a nanocluster together with PSKR1, belongs to group III along with CNGC14, CNGC15, CNGC16 and CNGC18.

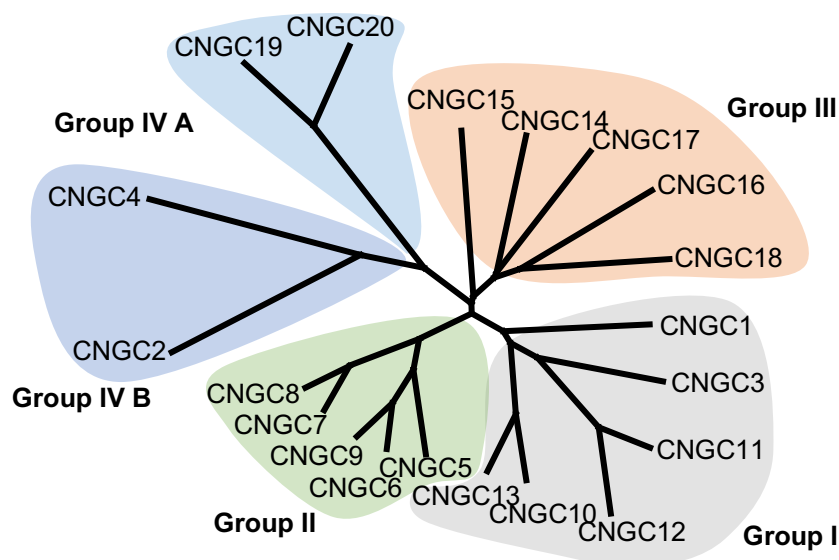


Figure 33: Phylogenetic tree of CNGCs in Arabidopsis.

Multiple sequence alignment of 20 CNGC protein sequences from Arabidopsis was performed with Clustal Omega (Madeira et al., 2019) and the phylogenetic tree with TreeView (Page, 2001).

RNA sequencing data deposited in the eFP-seq browser database (Sullivan et al., 2019) were used for expression analysis of the 20 *CNGC* genes (Figure 34). A broadly distributed expression in organs was observed with overall low expression levels. Strikingly, almost all *CNGC* genes were expressed in the shoot. *CNGC8*, *CNGC16* and *CNGC18* were expressed at elevated levels in pollen and expression of *CNGC14* was only observed in roots.

gene	root	root apical meristem	aerial	leaf	carpel	receptacle	st. 12 inflorescence	mature pollen
<i>CNGC1</i> (At5g53130)	28.6	17.2	80.8	96.9	107.9	89.7	53.6	0.3
<i>CNGC2</i> (At5g15410)	17.8	18.2	159.7	89.9	43.8	42.7	0.6	0.7
<i>CNGC3</i> (At2g46430)	22.1	3.4	44.5	38.7	2.8	12.2	0.6	0.3
<i>CNGC4</i> (At5g54250)	0.4	0.2	23.1	18.0	6.2	10.2	13.3	0.0
<i>CNGC5</i> (At5g57940)	24.9	16.0	35.8	38.3	49.0	41.7	32.7	0.0
<i>CNGC6</i> (At2g23980)	26.2	31.5	31.3	26.1	46.8	42.2	28.0	1.6
<i>CNGC7</i> (At1g15990)	0.1	0.0	14.2	43.5	1.3	6.9	31.1	10.9
<i>CNGC8</i> (At1g19780)	2.0	4.2	20.2	19.8	75.5	18.0	32.6	134.4
<i>CNGC9</i> (At4g30560)	25.2	15.3	5.9	9.5	25.9	26.1	19.2	6.0
<i>CNGC10</i> (At1g01340)	7.4	19.6	5.0	3.4	0.5	2.7	1.4	6.7
<i>CNGC11</i> (At2g46440)	5.9	1.4	126.1	93.8	2.9	9.9	1.6	0.4
<i>CNGC12</i> (At2g46450)	30.1	11.3	135.2	94.6	16.5	35.8	14.6	0.4
<i>CNGC13</i> (At4g01010)	3.6	0.9	17.3	13.9	0.9	6.9	1.8	43.4
<i>CNGC14</i> (At2g24610)	20.2	26.5	0.2	0.9	3.1	0.1	0.2	0.0
<i>CNGC15</i> (At2g28260)	10.4	5.2	15.2	14.3	18.3	8.0	18.4	0.0
<i>CNGC16</i> (At3g48010)	1.1	0.4	0.1	0.7	0.3	0.2	10.6	42.3
<i>CNGC17</i> (At4g30360)	59.8	9.9	31.5	40.4	62.7	63.3	44.1	0.0
<i>CNGC18</i> (At5g14870)	1.7	1.5	1.1	1.4	9.3	2.5	36.0	225.2
<i>CNGC19</i> (At3g17690)	0.7	0.7	1.0	2.2	6.5	1.6	1.9	0.0
<i>CNGC20</i> (At3g17700)	4.2	3.6	24.2	20.7	17.5	15.9	6.3	0.0

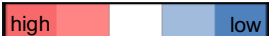
TPM  high low

Figure 34: Organ-specific expression of CNGCs in Arabidopsis.

Transcript levels per million (TPM) of *CNGC* genes in different organs are provided in numbers and as heat map (eFP-seq Browser) (Sullivan et al., 2019). The numbers are a mean of individual experiments. The RNA sequencing experiment numbers can be seen in Appendix Table 14.

We next compared gene expression specifically in guard cells in comparison to mesophyll cells using microarray data deposited in the eFP browser (Winter et al., 2007) (Figure 35). Of all 20 *CNGC* genes *CNGC1*, *CNGC5*, *CNGC6*, *CNGC15* and *CNGC20* showed elevated expression in guard cells. Compared with mesophyll cells, the expression in guard cells was at least three times higher in *CNGC5*, *CNGC6* and *CNGC20*, whereas *CNGC15* expression was almost 10 times higher. *CNGC15* was the only gene from group III with elevated transcripts in guard cells. In summary, the results revealed an overall broad distribution of *CNGC* expression in Arabidopsis. Higher expression of *CNGC1*, *CNGC5*, *CNGC6*, *CNGC15* and *CNGC20* in guard cells compared to mesophyll cells pointed to a specific function in stomata.

gene	guard cell	mesophyll cell
<i>CNGC1 (At5g53130)</i>	214.2	149.7
<i>CNGC2 (At5g15410)</i>	76.0	127.1
<i>CNGC3 (At2g46430)</i>	16.1	162.5
<i>CNGC4 (At5g54250)</i>	1.1	156.3
<i>CNGC5 (At5G57940)</i>	465.3	119.3
<i>CNGC6 (At2g23980)</i>	200.9	73.6
<i>CNGC7 (At1g15990)</i>	11.3	15.5
<i>CNGC8 (At1g19780)</i>	2.6	3.9
<i>CNGC9 (At4g30560)</i>	30.3	17.5
<i>CNGC10 (At1g01340)</i>	62.5	99.7
<i>CNGC11 (At2g46440)</i>	16.1	162.5
<i>CNGC12 (At2g46450)</i>	43.2	87.0
<i>CNGC13 (At4g01010)</i>	23.1	65.7
<i>CNGC14 (At2g24610)</i>	47.1	25.7
<i>CNGC15 (At2g28260)</i>	490.5	6.5
<i>CNGC16 (At3g48010)</i>	10.3	12.7
<i>CNGC17 (At4g30360)</i>	72.6	46.4
<i>CNGC18 (At5g14870)</i>	29.0	32.6
<i>CNGC19 (At3g17690)</i>	18.7	2.8
<i>CNGC20 (At3g17700)</i>	409.6	154.1

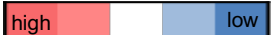
TPM  high low

Figure 35: Several *CNGC* genes are preferentially expressed in guard cells.

Transcript levels per million (TPM) of *CNGC* genes in guard cells and mesophyll cells are provided in numbers and as a heat map (eFP Browser) (Winter et al., 2007).

To independently verify group III *CNGC* expression in guard cells, *Promoter:GUS* reporter lines for group III *CNGCs* were generated. *CNGC18:GUS* lines were not generated since it was shown previously that *CNGC18* is exclusively expressed in pollen and its mutation causes male sterility (Frietsch et al., 2007). Promoter activities were analyzed in the 7th leaf of 3- to 4-week-old plants of the *GUS* reporter lines *CNGC14:GUS6*, *CNGC15:GUS9*, *CNGC16:GUS3* and *CNGC17:GUS10* (Figure 36). The promoters of *CNGC14* and *CNGC16* showed no activity in the 7th leaf (Figure 36A,C), supported by the low expression values obtained in RNAseq and microarray analysis. Low promoter activity was detected in the midvein for *CNGC17* (Figure 36D), whereas *CNGC15* was highly expressed in the midvein, trichomes and guard cells (Figure 36B,F,J).

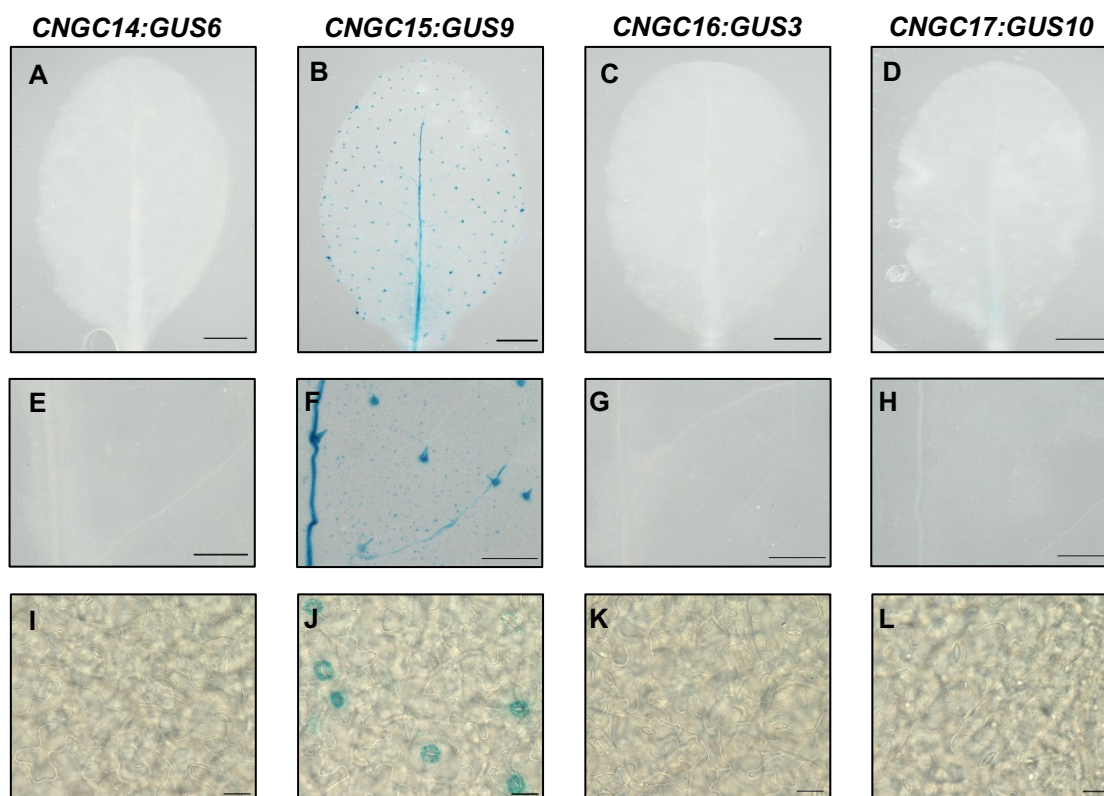


Figure 36: *CNGC15* is specifically expressed in guard cells.

Expression of *CNGC14*, *CNGC15*, *CNGC16* and *CNGC17* was analyzed in the 7th leaf of 3-4-week-old plants using GUS reporter lines indicated.

Scale bars = 5 mm (A-D), = 0.5 mm (E-H) and = 0.02 mm (I-L).

3.4.2 Knockout of *CNGCs* with the CRISPR/Cas9 technology

The expression analysis of *CNGCs* revealed that *CNGC17*, known to be part of the nanocluster with *PSKR1*, is not expressed in guard cells, whereas the closely related *CNGC15* has a specific expression in guard cells. To explore the physiological function of *CNGC15* and its potential role in *PSKR* signaling, a *cngc15* knock-out line was generated using the CRISPR/Cas9 technology. Since *CNGCs* in plants were shown to function together as heterotetramers (Pan et al., 2019), multiple gene knockouts of group III *CNGCs* were generated as well, even though *CNGC14*, *CNGC16* and *CNGC17* were expressed at low levels in guard cells.

The CRISPR/Cas9 technology was used to induce a larger deletion of several hundred base pairs in *CNGC15*. This was achieved by the use of two protospacers that bind to the *CNGC15* gene locus. Annotation analysis revealed two splicing variants of *CNGC15* (Cheng et al., 2017), both were considered while designing the protospacers. In this way, two double-strand breaks of the genomic DNA were induced, which led to a deletion of the intermediate sequence including the start codon and part of the ion transport domain (Figure 37A).

One advantage of this experimental design was that a complete gene sequence was deleted from the genome. In addition, as a result of the large deletion, we could use PCR to detect the gene mutation based on the size change of the amplified gene sequence (Figure 37B).

After stable transformation using *Agrobacteria*, the primary transformants (T1) for *cngc15* were selected by T-DNA-mediated BASTA resistance. Subsequently, from the resistant T1 plants, genomic DNA was extracted from a rosette leaf and genotyped with PCR. With the primers at the border of the deletion, a 1478 bp fragment should be amplified from the wild-type allele of *CNGC15*. Upon successful induction of both double-strand breaks, as well as the subsequent deletion of the intermediate sequence, an amplification of approximately 613 bp was expected (Figure 37B). Homozygous mutations with amplification at 613 bp as well as heterozygous mutations with amplification of two DNA sequences at 613 bp and 1478 bp could be identified. The next generations were screened for homozygous mutations, as well as for the out-crossing of the T-DNA, to avoid a still active CAS9 protein and to achieve a knock-out plant without transgene. To achieve a plant without T-DNA insertion, a PCR was performed with primers binding in the CAS9 sequence (Figure 37C).

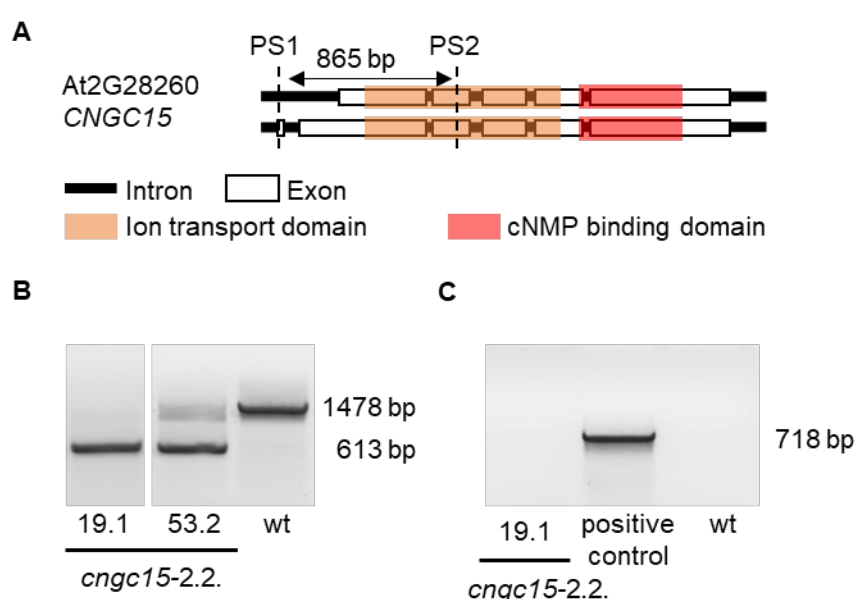


Figure 37: Selection strategy of CRISPR/Cas9-induced mutations.

A, Schematic structure of the two splicing variants of *CNGC15* with the ion transport and cNMP binding domains. The location of the protospacers (PS1, PS2) that induce an 865 bp deletion at the 5' end of the *CNGC15* gene are indicated.

B, Exemplary result of a PCR, genotyping *CNGC15* mutations induced by CRISPR/Cas9.

C, Exemplary result of a PCR, amplifying the *CAS9* sequence to select for plants without transgene. The plant samples of wild type (wt) and *cngc15-2.2.19.1* have no amplification for the *CAS9* sequence, whereas the positive control (*pDe-Cas9* vector) has an amplification at 718 bp.

4 DISCUSSION

The increasing number of signaling peptides and their receptors identified and characterized in recent years revealed diverse functions in plant growth and development, as well as in biotic and abiotic stress responses (Gancheva et al., 2019). One of these signaling peptides is PSK, which promotes plant growth through cell expansion (Kutschmar et al., 2009; Stührwohltdt et al., 2011a) and biotic stress responses (Loivamäki et al., 2010). Recent studies suggest that PSKR signaling is required during osmotic stress (Stührwohltdt et al., 2021; Reichardt et al., 2020; Rajamanickam et al., 2021) and maintains growth and delays leaf senescence under drought conditions (Rajamanickam et al., 2021). Based on the above findings, we investigated how PSKR signaling regulates the delay of senescence and thus positively affects plant survival under drought stress.

4.1 Transpiration control of leaves via stomatal closure by PSKR signaling

Leaf senescence caused by water deficit can be delayed by reducing transpiration (Rivero et al., 2007). The reduction in transpiration can occur in long-term adaptation through morphological changes, such as the reduction of leaf area and stomata numbers, or rapidly by stomatal closure (Nilson and Assmann, 2007). Specific expression of the PSK precursor *PSK4* and both PSK receptor genes (*PSKR1*, *PSKR2*) in guard cells indicated a function of PSK/PSKR signaling in guard cell regulation (3.1.1; Wu et al., 2016). Indeed, ABA-induced stomatal closure is impaired in PSKR deficient plants (3.1.4), leading to higher leaf transpiration (3.1.3). The results showed that ABA-induced stomatal closure acts in a PSK-independent and dependent manner, as the stomata were closed to some degree. Knockout of single PSKR genes or of both, *PSKR1* and *PSKR2*, impaired stomatal closure in response to ABA, suggesting that both receptors contribute to ABA-mediated stomatal closure (3.1.4). Previous findings showed that PSK-dependent root and hypocotyl growth is mainly transduced by PSKR1, whereas root and hypocotyl length is not altered in PSKR2 deficient *Arabidopsis* plants (Amano et al., 2007; Stührwohltdt et al., 2011). In immune responses to bacteria, PSKR1 was required in attenuation of *elf18*-mediated growth retardation and *elf18*-induced *Chitinase* and *FLG22-INDUCED RECEPTOR-LIKE KINASE1* expression, whereas PSKR2 was not (Igarashi et al., 2012). Interestingly, *PSKR2* expression data from the eFP-browser revealed high promoter activity in guard cells (3.1.1), but this was not verified with the *PSKR2:GUS* line available. The promoter region used may lack *cis*-elements required for guard cell-specific expression. Genome-wide expression

pattern analyses with *Promoter:GUS* lines of LRR-RLKs in Arabidopsis revealed promoter activity of *PSKR2* throughout the plant, including stomata (Wu et al., 2016), supporting a possible guard cell function for *PSKR2*. In addition to single knockout lines, overexpression lines of *PSKR1* and *PSKR2* showed rescue of ABA-induced stomatal closure indicating that both receptors are functional (3.1.4). It is conceivable that the function of *PSKR2* is specifically required at defined developmental stages or in specific stress responses. The genome-editing tool CRISPR-tissue specific knockout (CRISPR-TSKO) could help to determine organ- or tissue-specific functions of the two receptors by the knockout of *PSKR1* or *PSKR2* in a tissue-specific manner (Decaestecker et al., 2019) and the guard cell-specific promoter *GC1* would be an ideal tool to study the effect of *PSKR1* and *PSKR2* overexpressed specifically in guard cells (Yang et al., 2008).

In contrast to the promotion of cell elongation (Kutschmar et al., 2009; Stührwohltd et al., 2011a), *PSKR* signaling is required in ABA-induced stomatal closure, which is a consequence of guard cell shrinkage (Daszkowska-Golec and Szarejko, 2013), showing that *PSKR* signaling controls irreversible cell expansion during growth and reversible cell expansion of guard cells. Due to environmental stress, such as drought or pathogen infestation, plants reduce growth and activate defense responses. Notably, brassinosteroid (BR) signaling via the LRR-RLK *BRI1*, that is closely related to *PSKR*s (Planas-Riverola et al., 2019), promotes growth and regulates adaptation to environmental stress via the microbe-associated molecular pattern (MAMP)-triggered immunity by *FLS2*, ultimately leading to stomatal closure (Belkhadir et al., 2012; Shang et al., 2016; Wang, 2012). *BRI1* and *FLS2* are not in close proximity (Holzwardt et al., 2018) but share the same co-receptor, *BAK1*, which is suggested as the main mediator of both signals (Wang, 2012). The molecular mechanism for this regulation remains to be determined, but it is possible that *BAK1*, as a co-receptor of *PSKR1*, may also be a signaling coordinator. The present study showed that *PSKR* signaling is required for ABA-mediated stomatal closure. The fundamental question to be addressed is how the *PSKR* signaling pathway is integrated into ABA-induced stomatal closure and which component coordinates this crosstalk. Therefore, it is important to determine in which molecular mechanism during stomatal closure the *PSKR* pathway is integrated.

4.2 Interplay between PSKR and ROS signaling during ABA-induced stomatal closure

Signal transduction after ABA perception activates OST1 kinase in guard cells to regulate ion channels and transporters reducing the osmotic potential of the cell causing water efflux. Simultaneous, Ca^{2+} and ROS signaling is activated to maintain closure of stomata (Sierla et al., 2016). An increase in ROS levels in guard cells is induced by high carbon dioxide concentrations (Chater et al., 2015), ABA, and pathogens (Grondin et al., 2015; Rodrigues et al., 2017; Singh et al., 2017) and leads to stomatal closure. ROS are produced in the apoplast by the NADPH oxidases RBOHD and RBOHF (Torres et al., 1998, 2002; Bánfi et al., 2000; Kwak et al., 2002, 2003) and have been shown to enter guard cells by slow and limited diffusion or rapidly by the aquaporin PIP2;1, which facilitates the entry of H_2O_2 (Rodrigues et al., 2017; Bienert and Chaumont, 2014). Within guard cells, ROS promote an increase in cytosolic Ca^{2+} that activates CPKs that in turn phosphorylate the anion channel SLAC1 for anion efflux to keep the osmotic potential low (Brandt et al., 2012). CPKs also target and activate RBOHD/F for continuous ROS production that maintains stomatal closure (Pei et al., 2000; Konrad et al., 2018). Previous studies indicated that PSK/PSKR signaling is required for ROS production during cotton fiber elongation (Han et al., 2014) and pear pollen tube growth (Kou et al., 2020). This is supported by the finding that PSKR1 and RBOHD were identified in a co-immunoprecipitation (AG Sauter, personal communication), which prompted us to analyze the link between PSKR signaling and ROS production during stomatal closure. The results showed that ABA-induced ROS elevation in guard cells was impaired in *pskr1-3 pskr2-1* (3.2.2), suggesting that PSKRs are required for ABA-induced ROS accumulation during stomatal closure. Treatment of *pskr1-3 pskr2-1* guard cells with H_2O_2 affirmed this assumption when stomatal closure was fully restored in response to ABA (3.2.2).

ROS accumulation during stomatal closure is controlled by several other proteins, such as OST1, BIK1 and CPKs, and signaling cascades via FLS2 and BRI1 (Kimura et al., 2017; Acharya et al., 2013). Why the PSKR signaling pathway in particular is required for ROS accumulation during ABA-mediated stomatal closure, remains to be determined. The advantage of an LRR-RLK signaling pathway is that the binding of a ligand can induce the formation of a multiprotein complex with co-receptors or cytoplasmic kinases that trigger signal transduction and activate further cellular responses, such as ROS production. Moreover, binding of a ligand may provide specificity for organ, tissue and cell-dependent ROS signaling. Full biological activity of PSK is obtained by sulfation of the two tyrosine residues (Kutschmar et al., 2009; Wang et al., 2015b) catalyzed by TPST, that is encoded by a single gene in Arabidopsis (Komori et al., 2009). ABA-induced stomatal closure was

impaired in *tpst-1* but the application of PSK was sufficient to rescue stomatal closure in response to ABA in *TPST* deficient plants (3.1.5) suggesting that the binding of PSK is required to promote ABA-induced stomatal closure.

Many LRR-RLKs are functionally linked to ROS elevation in stomata during immune responses, such as FLS2, EF-Tu receptor (EFR), PEP receptor 1 and 2 (PEPR1/2) and BRI1, mainly via the receptor-like cytoplasmic kinase (RLCK) BIK1 (Kimura et al., 2017). Stomata are not only required for gas exchange and regulation of water transpiration, but they are also the gateways for pathogens, and therefore stomatal closure is an efficient response to prevent pathogen invasion. Many pathogens enter plants through wounds or stomata, which requires rapid control of stomata (Tucker and Talbot, 2001; Ye et al., 2020; Melotto et al., 2017). ROS elevation is needed for the rapid closure of stomata (Zhang et al., 2018c; Li et al., 2014). The secreted peptide PIP1, an elicitor for immune responses, triggers stomatal closure by activating anion channels and promoting the increase of ROS and Ca^{2+} by OST1 in the cytosol (Shen et al., 2020). A requirement for PSKRs for the ROS burst in stomata suggests that PSKRs may contribute to biotic stress resistance through their control of stoma closure. Knockout of PSKR1 induced high susceptibility to *Alternaria brassicicola*, and application of PSK on tomato leaves helped the plant reduce susceptibility to *Botrytis cinerea* (Mosher et al., 2013; Zhang et al., 2018b), pointing to a role of PSK signaling in resistance against necrotrophic pathogens. It is conceivable that PSKR signaling mediates pathogen-induced stomatal closure.

To determine the role of PSKR signaling for ROS accumulation in ABA-induced stomatal closure, it is first necessary to understand in which regulatory process the signaling pathway is involved to increase the ROS content in the cell. In the remaining part we discuss the results on possible regulatory mechanisms that PSKR signaling controls to induce an accumulation of ROS in the guard cells during ABA-induced stomatal closure. Figure 38 shows a model of PSKR-dependent ABA-induced stomatal closure. One possible regulatory mechanism could be an activating phosphorylation of RBOH by PSKR1 kinase or regulation of PIP2;1 to facilitate entry of H_2O_2 into guard cells. Another mechanism could be that PSKR1 together with CNGCs increase Ca^{2+} in the cell which then activates RBOHs.

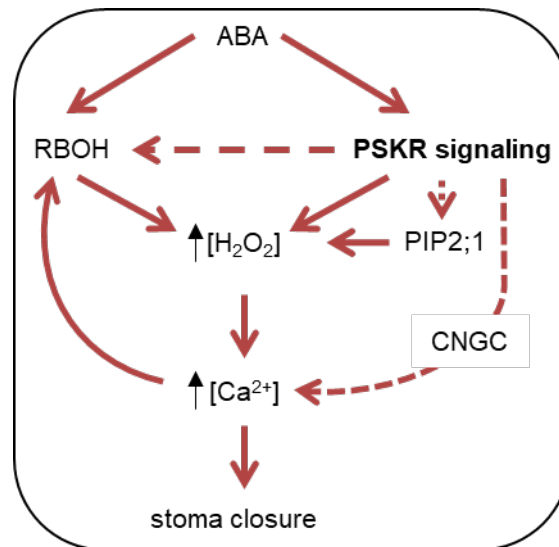


Figure 38: Model of PSKR-dependent ABA-induced stomatal closure.

ABA signaling activates RBOHs that generate ROS in the apoplast. PIP2;1 facilitates the entry of H_2O_2 into the cell, resulting in an H_2O_2 burst. Increasing H_2O_2 levels in the guard cell leads to activation of channels that increase Ca^{2+} levels in guard cells, which in turn leads to stoma closure. PSKR signaling is required to promote H_2O_2 elevation. The dashed arrows indicate three pathways by which PSKR might act in guard cells. First, activating phosphorylation of RBOH to produce ROS; second, control of PIP2;1 to facilitate entry of H_2O_2 into the cell; and third, regulation of CNGCs to facilitate entry of Ca^{2+} that activates RBOHs.

4.2.1 Regulation of RBOH by PSKR kinase *in vitro*

ROS are generated in multiple organelles of the cell, such as chloroplasts, mitochondria and peroxisomes during photorespiration and other metabolic processes (Noctor and Foyer, 2016; Janku et al., 2019). Biotic and abiotic stress responses mainly utilize extracellular produced ROS from plasma membrane-bound NADPH oxidases (Kimura et al., 2017). The NADPH oxidase RBOHF is the major isoform contributing to ABA-mediated signaling whereas RBOHD mainly contributes to pathogen defense but also to ABA-induced stomatal closure (Kwak et al., 2003; Qi et al., 2017). RBOHD and RBOHF are activated by phosphorylation of their N- and C-termini and Ca^{2+} -binding to helix-loop-helix structural domains called EF-hands (Oda et al., 2010).

PSKR and RBOHD or RBOHF could directly interact at the plasma membrane as suggested by co-immunoprecipitation of PSKR1 and RBOHD from Arabidopsis leaves (AG Sauter, personal communication). Previous research on RBOHD showed that the N- and C-termini of RBOHD are in the cytosol, harboring EF-hands at its N-terminus and FAD and NADPH binding sites at the C-terminus (Kimura et al., 2020). The C-terminus is required for the synthesis of superoxide anions in the apoplast, whereas the N-terminus may have regulatory functions since it is multiply phosphorylated by various protein kinases (Chen et al., 2017; Zhang et al., 2018d; Kimura et al., 2020; Kadota et al., 2014; Dubiella et al., 2013). Interestingly also the C-terminus of RBOHD was recently shown to

be phosphorylated (Kimura et al., 2020). As described above, phosphorylation of RBOHD during stomatal closure has so far been studied only in the context of an immune response. The kinase domain of PSKR1 shows auto- and transphosphorylation activity (Hartmann et al., 2014) and phosphorylates its co-receptor BAK1 and the proton pump AHA1 *in vitro* (Kaufmann, 2018). FRET-AB analysis demonstrated that PSKR1 and RBOHD/F are in proximity (3.2.4) and *in vitro* analysis showed transphosphorylation by the PSKR1 kinase (3.2.5). RBOHF is phosphorylated by CIPK26 and OST1 at its N-terminus, but the physiological role of the phosphorylation remains to be characterized (Sirichandra et al., 2009). This study showed that the region of the FAD binding domain (RBOHF-Loop2) was phosphorylated *in vitro* by the PSKR1 kinase (3.2.5), whereas the NADPH binding domain of RBOHF (RBOHF-Cterm) was not. Phosphorylation in the FAD binding domain was previously shown for RBOHD *in vitro* (Kimura et al., 2020). The phosphorylation sites S611 and S703 were identified and both sites are conserved in RBOHF (S622, S714), suggesting that these residues may have regulatory function. It was also shown that S862 of RBOHD, located in the NADPH binding domain, is phosphorylated (Kimura et al., 2020). However, this site is not conserved in RBOHF, matching to our finding that RBOHF-Cterm, harboring the NADPH domain, is not phosphorylated. This result provides evidence that ROS production at the plasma membrane is regulated by PSKR. Mass-spectrometry (MS) analysis will identify the specific phosphorylation sites of RBOHD and RBOHF by PSKR1 kinase. Once the sites of RBOHD and RBOHF that are phosphorylated by PSKR1 are identified, the functional relevance of these sites in guard cells can be studied in plants expressing point-mutated RBOH isoforms. Whether or not RBOHD/F is the target of different signaling pathways remains to be determined.

4.2.2 The aquaporin PIP2;1 as part of the PSKR signaling complex

Plant growth relies on cell division and cell expansion and is regulated by environmental changes. Cell expansion is the result of osmotically driven water influx and cell wall yielding. In contrast to cell expansion, stomatal closure requires rapid water movement out of guard cells (Cosgrove, 2014; Dünser and Kleine-Vehn, 2015). Diffusion of water across the cell membrane is facilitated by aquaporins, which are classified in two groups, tonoplast intrinsic proteins (TIPs) and PLASMA MEMBRANE INTRINSIC PROTEINS (PIPs), with PIPs as the larger subfamily divided into two subgroups, PIP1 (5 members) and PIP2 (8 members) in Arabidopsis (Chaumont et al., 2001; Johanson et al., 2001). All PIP2 proteins were shown to have high water channel activity tested in heterologous systems, whereas it was lower for PIP1 (Chaumont et al., 2001; Yaneff et al., 2015; Groszmann et al., 2021).

Aquaporins are hypothesized to contribute to cell elongation by allowing water to cross the plasma membrane (Maurel et al., 2008). PSKR signaling is known to promote cell expansion (Kutschmar et al., 2009; Stührwohldt et al., 2011) making it conceivable that the nanocluster complex of PSKR1 harbors an aquaporin that facilitates water movement across the plasma membrane. In this study, we showed that the aquaporin PIP2;1 contributes to PSK-dependent root elongation and expansion of protoplasts from hypocotyl (3.3.1). In rose, *RhPIP2;1* was found to be required in petal cell expansion (Ma et al., 2008) and a requirement in lateral root emergence was reported for Arabidopsis (Péret et al., 2012). It cannot be excluded that PIP2;1 exclusively is required for rapid cell growth but PIP proteins are widely expressed throughout the plant and *PIP2;1*, *PIP2;2* and *PIP2;7* are highly expressed in both root and shoot of Arabidopsis (Jang et al., 2004; Alexandersson et al., 2005; Monneuse et al., 2011) suggesting additional functions.

Both growth by cell expansion and stomatal control of photosynthetic gas exchange require maintenance of turgor pressure, which depends on water status regulated by the water stress-induced phytohormone ABA. ABA-treated guard cell protoplasts require PIP2;1 for water transport and associated ABA-induced stomatal closure to reduce leaf transpiration (Grondin et al., 2015; Rodrigues et al., 2017; 3.3.3). In addition to its water channel activity, PIPs also facilitate entry of H₂O₂ into the cell (Bienert and Chaumont, 2014). Specifically, PIP2;1 is required for the entry of H₂O₂ in ABA-induced stomatal closure (Rodrigues et al., 2017). This together with the finding that PSKR signaling is required for ROS elevation in ABA-induced stomatal closure and PIP2;1 contributes in PSK-dependent growth, let us hypothesize that PIP2;1 is a target of PSKR. PIP2;1 facilitate water and H₂O₂ movement and could contribute either to PSKR-dependent cell growth or reversible volume change of guard cells. *PIP2;1* transcript level was independent of PSKR (3.3.2), which make it conceivable that regulation of PIP2;1 by PSKR occurs at the protein level. Response of plants to environmental and hormonal stimuli is mediated by transcriptional and post-translational regulation of aquaporin function, specifically, phosphorylation is a requirement in stress responses (Péret et al., 2012; Grondin et al., 2015). As mentioned above, the PSKR1 kinase domain has a transphosphorylation activity (Hartmann et al., 2014), which was shown to phosphorylate co-receptor BAK1 and proton pump AHA1 *in vitro* (Kaufmann, 2018). In this study, we could show that PSKR1 kinase transphosphorylates the cytosolic domains of PIP2;1 *in vitro* (3.3.4). Mass spectrometry analyses will identify the specific phosphorylation sites, which could be analyzed for their functional relevance in ROS-dependent stomatal closure. Phosphorylation of PIP2;1 was shown to have a major impact on the functionality of the protein. Phosphorylation of S121 in loop 1 is necessary and sufficient for ABA-dependent stomatal closure in Arabidopsis (Grondin et al., 2015). In contrast, the C-terminal phosphorylation of PIP2;1 at S280 and

S283 (Prak et al., 2008; Kline et al., 2010; Prado et al., 2013) contributes to the closure of the aquaporin, whereas dephosphorylation of S115 (conserved site S121 in Arabidopsis) and S274 (conserved site S280 in Arabidopsis) in spinach destabilized the protein conformation and closed the water channel (Törnroth-Horsefield et al., 2006). We observed that S280 and S283 are not required for ABA-mediated stomatal closure (3.3.3), indicating that other posttranslational modifications may be required for PIP2;1 regulation by PSKR in ABA-induced stomatal closure. Interestingly, ABA reduces phosphorylation of PIP2;1 (Kline et al., 2010), decreasing water flux and maintained seeds in a dormant state. In contrast to that, osmotic stress induced phosphorylation of PIP2;6 (Niittylä et al., 2007). Specific phosphorylation events in different tissues and organs suggest specific regulation by different stimuli at distinct phosphorylation sites of PIP2;1. Guard cell- and growth-specific regulation of PIP2;1 by PSKR could provide a way to integrate growth and drought stress signals.

4.2.3 PSKR could increase cellular Ca^{2+} by activating CNGCs in guard cells

Calcium acts as a second messenger in the regulation of plant development and growth as well as abiotic and biotic stress responses. Cellular concentrations of Ca^{2+} change in response to drought, salt, temperature, light and plant hormones, inducing specific responses (Sanders et al., 1999). Ca^{2+} accumulation in guard cells is induced by ABA, ROS and CO_2 (Murata et al., 2001; Young et al., 2006) and regulates the closure of stomata (Hubbard et al., 2012; Brandt et al., 2015). The elevation of cytosolic Ca^{2+} is either achieved by yet unknown Ca^{2+} -permeable cation channels localized at the plasma membrane or through release from intracellular Ca^{2+} stores (Kim et al., 2010). Increased Ca^{2+} levels in the cell leads to the binding of Ca^{2+} to the Ca^{2+} -activation domain of CPKs (Bender et al., 2018) and triggers crucial phosphorylation of the anion channel SLAC1 and the NADPH oxidase RBOHD during stomatal closure (Geiger et al., 2009; Dubiella et al., 2013). The major S-type anion channel SLAC1 is activated either through OST1 (Geiger et al., 2009) or through CPK5, CPK6, CPK21 and CPK23 (Geiger et al., 2010; Brandt et al., 2012) driving the depolarization of the plasma membrane. CPK4-6 and CPK11 were shown to phosphorylate and activate RBOHD resulting in ROS production (Dubiella et al., 2013; Sierla et al., 2016) and binding of Ca^{2+} to EF-hands at the N-terminus of OsRBOHB is of higher importance for its activity in rice (Oda et al., 2010), indicating the importance of Ca^{2+} for the activation of ROS production.

The CNGC protein family in Arabidopsis includes 20 members, known to mediate cation influx (Talke et al., 2003), with CNGC2, CNGC4-5, CNGC7-10, CNGC12, CNGC14, CNGC16 and CNGC18-20 facilitating the entry of Ca^{2+} into the cell (Tian et al., 2019a; Wang

et al., 2017; Zhang et al., 2017, 2019; Wang et al., 2013; Zeb et al., 2020; Gu et al., 2016; Pan et al., 2019; Yu et al., 2019). Transcriptome analyses reveal a specific expression of *CNGC1*, *CNGC5*, *CNGC6*, *CNGC15* and *CNGC20* in Arabidopsis guard cells (3.4.1). The cation channels *CNGC5* and *CNGC6* were identified as cGMP-activated nonselective Ca^{2+} -permeable cation channels, but mutations of both did not impair Ca^{2+} channel activity in guard cells (Wang et al., 2013). *CNGC20* was identified as a Ca^{2+} -permeable channel but its function in Arabidopsis guard cells remain unclear (Yu et al., 2019). *CNGC15* belongs to group III with *CNGC14*, *CNGC16*, *CNGC17* and *CNGC18* (Talke et al., 2003). The physiological function and ion specificity of *CNGC15* remain to be determined. Specific expression of individual CNGCs in guard cells provides evidence that they may have a function in stomatal closure, which need to be concluded in further studies.

PSKR signaling is required for ABA-mediated stomatal closure by elevating ROS levels in guard cells (3.2.2). We have discussed the hypothesis that regulation of ROS level via PSKRs is controlled through direct interaction with the NADPH oxidases RBOHD/F or with PIP2;1 that imports H_2O_2 from the apoplast into the guard cell. Based on the knowledge that PSKR1 is part of a nanocluster complex together with *CNGC17* (Ladwig et al., 2015), it is also conceivable that PSKR1 controls Ca^{2+} influx via CNGCs to promote Ca^{2+} -dependent RBOH activity, whereas the ion specificity of *CNGC17* is not known yet. CNGCs are known to harbor a CaM and cNMP binding domain at the C-terminus (Arazi et al., 2000; Hua et al., 2003). PSKR1 harbors an GC-domain in the cytosol which possibly contributes to the PSK-induced protoplast expansion via the second messenger cGMP to target *CNGC17* (Ladwig et al., 2015). The role of cNMPs in CNGC regulation is discussed and not clear yet (Dietrich et al., 2020), but a cNMP binding site is present in several CNGCs (Zhou et al., 2014; Gao et al., 2016). In the last years, it has become clear that regulation of CNGCs does not occur only through CaM and cNMP binding. It was hypothesized that CPKs regulate CNGCs (Zhou et al., 2014; Dietrich et al., 2020). Phosphorylation of *CNGC4* occurs following MAMP/PAMP recognition is required to induce immune responses (Tian et al., 2019b). The possibility of CNGC regulation through phosphorylation by PSKR1 seems low since both proteins are not in close proximity and not physically interacting (Ladwig et al., 2015). But BAK1, the co-receptor of PSKR1, could be a signal transducer that physically interacts with *CNGC17* (Ladwig et al., 2015). Recent studies indicated that BAK1 phosphorylates the cytosolic domain of *CNGC19* and *CNGC20*, increasing the protein stability of the heteromer which positively regulates cell death, whereas the regulatory mechanism remains to be determined (Yu et al., 2019). Thus, BAK1 could act as signal mediator in the PSKR/BAK1 complex, as discussed in Chapter 4.1. Due to the importance of changes in Ca^{2+} level during stomatal closure and its regulatory effect

on ROS production, regulation of CNGCs by the PSKR signaling pathway should be considered and further investigated.

In future, guard cell-specific functions of CNGCs can be determined using CRISPR-TSKO to investigate their requirement for ABA-mediated stomatal closure in a tissue-specific manner (Decaestecker et al., 2019). The guard cell-specific promoter *GC1* would help to solve this question by specific overexpression of associated CNGCs in guard cells (Yang et al., 2008). To link the Ca^{2+} increase in guard cells during stomatal closure to PSKR signaling, it should be analyzed if Ca^{2+} -accumulation in guard cells is impaired in *pskr1-3 pskr2-1* by using live cell imaging with a calcium sensor, such as *R-GECO1-mTurquoise* (Waadt et al., 2017). These approaches could be used in future to address the question of whether CNGCs are required for the Ca^{2+} elevation in guard cells and whether PSKRs control this mechanism to activate ROS production at the plasma membrane.

4.3 Conclusion

This study showed that PSKR signaling plays a role in ABA-induced stomatal closure, representing another signaling pathway that needs to be integrated into the network of signals controlling stomatal closure. The enhanced leaf senescence during water deficit in PSKR-deficient plants may be caused by increased transpiration due to impaired stomatal closure. The challenge now is to understand how the PSKR pathway is integrated into the complex signaling network of stomatal closure and how the different signaling pathways are coordinated to trigger an integrated response. We showed that PSKR signaling is required in ABA-dependent ROS accumulation in guard cells leading to stomatal closure. In determining the role of PSKR signaling for ROS accumulation, we identified RBOHD/F and PIP2;1 as novel targets of the PSKR1 kinase. The phosphorylation of RBOHD/F and/or PIP2;1 by PSKR1 could stimulate ROS production at the plasma membrane and facilitate the entry of H_2O_2 into guard cells. Whether or not RBOHD/F and/or PIP2;1 integrate different signaling pathways to induce stomatal closure in response to abiotic and biotic stress remains to be determined. We also provide expression analyses of CNGCs and novel mutant lines as tools for future analyses to determine whether CNGCs are required for Ca^{2+} signaling during stomatal closure. Overall, understanding the interplay of different signaling pathways is becoming increasingly important to understand the integrated regulation of stress responses (Nemhauser et al., 2006; Gui et al., 2016; Wang, 2012).

5 LIST OF REFERENCES

- Acharya, B.R., Jeon, B.W., Zhang, W., and Assmann, S.M.** (2013). Open Stomata 1 (OST1) is limiting in abscisic acid responses of Arabidopsis guard cells. *New Phytol.* **200**: 1049–1063.
- Alexandersson, E., Frayse, L., Sjövall-Larsen, S., Gustavsson, S., Fellert, M., Karlsson, M., Johanson, U., and Kjellbom, P.** (2005). Whole gene family expression and drought stress regulation of aquaporins. *Plant Mol. Biol.* **59**: 469–484.
- Amano, Y., Tsubouchi, H., Shinohara, H., Ogawa, M., and Matsubayashi, Y.** (2007). Tyrosine-sulfated glycopeptide involved in cellular proliferation and expansion in Arabidopsis. *Proc. Natl. Acad. Sci.* **104**: 18333–18338.
- Arazi, T., Kaplan, B., and Fromm, H.** (2000). A high-affinity calmodulin-binding site in a tobacco plasma-membrane channel protein coincides with a characteristic element of cyclic nucleotide-binding domains. *Plant Mol. Biol.* **42**: 591–601.
- Bánfi, B., Maturana, A., Jaconi, S., Arnaudeau, S., Laforge, T., Sinha, B., Erzsébet, L., Demaurex, N., and Krause, K.-H.** (2000). A Mammalian H⁺ Channel Generated Through Alternative Splicing of the NADPH Oxidase Homolog NOH-1. *Science* (80-.). **287**: 138–142.
- Bauer, H. et al.** (2013). The stomatal response to reduced relative humidity requires guard cell-autonomous ABA synthesis. *Curr. Biol.* **23**: 53–57.
- Belkhadir, Y., Jaillais, Y., Eppe, P., Balsemão-Pires, E., Dangl, J.L., and Chory, J.** (2012). Brassinosteroids modulate the efficiency of plant immune responses to microbe-associated molecular patterns. *Proc. Natl. Acad. Sci. U. S. A.* **109**: 297–302.
- Bender, K.W., Zielinski, R.E., and Huber, S.C.** (2018). Revisiting paradigms of Ca²⁺ signaling protein kinase regulation in plants. *Biochem. J.* **475**: 207–223.
- Bienert, G.P. and Chaumont, F.** (2014). Aquaporin-facilitated transmembrane diffusion of hydrogen peroxide. *Biochim. Biophys. Acta - Gen. Subj.* **1840**: 1596–1604.
- Bittner, F., Oreb, M., and Mendel, R.R.** (2001). ABA3 Is a Molybdenum Cofactor Sulfurase Required for Activation of Aldehyde Oxidase and Xanthine Dehydrogenase in Arabidopsis thaliana. *J. Biol. Chem.* **276**: 40381–40384.
- Brandt, B., Brodsky, D.E., Xue, S., Negi, J., Iba, K., Kangasjärvi, J., Ghassemian, M., Stephan, A.B., Hu, H., and Schroeder, J.I.** (2012). Reconstitution of abscisic acid activation of SLAC1 anion channel by CPK6 and OST1 kinases and branched ABI1 PP2C phosphatase action. *Proc. Natl. Acad. Sci. U. S. A.* **109**: 10593–10598.

- Brandt, B., Munemasa, S., Wang, C., Nguyen, D., Yong, T., Yang, P.G., Poretsky, E., Belknap, T.F., Waadt, R., Alemañ, F., and Schroeder, J.I.** (2015). Calcium specificity signaling mechanisms in abscisic acid signal transduction in arabidopsis guard cells. *Elife* **4**: 1–25.
- Caesar, K., Elgass, K., Chen, Z., Huppenberger, P., Witthöft, J., Schleifenbaum, F., Blatt, M.R., Oecking, C., and Harter, K.** (2011). A fast brassinolide-regulated response pathway in the plasma membrane of *Arabidopsis thaliana*. *Plant J.* **66**: 528–540.
- Cardoso, A.A., Gori, A., Da-Silva, C.J., and Brunetti, C.** (2020). Abscisic acid biosynthesis and signaling in plants: Key targets to improve water use efficiency and drought tolerance. *Appl. Sci.* **10**: 1–15.
- Ceciliato, P.H.O., Zhang, J., Liu, Q., Shen, X., Hu, H., Liu, C., Schäffner, A.R., and Schroeder, J.I.** (2019). Intact leaf gas exchange provides a robust method for measuring the kinetics of stomatal conductance responses to abscisic acid and other small molecules in *Arabidopsis* and grasses. *Plant Methods* **15**: 1–10.
- Chater, C. et al.** (2015). Elevated CO₂-Induced Responses in Stomata Require ABA and ABA Signaling. *Curr. Biol.* **25**: 2709–2716.
- Chaumont, F., Barrieu, F., Wojcik, E., Chrispeels, M.J., and Jung, R.** (2001). Aquaporins constitute a large and highly divergent protein family in maize. *Plant Physiol.* **125**: 1206–1215.
- Chen, D., Cao, Y., Li, H., Kim, D., Ahsan, N., Thelen, J., and Stacey, G.** (2017). Extracellular ATP elicits DORN1-mediated RBOHD phosphorylation to regulate stomatal aperture. *Nat. Commun.* **8**: 1–13.
- Chen, Y., Matsubayashi, Y., and Sakagami, Y.** (2000). Peptide growth factor phytosulfokine-a contributes to the pollen population effect. *Plant Mol. Biol.* **211**: 752–755.
- Chen, Y.L., Fan, K.T., Hung, S.C., and Chen, Y.R.** (2020). The role of peptides cleaved from protein precursors in eliciting plant stress reactions. *New Phytol.* **225**: 2267–2282.
- Cheng, C.Y., Krishnakumar, V., Chan, A.P., Thibaud-Nissen, F., Schobel, S., and Town, C.D.** (2017). Araport11: a complete reannotation of the *Arabidopsis thaliana* reference genome. *Plant J.* **89**: 789–804.
- Chien, P.S., Nam, H.G., and Chen, Y.R.** (2015). A salt-regulated peptide derived from the CAP superfamily protein negatively regulates salt-stress tolerance in *Arabidopsis*. *J. Exp. Bot.* **66**: 5301–5313.

- Chinchilla, D., Bauer, Z., Regenass, M., Boller, T., and Felix, G.** (2006). The Arabidopsis receptor kinase FLS2 binds flg22 and determines the specificity of flagellin perception. *Plant Cell* **18**: 465–476.
- Chinchilla, D., Shan, L., He, P., de Vries, S., and Kemmerling, B.** (2009). One for all: the receptor-associated kinase BAK1. *Trends Plant Sci.* **14**: 535–541.
- Clough, S.J. and Bent, A.F.** (1998). Floral dip: A simplified method for *Agrobacterium*-mediated transformation of *Arabidopsis thaliana*. *Plant J.* **16**: 735–743.
- Cosgrove, D.J.** (2014). *Plant Cell Growth and Elongation*. eLS: 1–12.
- Daszkowska-Golec, A. and Szarejko, I.** (2013). Open or close the gate – stomata action under the control of phytohormones in drought stress conditions. *Front. Plant Sci.* **4**: 1–16.
- Davies, W.J., Kudoyarova, G., and Hartung, W.** (2005). Long-distance ABA signaling and its relation to other signaling pathways in the detection of soil drying and the mediation of the plant's response to drought. *J. Plant Growth Regul.* **24**: 285–295.
- Decaestecker, W., Buono, R.A., Pfeiffer, M.L., Vangheluwe, N., Jourquin, J., Karimi, M., van Isterdael, G., Beeckman, T., Nowack, M.K., and Jacobs, T.B.** (2019). CRISPR-Tsko: A technique for efficient mutagenesis in specific cell types, tissues, or organs in *Arabidopsis*. *Plant Cell* **31**: 2868–2887.
- DeFalco, T.A., Marshall, C.B., Munro, K., Kang, H.G., Moeder, W., Ikura, M., Snedden, W.A., and Yoshioka, K.** (2016). Multiple calmodulin-binding sites positively and negatively regulate arabidopsis CYCLIC NUCLEOTIDE-GATED CHANNEL12. *Plant Cell* **28**: 1738–1751.
- Dietrich, P., Moeder, W., and Yoshioka, K.** (2020). Plant cyclic nucleotide-gated channels: New insights on their functions and regulation1. *Plant Physiol.* **184**: 27–38.
- Drerup, M.M., Schluecking, K., Hashimoto, K., and Manishankar, P.** (2013). The Calcineurin B-Like Calcium Sensors CBL1 and CBL9 Together with Their Interacting Protein Kinase CIPK26 Regulate the Arabidopsis NADPH Oxidase RBOHF. *Mol. Plant* **6**: 559–569.
- Dubiella, U., Seybold, H., Durian, G., Komander, E., Lassig, R., Witte, C.P., Schulze, W.X., and Romeis, T.** (2013). Calcium-dependent protein kinase/NADPH oxidase activation circuit is required for rapid defense signal propagation. *Proc. Natl. Acad. Sci. U. S. A.* **110**: 8744–8749.
- Dünser, K. and Kleine-Vehn, J.** (2015). Differential growth regulation in plants-the acid growth balloon theory. *Curr. Opin. Plant Biol.* **28**: 55–59.

- Eisele, J.F., Fäßler, F., Bürgel, P.F., and Chaban, C.** (2016). A rapid and simple method for microscopy-based stomata analyses. *PLoS One* **11**: 1–13.
- Faroux, M.** (2021). The aquaporin PIP2 ; 1 as a potential interaction partner of PSKR1.
- Finkelstein, R.** (2013). Absciscic Acid Synthesis and Response. *Arab. B.* **11**: 1–36.
- Fischer, C., Kugler, A., Hoth, S., and Dietrich, P.** (2013). An IQ domain mediates the interaction with calmodulin in a plant cyclic nucleotide-gated channel. *Plant Cell Physiol.* **54**: 573–584.
- Foxx, A.J. and Fort, F.** (2019). Root and shoot competition lead to contrasting competitive outcomes under water stress: A systematic review and meta-analysis. *PLoS One* **14**: 1–17.
- Foyer, C.H. and Harbinson, J.** (1994). Oxygen Metabolism and the Regulation of Photosynthetic Electron Transport. In *Causes of Photooxidative Stress and Amelioration of Denfense Systems in Plants*, pp. 1–42.
- Frietsch, S., Wang, Y.-F., Sladek, C., Poulsen, L.R., Romanowsky, S.M., Schroeder, J.I., and Harper, J.F.** (2007). A cyclic nucleotide-gated channel is essential for polarized tip growth of pollen. *PNAS* **104**: 14531–14536.
- Fuglsang, A.T., Kristensen, A., Cuin, T.A., Schulze, W.X., Persson, J., Thuesen, K.H., Ytting, C.K., Oehlenschläger, C.B., Mahmood, K., Sondergaard, T.E., Shabala, S., and Palmgren, M.G.** (2014). Receptor kinase-mediated control of primary active proton pumping at the plasma membrane. *Plant J.* **80**: 951–964.
- Gancheva, M.S., Malovichko, Y. V., Poliushkevich, L.O., Dodueva, I.E., and Lutova, L.A.** (2019). Plant Peptide Hormones. *Russ. J. Plant Physiol.* **66**: 171–189.
- Gao, Q.F., Gu, L.L., Wang, H.Q., Fei, C.F., Fang, X., Hussain, J., Sun, S.J., Dong, J.Y., Liu, H., and Wang, Y.F.** (2016). Cyclic nucleotide-gated channel 18 is an essential Ca²⁺ channel in pollen tube tips for pollen tube guidance to ovules in Arabidopsis. *Proc. Natl. Acad. Sci. U. S. A.* **113**: 3096–3101.
- Geiger, D., Scherzer, S., Mumm, P., Marten, I., Ache, P., Matschi, S., Liese, A., Wellmann, C., Al-Rasheid, K.A.S., Grill, E., Romeis, T., and Hedrich, R.** (2010). Guard cell anion channel SLAC1 is regulated by CDPK protein kinases with distinct Ca²⁺ affinities. *Proc. Natl. Acad. Sci. U. S. A.* **107**: 8023–8028.
- Geiger, D., Scherzer, S., Mumm, P., Stange, A., Marten, I., Bauer, H., Ache, P., Matschi, S., Liese, A., Al-Rasheid, K.A.S., Romeis, T., and Hedrich, R.** (2009). Activity of guard cell anion channel SLAC1 is controlled by drought-stress signaling kinase-phosphatase pair. *Proc. Natl. Acad. Sci. U. S. A.* **106**: 21425–21430.

- Ghorbani, S.** (2014). Signaling Peptides in Plants. *Cell Dev. Biol.* **03**: 98–101.
- Grondin, A., Rodrigues, O., Verdoucq, L., Merlot, S., Leonhardt, N., and Maurel, C.** (2015). Aquaporins Contribute to ABA-Triggered Stomatal Closure through OST1-Mediated Phosphorylation. *Plant Cell* **27**: 1945–1954.
- Groszmann, M., Rosa, A. De, Chen, W., Qiu, J., and Mcgaughey, S.A.** (2021). Permeability profiling of all 13 Arabidopsis PIP aquaporin s using a high throughput yeast approach. *bioRxiv* doi:<https://doi.org/10.1101/2021.05.09.443061>
- Gu, L., Gao, Q., and Wang, Y.** (2016). Cyclic nucleotide-gated channel 18 is essential for pollen germination and pollen tube growth in. **2324**: 17–19.
- Gui, J., Zheng, S., Liu, C., Shen, J., Li, J., and Li, L.** (2016). OsREM4.1 Interacts with OsSERK1 to Coordinate the Interlinking between Absciscic Acid and Brassinosteroid Signaling in Rice. *Dev. Cell* **38**: 201–213.
- Hager, A.** (2003). Role of the plasma membrane H⁺-ATPase in auxin-induced elongation growth: Historical and new aspects. *J. Plant Res.* **116**: 483–505.
- Han, J., Tan, J., Tu, L., and Zhang, X.** (2014). A peptide hormone gene, GhPSK promotes fibre elongation and contributes to longer and finer cotton fibre. *Plant Biotechnol. J.* **12**: 861–871.
- Hartmann, J., Fischer, C., Dietrich, P., and Sauter, M.** (2014). Kinase activity and calmodulin binding are essential for growth signaling by the phytosulfokine receptor PSKR1. *Plant J.* **78**: 192–202.
- Hartmann, J., Stührwohldt, N., Dahlke, R.I., and Sauter, M.** (2013). Phytosulfokine control of growth occurs in the epidermis, is likely to be non-cell autonomous and is dependent on brassinosteroids. *Plant J.* **73**: 579–590.
- Haruta, M., Burch, H.L., Nelson, R.B., Barrett-Wilt, G., Kline, K.G., Mohsin, S.B., Young, J.C., Otegui, M.S., and Sussman, M.R.** (2010). Molecular characterization of mutant Arabidopsis plants with reduced plasma membrane proton pump activity. *J. Biol. Chem.* **285**: 17918–17929.
- Holzwardt, E., Huerta, A.I., Glöckner, N., Garnelo Gómez, B., Wanke, F., Augustin, S., Askani, J.C., Schürholz, A.-K., Harter, K., and Wolf, S.** (2018). BRI1 controls vascular cell fate in the Arabidopsis root through RLP44 and phytosulfokine signaling. *Proc. Natl. Acad. Sci.* **115**: 11838–11843.
- Hosy, E. et al.** (2003). The Arabidopsis outward K⁺ channel GORK is involved in regulation of stomatal movements and plant transpiration. *Proc. Natl. Acad. Sci. U. S. A.* **100**: 5549–5554.

- Hou, S., Wang, X., Chen, D., Yang, X., Wang, M., Turrà, D., Di Pietro, A., and Zhang, W. (2014). The Secreted Peptide PIP1 Amplifies Immunity through Receptor-Like Kinase 7. *PLoS Pathog.* **10**: 1–15.
- Hua, B.G., Mercier, R.W., Zielinski, R.E., and Berkowitz, G.A. (2003). Functional interaction of calmodulin with a plant cyclic nucleotide gated cation channel. *Plant Physiol. Biochem.* **41**: 945–954.
- Hua, D., Wang, C., He, J., Liao, H., Duan, Y., Zhu, Z., Guo, Y., Chen, Z., and Gong, Z. (2012). A Plasma Membrane Receptor Kinase, GHR1, Mediates Absciscic Acid- and Hydrogen Peroxide-Regulated Stomatal Movement in *Arabidopsis*. *Plant Cell* **24**: 2546–2561.
- Huang, S., Waadt, R., Nuhkat, M., Kollist, H., Hedrich, R., and Roelfsema, M.R.G. (2019). Calcium signals in guard cells enhance the efficiency by which absciscic acid triggers stomatal closure. *New Phytol.* **224**: 177–187.
- Hubbard, K.E., Siegel, R.S., Valerio, G., Brandt, B., and Schroeder, J.I. (2012). Absciscic acid and CO₂ signalling via calcium sensitivity priming in guard cells, new CDPK mutant phenotypes and a method for improved resolution of stomatal stimulus-response analyses. *Ann. Bot.* **109**: 5–17.
- Igarashi, D., Tsuda, K., and Katagiri, F. (2012). The peptide growth factor, phytosulfokine, attenuates pattern-triggered immunity. *Plant J.* **71**: 194–204.
- Igasaki, T., Akashi, N., Ujino-Ihara, T., Matsubayashi, Y., Sakagami, Y., and Shinohara, K. (2003). Phytosulfokine Stimulates Somatic Embryogenesis in *Cryptomeria japonica*. *Plant Cell Physiol.* **44**: 1412–1416.
- Imes, D., Mumm, P., Böhm, J., Al-Rasheid, K.A.S., Marten, I., Geiger, D., and Hedrich, R. (2013). Open stomata 1 (OST1) kinase controls R-type anion channel QUAC1 in *Arabidopsis* guard cells. *Plant J.* **74**: 372–382.
- Da Ines, O., Graf, W., Franck, K.I., Albert, A., Winkler, J.B., Scherb, H., Stichler, W., and Schäffner, A.R. (2010). Kinetic analyses of plant water relocation using deuterium as tracer - reduced water flux of *Arabidopsis* pip2 aquaporin knockout mutants. *Plant Biol.* **12**: 129–139.
- Iwai, S., Ogata, S., Yamada, N., Onjo, M., Sonoike, K., and Shimazaki, K. ichiro (2019). Guard cell photosynthesis is crucial in absciscic acid-induced stomatal closure. *Plant Direct* **3**: 1–10.

- Jammes, F. et al.** (2009). MAP kinases MPK9 and MPK12 are preferentially expressed in guard cells and positively regulate ROS-mediated ABA signaling. *Proc. Natl. Acad. Sci. U. S. A.* **106**: 20520–20525.
- Jang, J.Y., Kim, D.G., Kim, Y.O., Kim, J.S., and Kang, H.** (2004). An expression analysis of a gene family encoding plasma membrane aquaporins in response to abiotic stresses in *Arabidopsis thaliana*. *Plant Mol. Biol.* **54**: 713–725.
- Janku, M., Luhová, L., and Petrivalský, M.** (2019). On the origin and fate of reactive oxygen species in plant cell compartments. *Antioxidants* **8**: 1–15.
- Jiang, F., Zhu, J., and Liu, H.L.** (2013). Protoplasts: A useful research system for plant cell biology, especially dedifferentiation. *Protoplasma* **250**: 1231–1238.
- Johanson, U., Karlsson, M., Johansson, I., Gustavsson, S., Sjövall, S., Frayssé, L., Weig, A.R., and Kjellbom, P.** (2001). The complete set of genes encoding major intrinsic proteins in *Arabidopsis* provides a framework for a new nomenclature for major intrinsic proteins in plants. *Plant Physiol.* **126**: 1358–1369.
- Kadota, Y., Sklenar, J., Derbyshire, P., Stransfeld, L., Asai, S., Ntoukakis, V., Jones, J.D., Shirasu, K., Menke, F., Jones, A., and Zipfel, C.** (2014). Direct Regulation of the NADPH Oxidase RBOHD by the PRR-Associated Kinase BIK1 during Plant Immunity. *Mol. Cell* **54**: 43–55.
- Karimi, M., Inzé, D., and Depicker, A.** (2002). GATEWAY vectors for *Agrobacterium*-mediated plant. *Trends Plant Sci.* **7**: 193–195.
- Kaufmann, C.** (2018). Regulation and activities of phytosulfokine receptor PSKR1 in *Arabidopsis thaliana*. Dissertation.
- Kaufmann, C. and Sauter, M.** (2019). Sulfated plant peptide hormones. *J. Exp. Bot.*: 1–11.
- Kaufmann, C., Stührwoldt, N., and Sauter, M.** (2021). TPST-dependent and -independent regulation of root development and signaling by PSK LRR receptor kinases in *Arabidopsis*. *J. Exp. Bot.*: 1–14.
- Keller, T., Damude, H.G., Werner, D., Doerner, P., Dixon, R.A., and Lamb, C.** (1998). A Plant Homolog of the Neutrophil NADPH Oxidase gp91 phox Subunit Gene Encodes a Plasma Membrane Protein with Ca²⁺ Binding Motifs. *Plant Cell* **10**: 255–266.
- Kilian, J., Whitehead, D., Horak, J., Wanke, D., Weinl, S., Batistic, O., D'Angelo, C., Bornberg-Bauer, E., Kudla, J., and Harter, K.** (2007). The AtGenExpress global stress expression data set: Protocols, evaluation and model data analysis of UV-B light, drought and cold stress responses. *Plant J.* **50**: 347–363.

- Kim, T.-H., Bohmer, M., Hu, H., Nishimura, N., and Schroeder, J.I.** (2010). Guard cells signal transduction network: advances in understanding abscisic acid CO₂, and Ca²⁺ signalling. *Annu. Rev. Plant Biol.* **61**: 561–591.
- Kimura, S., Hunter, K., Vaahtera, L., Tran, H.C., Citterico, M., Vaattovaara, A., Rokka, A., Stolze, S.C., Harzen, A., Meißner, L., Wilkens, M.M.T., Hamann, T., Toyota, M., Nakagami H. and Wrzaczek M.** (2020). CRK2 and C-terminal phosphorylation of NADPH oxidase RBOHD regulate reactive oxygen species production in arabidopsis. *Plant Cell* **32**: 1063–1080.
- Kimura, S., Kawarazaki, T., Nibori, H., Michikawa, M., Imai, A., Kaya, H., and Kuchitsu, K.** (2013). The CBL-interacting protein kinase CIPK26 is a novel interactor of Arabidopsis NADPH oxidase AtRbohF that negatively modulates its ROS-producing activity in a heterologous expression system. *J. Biochem.* **153**: 191–195.
- Kimura, S., Waszczak, C., Hunter, K., and Wrzaczek, M.** (2017). Bound by Fate: The Role of Reactive Oxygen Species in Receptor-Like Kinase Signaling. *Plant Cell* **29**: 638–654.
- Kinoshita, T., Caño-Delgado, A., Seto, H., Hiranuma, S., Fujioka, S., Yoshida, S., and Chory, J.** (2005). Binding of brassinosteroids to the extracellular domain of plant receptor kinase BRI1. *Nature* **433**: 167–171.
- Kline, K.G., Barrett-Wilt, G.A., and Sussman, M.R.** (2010). In planta changes in protein phosphorylation induced by the plant hormone abscisic acid. *Proc. Natl. Acad. Sci. U. S. A.* **107**: 15986–15991.
- Kobayashi, T., Eun, C.H., Hanai, H., Matsubayashi, Y., Sakagami, Y., and Kamada, H.** (1999). Phytosulphokine- α , a peptidyl plant growth factor, stimulates somatic embryogenesis in carrot. *J. Exp. Bot.* **50**: 1123–1128.
- Köhler, B. and Blatt, M.R.** (2002). Protein phosphorylation activates the guard cell Ca²⁺ channel and is a prerequisite for gating by abscisic acid. *Plant J.* **32**: 185–194.
- Komori, R., Amano, Y., Ogawa-Ohnishi, M., and Matsubayashi, Y.** (2009). Identification of tyrosylprotein sulfotransferase in Arabidopsis. *Proc. Natl. Acad. Sci. U. S. A.* **106**: 15067–15072.
- Kong, X. et al.** (2018). PHB3 Maintains Root Stem Cell Niche Identity through ROS-Responsive AP2/ERF Transcription Factors in Arabidopsis. *Cell Rep.* **22**: 1350–1363.
- Konrad, K.R., Maierhofer, T., and Hedrich, R.** (2018). Spatio-temporal aspects of Ca²⁺ signalling: lessons from guard cells and pollen tubes. *J. Exp. Bot.* **69**: 4195–4214.

- Koornneef, M., Jorna, M.L., Brinkhorst-van der Swan, D.L.C., and Karssen, C.M.** (1982). The isolation of abscisic acid (ABA) deficient mutants by selection of induced revertants in non-germinating gibberellin sensitive lines of *Arabidopsis thaliana* (L.) heynh. *Theor. Appl. Genet.* **61**: 385–393.
- Kou, X., Liu, Q., Sun, Y., Wang, P., Zhang, S., and Wu, J.** (2020). The Peptide PbrPSK2 From Phytosulfokine Family Induces Reactive Oxygen Species (ROS) Production to Regulate Pear Pollen Tube Growth. *Front. Plant Sci.* **11**: 1–14.
- Kutschmar, A., Rzewuski, G., Stührwohldt, N., Beemster, G.T.S., Inzé, D., and Sauter, M.** (2009). PSK- α promotes root growth in *Arabidopsis*. *New Phytol.* **181**: 820–831.
- Kwak, J.M., Moon, J.H., Murata, Y., Kuchitsu, K., Leonhardt, N., DeLong, A., and Schroeder, J.I.** (2002). Disruption of a guard cell-expressed protein phosphatase 2A regulatory subunit, RCN1, confers abscisic acid insensitivity in *arabidopsis*. *Plant Cell* **14**: 2849–2861.
- Kwak, J.M., Mori, I.C., Pei, Z.M., Leonhard, N., Angel Torres, M., Dangl, J.L., Bloom, R.E., Bodde, S., Jones, J.D.G., and Schroeder, J.I.** (2003). NADPH oxidase AtrbohD and AtrbohF genes function in ROS-dependent ABA signaling in *arabidopsis*. *EMBO J.* **22**: 2623–2633.
- Kwezi, L., Ruzvidzo, O., Wheeler, J.I., Govender, K., Iacuone, S., Thompson, P.E., Gehring, C., and Irving, H.R.** (2011). The phytosulfokine (PSK) receptor is capable of guanylate cyclase activity and enabling cyclic GMP-dependent signaling in plants. *J. Biol. Chem.* **286**: 22580–22588.
- Ladwig, F., Dahlke, R.I., Stührwohldt, N., Hartmann, J., Harter, K., and Sauter, M.** (2015). Phytosulfokine Regulates Growth in *Arabidopsis* through a Response Module at the Plasma Membrane That Includes CYCLIC NUCLEOTIDE-GATED CHANNEL17, H⁺-ATPase, and BAK1. *Plant Cell* **27**: 1718–1729.
- Laemmli, U.K.** (1970). Cleavage of structural proteins during the assembly of the head of bacteriophage T4. *Nature* **227**: 680–685.
- Lee, Y., Kim, Y.J., Kim, M.H., and Kwak, J.M.** (2016). MAPK cascades in guard cell signal transduction. *Front. Plant Sci.* **7**: 1–8.
- Leng, Q., Mercier, R.W., Yao, W., and Berkowitz, G.A.** (1999). Cloning and first functional characterization of a plant cyclic nucleotide-gated cation channel. *Plant Physiol.* **121**: 753–761.

- Li, L., Li, M., Yu, L., Zhou, Z., Liang, X., Liu, Z., Cai, G., Gao, L., Zhang, X., Wang, Y., Chen, S., and Zhou, J.M.** (2014). The FLS2-associated kinase BIK1 directly phosphorylates the NADPH oxidase RbohD to control plant immunity. *Cell Host Microbe* **15**: 329–338.
- Loivamäki, M., Stührwohltd, N., Deeken, R., Steffens, B., Roitsch, T., Hedrich, R., and Sauter, M.** (2010). A role for PSK signaling in wounding and microbial interactions in Arabidopsis. *Physiol. Plant.* **139**: 348–357.
- Lorbiecke, R. and Sauter, M.** (2002). Comparative analysis of PSK peptide growth factor precursor homologs. *Plant Sci.* **163**: 321–332.
- Ma, N., Xue, J., Li, Y., Liu, X., Dai, F., Jia, W., Luo, Y., and Gao, J.** (2008). Rh-PIP2;1, a rose aquaporin gene, is involved in ethylene-regulated petal expansion. *Plant Physiol.* **148**: 894–907.
- Madeira, F., Park, Y.M., Lee, J., Buso, N., Gur, T., Madhusoodanan, N., Basutkar, P., Tivey, A.R.N., Potter, S.C., Finn, R.D., and Lopez, R.** (2019). The EMBL-EBI search and sequence analysis tools APIs in 2019. *Nucleic Acids Res.* **47**: W636–W641.
- Marino, D., Dunand, C., Puppo, A., and Pauly, N.** (2012). A burst of plant NADPH oxidases. *Trends Plant Sci.* **17**: 9–15.
- Matsubayashi, Y.** (2006). Disruption and Overexpression of Arabidopsis Phytosulfokine Receptor Gene Affects Cellular Longevity and Potential for Growth. *Plant Physiol.* **142**: 45–53.
- Matsubayashi, Y.** (2014). Posttranslationally modified small-peptide signals in plants. *Annu. Rev. Plant Biol.* **65**: 385–413.
- Matsubayashi, Y.** (2011). Recent progress in research on small post-translationally modified peptide signals in plants. In *The Arabidopsis Book - Peptide Signals in Arabidopsis*, pp. 1–10.
- Matsubayashi, Y., Hanai, H., Hara, O., and Sakagami, Y.** (1996). Active Fragments and Analogs of the Plant Growth Factor , Phytosulfokine : Structure – Activity Relationships Proliferation of dispersed plant cells in culture is strictly dependent on cell density , and cells in a low density culture can only grow in the. *Biochem. Biophys. Res. Commun.* **225**: 209–214.
- Matsubayashi, Y., Ogawa, M., Morita, A., and Sakagami, Y.** (2002). An LRR receptor kinase involved in perception of a peptide plant hormone, phytosulfokine. *Science* (80-.). **296**: 1470–1472.

- Matsubayashi, Y. and Sakagami, Y.** (1996). Phytosulfokine, sulfated peptides that induce the proliferation of single mesophyll cells of *Asparagus officinalis* L. *Proc. Natl. Acad. Sci. U. S. A.* **93**: 7623–7627.
- Matsuzaki, Y., Ogawa-Ohnishi, M., Mori, A., and Matsubayashi, Y.** (2010). Secreted peptide signals required for maintenance of root stem cell niche in *Arabidopsis*. *Science* (80-.). **329**: 1065–1067.
- Maurel, C., Verdoucq, L., Luu, D.T., and Santoni, V.** (2008). Plant aquaporins: Membrane channels with multiple integrated functions. *Annu. Rev. Plant Biol.* **59**: 595–624.
- McAdam, S.A.M., Brodribb, T.J., and Ross, J.J.** (2016a). Shoot-derived abscisic acid promotes root growth. *Plant Cell Environ.* **39**: 652–659.
- McAdam, S.A.M., Manzi, M., Ross, J.J., Brodribb, T.J., and Gómez-Cadenas, A.** (2016b). Uprooting an abscisic acid paradigm: Shoots are the primary source. *Plant Signal. Behav.* **11**: 1–2.
- Meinhard, M., Rodriguez, P.L., and Grill, E.** (2002). The sensitivity of ABI2 to hydrogen peroxide links the abscisic acid-response regulator to redox signalling. *Planta* **214**: 775–782.
- Melotto, M., Zhang, L., Oblessuc, P.R., and He, S.Y.** (2017). Stomatal defense a decade later. *Plant Physiol.* **174**: 561–571.
- Merilo, E., Yarmolinsky, D., Jalakas, P., Parik, H., Tulva, I., Rasulov, B., Kilk, K., and Kollist, H.** (2018). Stomatal VPD response: there is more to the story than ABA. *Plant Physiol.* **176**: 851–864.
- Monneuse, J.M., Sugano, M., Becue, T., Santoni, V., Hem, S., and Rossignol, M.** (2011). Towards the profiling of the *Arabidopsis thaliana* plasma membrane transportome by targeted proteomics. *Proteomics* **11**: 1789–1797.
- Moore, K.L.** (2003). The Biology and Enzymology of Protein Tyrosine O-Sulfation. *J. Biol. Chem.* **278**: 24243–24246.
- Mori, I.C. and Schroeder, J.I.** (2004). Reactive oxygen species activation of plant Ca²⁺ channels. A signaling mechanism in polar growth, hormone transduction, stress signaling, and hypothetically mechanotransduction. *Plant Physiol.* **135**: 702–708.
- Mosher, S., Seybold, H., Rodriguez, P., Stahl, M., Davies, K.A., Dayaratne, S., Morillo, S.A., Wierzbza, M., Favery, B., Keller, H., Tax, F.E., and Kemmerling, B.** (2013). The tyrosine-sulfated peptide receptors PSKR1 and PSY1R modify the immunity of *Arabidopsis* to biotrophic and necrotrophic pathogens in an antagonistic manner. *Plant J.* **73**: 469–482.

- Munemasa, S., Hauser, F., Park, J., Waadt, R., Brandt, B., and Schroeder, J.I.** (2015). Mechanisms of abscisic acid-mediated control of stomatal aperture. *Curr. Opin. Plant Biol.* **28**: 154–162.
- Murata, Y., Pei, Z.M., Mori, I.C., and Schroeder, J.** (2001). Absciscic Acid Activation of plasma membrane Ca^{2+} channels in guard cells requires cytosolic NAD(P)H and is differentially disrupted upstream and downstream of reactive oxygen species production in *abi1-1* and *abi2-1* protein phosphatase 2C mutants. *Plant Cell* **13**: 2513–2523.
- Nakaminami, K. et al.** (2018). AtPep3 is a hormone-like peptide that plays a role in the salinity stress tolerance of plants. *Proc. Natl. Acad. Sci. U. S. A.* **115**: 5810–5815.
- Nemhauser, J.L., Hong, F., and Chory, J.** (2006). Different Plant Hormones Regulate Similar Processes through Largely Nonoverlapping Transcriptional Responses. *Cell* **126**: 467–475.
- Niittylä, T., Fuglsang, A.T., Palmgren, M.G., Frommer, W.B., and Schulze, W.X.** (2007). Temporal analysis of sucrose-induced phosphorylation changes in plasma membrane proteins of *Arabidopsis*. *Mol. Cell. Proteomics* **6**: 1711–1726.
- Nilson, S.E. and Assmann, S.M.** (2007). The control of transpiration. Insights from *Arabidopsis*. *Plant Physiol.* **143**: 19–27.
- Noctor, G. and Foyer, C.H.** (2016). Intracellular redox compartmentation and ROS-related communication in regulation and signaling. *Plant Physiol.* **171**: 1581–1592.
- North, H.M., Almeida, A. De, Boutin, J.P., Frey, A., To, A., Botran, L., Sotta, B., and Marion-Poll, A.** (2007). The *Arabidopsis* ABA-deficient mutant *aba4* demonstrates that the major route for stress-induced ABA accumulation is via neoxanthin isomers. *Plant J.* **50**: 810–824.
- Oda, T., Hashimoto, H., Kuwabara, N., Akashi, S., Hayashi, K., Kojima, C., Wong, H.L., Kawasaki, T., Shimamoto, K., Sato, M., and Shimizu, T.** (2010). Structure of the N-terminal regulatory domain of a plant NADPH oxidase and its functional implications. *J. Biol. Chem.* **285**: 1435–1445.
- Ogasawara, Y. et al.** (2008). Synergistic activation of the *Arabidopsis* NADPH oxidase AtrobohD by Ca^{2+} and phosphorylation. *J. Biol. Chem.* **283**: 8885–8892.
- Ogawa, M., Shinohara, H., Sakagami, Y., and Matsubayashi, Y.** (2008). *Arabidopsis* CLV3 peptide directly binds CLV1 ectodomain. *Science* (80-.). **319**: 294.

- Omasits, U., Ahrens, C.H., Müller, S., and Wollscheid, B.** (2014). Protter: Interactive protein feature visualization and integration with experimental proteomic data. *Bioinformatics* **30**: 884–886.
- Osakabe, Y. et al.** (2013). Osmotic Stress Responses and Plant Growth Controlled by Potassium Transporters in Arabidopsis. *Plant Cell* **25**: 609–624.
- Pan, Y., Chai, X., Gao, Q., Zhou, L., Zhang, S., Li, L., and Luan, S.** (2019). Dynamic Interactions of Plant CNGC Subunits and Calmodulins Drive Oscillatory Ca²⁺ Channel Activities. *Dev. Cell* **48**: 710–725.
- Park, S.S.-Y. et al.** (2009). Absciscic Acid Inhibits Type 2C Protein Phosphatases via the PYR/ PYL Family of START Proteins. *Science* (80-.). **324**: 1068–1069.
- Pei, Z., Murata, Y., Benning, G., Thomine, Â., Klüsener, B., Allen, G.J., Grill, E., and Schroeder, J.I.** (2000). Calcium channels activated by hydrogen peroxide mediate abscisic acid signalling in guard cells. *Nature* **406**: 731–734.
- Péret, B. et al.** (2012). Auxin regulates aquaporin function to facilitate lateral root emergence. *Nat. Cell Biol.* **14**: 991–998.
- Pfaffl, M.W.** (2001). A new mathematical model for relative quantification in real-time RT-PCR. *Nucleic Acids Res.* **29**: 2002–2007.
- Piston, D.W. and Kremers, G.J.** (2007). Fluorescent protein FRET: the good, the bad and the ugly. *Trends Biochem. Sci.* **32**: 407–414.
- Planas-Riverola, A., Gupta, A., Betegoñ-Putze, I., Bosch, N., Ibanes, M., and Cano-Delgado, A.I.** (2019). Brassinosteroid signaling in plant development and adaptation to stress. *Dev.* **146**: 1–11.
- Postiglione, A.E. and Muday, G.K.** (2020). The Role of ROS Homeostasis in ABA-Induced Guard Cell Signaling. *Front. Plant Sci.* **11**: 1–9.
- Prado, K., Boursiac, Y., Tournaire-Roux, C., Monneuse, J.-M., Postaire, O., Da Ines, O., Schaffner, A.R., Hem, S., Santoni, V., and Maurel, C.** (2013). Regulation of Arabidopsis Leaf Hydraulics Involves Light-Dependent Phosphorylation of Aquaporins in Veins. *Plant Cell* **25**: 1029–1039.
- Prak, S., Hem, S., Boudet, J., Viennois, G., Sommerer, N., Rossignol, M., Maurel, C., and Santoni, V.** (2008). Multiple Phosphorylations in the C-terminal Tail of Plant Plasma Membrane Aquaporins. *Mol. Cell. Proteomics* **7**: 1019–1030.
- Qi, J., Wang, J., Gong, Z., and Zhou, J.M.** (2017). Apoplastic ROS signaling in plant immunity. *Curr. Opin. Plant Biol.* **38**: 92–100.

- Qiu, J., McGaughey, S.A., Groszmann, M., Tyerman, S.D., and Byrt, C.S.** (2020). Phosphorylation influences water and ion channel function of AtPIP2;1. *Plant Cell Environ.* **43**: 2428–2442.
- Rajamanickam, K., Schönhof, M.D., Hause, B., and Sauter, M.** (2021). PSK signaling controls ABA homeostasis and signaling genes and maintains shoot growth under osmotic stress. *bioRxiv* doi: <https://doi.org/10.1101/2020.10.20.347674>
- Reichardt, A.S., Piepho, H., Stintzi, A., and Schaller, A.** (2020). Peptide signaling for drought-induced tomato flower drop. *Science* (80-.). **367**: 1482–1485.
- Rienmüller, F., Beyhl, D., Lautner, S., Fromm, J., Al-Rasheid, K.A.S., Ache, P., Farmer, E.E., Marten, I., and Hedrich, R.** (2010). Guard cell-specific calcium sensitivity of high density and activity SV/TPC1 channels. *Plant Cell Physiol.* **51**: 1548–1554.
- Rivero, R.M., Kojima, M., Gepstein, A., Sakakibara, H., Mittler, R., Gepstein, S., and Blumwald, E.** (2007). Delayed leaf senescence induces extreme drought tolerance in a flowering plant. *Proc. Natl. Acad. Sci. U. S. A.* **104**: 19631–19636.
- Rock, C.D. and Zeevaart, J.A.D.** (1991). The aba mutant of *Arabidopsis thaliana* is impaired in epoxy-carotenoid biosynthesis. *Proc. Natl. Acad. Sci. U. S. A.* **88**: 7496–7499.
- Rodrigues, O., Reshetnyak, G., Grondin, A., Saijo, Y., Leonhardt, N., Maurel, C., and Verdoucq, L.** (2017). Aquaporins facilitate hydrogen peroxide entry into guard cells to mediate ABA- and pathogen-triggered stomatal closure. *Proc. Natl. Acad. Sci.* **114**: 9200–9205.
- Russinova, E., Borst, J.W., Kwaaitaal, M., Caño-Delgado, A., Yin, Y., Chory, J., and De Vries, S.C.** (2004). Heterodimerization and endocytosis of *Arabidopsis* brassinosteroid receptors BRI1 and AtSERK3 (BAK1). *Plant Cell* **16**: 3216–3229.
- Sanders, D., Brownlee, C., and Harper, J.F.** (1999). Communicating with calcium. *Plant Cell* **11**: 691–706.
- Schindelin, J. et al.** (2012). Fiji: an open-source platform for biological-image analysis. *Nat. Methods* **9**: 676.
- Schroeder, J.I.** (2003). Knockout of the guard cell K⁺out channel and stomatal movements. *Proc. Natl. Acad. Sci. U. S. A.* **100**: 4976–4977.
- Schwartz, S.H., Léon-Kloosterziel, K.M., Koornneef, M., and Zeevaart, J. a D.** (1997). Biochemical Characterization of the aba2 and aba3 Mutants in *Arabidopsis thaliana*. *Plant Physiol.* **114**: 161–166.

- Shang, Y., Dai, C., Lee, M.M., Kwak, J.M., and Nam, K.H.** (2016). BRI1-Associated Receptor Kinase 1 Regulates Guard Cell ABA Signaling Mediated by Open Stomata 1 in Arabidopsis. *Mol. Plant* **9**: 447–460.
- Shen, J., Diao, W., Zhang, L., Acharya, B.R., Wang, M., Zhao, X., Chen, D., and Zhang, W.** (2020). Secreted Peptide PIP1 Induces Stomatal Closure by Activation of Guard Cell Anion Channels in Arabidopsis. *Front. Plant Sci.* **11**: 1–10.
- Shiu, S.H. and Bleecker, A.B.** (2003). Expansion of the receptor-like kinase/Pelle gene family and receptor-like proteins in Arabidopsis. *Plant Physiol.* **132**: 530–543.
- Shiu, S.H. and Bleecker, A.B.** (2001). Receptor-like kinases from Arabidopsis form a monophyletic gene family related to animal receptor kinases. *Proc. Natl. Acad. Sci. U. S. A.* **98**: 10763–10768.
- Sierla, M. et al.** (2018). The receptor-like pseudokinase GHR1 is required for stomatal closure. *Plant Cell* **30**: 2813–2837.
- Sierla, M., Waszczak, C., Vahisalu, T., and Kangasjärvi, J.** (2016). Reactive Oxygen Species in the Regulation of Stomatal Movements. *Plant Physiol.* **171**: 1569–1580.
- Sievers, F., Wilm, A., Dineen, D., Gibson, T.J., Karplus, K., Li, W., Lopez, R., Thompson, J.D., Higgins, D.G., McWilliam, H., Remmert, M., and So, J.** (2011). Fast , scalable generation of high-quality protein multiple sequence alignments using Clustal Omega. *Mol. Syst. Biol.* **7**: 1–6.
- Singh, R., Parihar, P., Singh, S., Mishra, R.K., Singh, V.P., and Prasad, S.M.** (2017). Reactive oxygen species signaling and stomatal movement: Current updates and future perspectives. *Redox Biol.* **11**: 213–218.
- Sirichandra, C., Gu, D., Hu, H., Davanture, M., Lee, S., Djaoui, M., Valot, B., Zivy, M., Leung, J., Merlot, S., and Kwak, J.M.** (2009). Phosphorylation of the Arabidopsis AttrbohF NADPH oxidase by OST1 protein kinase. *FEBS Lett.* **583**: 2982–2986.
- Srivastava, R., Liu, J.X., and Howell, S.H.** (2008). Proteolytic processing of a precursor protein for a growth-promoting peptide by a subtilisin serine protease in Arabidopsis. *Plant J.* **56**: 219–227.
- Stührwohldt, N., Bühler, E., Sauter, M., and Schaller, A.** (2021). Phytosulfokine (PSK) precursor processing by subtilase SBT3.8 and PSK signaling improve drought stress tolerance in Arabidopsis. *J. Exp. Bot.* **72**: 3427–3440.
- Stührwohldt, N., Dahlke, R.I., Kutschmar, A., Peng, X., Sun, M.X., and Sauter, M.** (2015). Phytosulfokine peptide signaling controls pollen tube growth and funicular pollen tube guidance in Arabidopsis thaliana. *Physiol. Plant.* **153**: 643–653.

- Stührwohldt, N., Dahlke, R.I., Steffens, B., Johnson, A., and Sauter, M.** (2011). Phytosulfokine- a Controls Hypocotyl Length and Cell Expansion in *Arabidopsis thaliana* through Phytosulfokine Receptor 1. **6**.
- Sullivan, A. et al.** (2019). An 'eFP-Seq Browser' for visualizing and exploring RNA sequencing data. *Plant J.* **100**: 641–654.
- Sussmilch, F.C., Roelfsema, M.R.G., and Hedrich, R.** (2019). On the origins of osmotically driven stomatal movements. *New Phytol.* **222**: 84–90.
- Takahashi, F., Suzuki, T., Osakabe, Y., Betsuyaku, S., Kondo, Y., Dohmae, N., Fukuda, H., Yamaguchi-Shinozaki, K., and Shinozaki, K.** (2018). A small peptide modulates stomatal control via abscisic acid in long-distance signaling. *Nature* **556**: 235–238.
- Talke, I.N., Blaudez, D., Maathuis, F.J.M., and Sanders, D.** (2003). CNGCs: Prime targets of plant cyclic nucleotide signalling? *Trends Plant Sci.* **8**: 286–293.
- Tavormina, P., De Coninck, B., Nikonorova, N., De Smet, I., and Cammuea, B.P.A.** (2015). The plant peptidome: An expanding repertoire of structural features and biological functions. *Plant Cell* **27**: 2095–2118.
- Thor, K. et al.** (2020). The calcium-permeable channel OSCA1.3 regulates plant stomatal immunity. *Nature* **585**: 569–573.
- Tian, W., Hou, C., Ren, Z., Wang, C., Zhao, F., Dahlbeck, D., Hu, S., Zhang, L., Niu, Q., Li, L., Staskawicz, B.J., and Luan, S.** (2019a). A calmodulin-gated calcium channel links pathogen patterns to plant immunity. *Nature* **572**: 131–135.
- Tian, W., Hou, C., Ren, Z., Wang, C., Zhao, F., Dahlbeck, D., Hu, S., Zhang, L., Niu, Q., Li, L., Staskawicz, B.J., and Luan, S.** (2019b). A calmodulin-gated calcium channel links pathogen patterns to plant immunity. *Nature* **572**: 131–135.
- Törnroth-Horsefield, S., Wang, Y., Hedfalk, K., Johanson, U., Karlsson, M., Tajkhorshid, E., Neutze, R., and Kjellbom, P.** (2006). Structural mechanism of plant aquaporin gating. *Nature* **439**: 688–694.
- Torres, M.A., Dangl, J.L., and Jones, J.D.G.** (2002). *Arabidopsis* gp91phox homologues AtrbohD and AtrbohF are required for accumulation of reactive oxygen intermediates in the plant defense response. *Proc. Natl. Acad. Sci. U. S. A.* **99**: 517–522.
- Torres, M.A., Onouchi, H., Hamada, S., Machida, C., Hammond-Kosack, K.E., and Jones, J.D.G.** (1998). Six *Arabidopsis thaliana* homologues of the human respiratory burst oxidase (gp91(phox)). *Plant J.* **14**: 365–370.
- Tsirigos, K.D., Peters, C., Shu, N., Käll, L., and Elofsson, A.** (2015). The TOPCONS web

- server for consensus prediction of membrane protein topology and signal peptides. *Nucleic Acids Res.* **43**: W401–W407.
- Tucker, S.L. and Talbot, N.J.** (2001). Surface attachment and Pre -Penetration Stage Development By Plant Pathogenic Fungi. *Annu. Rev. Phytopathol.* **39**: 385–417.
- Tunc-Ozdemir, M., Tang, C., Ishka, M.R., Brown, E., Groves, N.R., Myers, C.T., Rato, C., Poulsen, L.R., McDowell, S., Miller, G., Mittler, R., and Harper, J.F.** (2013). A Cyclic Nucleotide-Gated Channel (CNGC16) in Pollen Is Critical for Stress Tolerance in Pollen Reproductive Development. *Plant Physiol.* **161**: 1010–1020.
- Turner, N.C.** (2018). Turgor maintenance by osmotic adjustment: 40 years of progress. *J. Exp. Bot.* **69**: 3223–3233.
- Umezawa, T., Nakashima, K., Miyakawa, T., Kuromori, T., Tanokura, M., Shinozaki, K., and Yamaguchi-Shinozaki, K.** (2010). Molecular basis of the core regulatory network in ABA responses: Sensing, signaling and transport. *Plant Cell Physiol.* **51**: 1821–1839.
- Vahisalu, T., Kollist, H., Wang, Y.F., Nishimura, N., Chan, W.Y., Valerio, G., Lamminmäki, A., Brosché, M., Moldau, H., Desikan, R., Schroeder, J.I., and Kangasjärvi, J.** (2008). SLAC1 is required for plant guard cell S-type anion channel function in stomatal signalling. *Nature* **452**: 487–491.
- Vandesompele, J., De Preter, K., Pattyn, F., Poppe, B., Van Roy, N., De Paepe, A., and Speleman, F.** (2002). Accurate normalization of real-time quantitative RT-PCR data by geometric averaging of multiple internal control genes. *Genome Biol.* **3**: 1–12.
- Wang, C., Hu, H., Qin, X., Zeise, B., Xu, D., Rappel, W.J., Boron, W.F., and Schroeder, J.I.** (2015a). Reconstitution of CO₂ regulation of SLAC1 anion channel and function of CO₂-permeable PIP₂;1 aquaporin as CARBONIC ANHYDRASE4 interactor. *Plant Cell* **28**: 568–582.
- Wang, J., Li, H., Han, Z., Zhang, H., Wang, T., Lin, G., Chang, J., Yang, W., and Chai, J.** (2015b). Allosteric receptor activation by the plant peptide hormone phytosulfokine. *Nature* **525**: 265–268.
- Wang, P. and Song, C.P.** (2008). Guard-cell signalling for hydrogen peroxide and abscisic acid. *New Phytol.* **178**: 703–718.
- Wang, Y.-F., Munemasa, S., Nishimura, N., Ren, H.-M., Robert, N., Han, M., Puzorjova, I., Kollist, H., Lee, S., Mori, I., and Schroeder, J.I.** (2013). Identification of Cyclic GMP-Activated Nonselective Ca²⁺-Permeable Cation Channels and Associated CNGC5 and CNGC6 Genes in Arabidopsis Guard Cells. *Plant Physiol.* **163**: 578–590.

- Wang, Y., Kang, Y., Ma, C., Miao, R., Wu, C., Long, Y., Ge, T., Wu, Z., Hou, X., Zhang, J., and Qi, Z.** (2017). CNGC2 is a Ca²⁺ influx channel that prevents accumulation of apoplastic Ca²⁺ in the leaf. *Plant Physiol.* **173**: 1342–1354.
- Wang, Z.Y.** (2012). Brassinosteroids modulate plant immunity at multiple levels. *Proc. Natl. Acad. Sci. U. S. A.* **109**: 7–8.
- Wheeler, J.I. and Irving, H.R.** (2010). Evolutionary advantages of secreted peptide signalling molecules in plants. *Funct. Plant Biol.* **37**: 382–394.
- Winter, D., Vinegar, B., Nahal, H., Ammar, R., Wilson, G. V., and Provart, N.J.** (2007). An “electronic fluorescent pictograph” Browser for exploring and analyzing large-scale biological data sets. *PLoS One* **2**: 1–12.
- Wolf, S. et al.** (2014). A receptor-like protein mediates the response to pectin modification by activating brassinosteroid signaling. *PNAS* **111**: 15261–15266.
- Wu, Y., Xun, Q., Guo, Y., Zhang, J., Cheng, K., Shi, T., He, K., Hou, S., Gou, X., and Li, J.** (2016). Genome-Wide Expression Pattern Analyses of the Arabidopsis Leucine-Rich Repeat Receptor-Like Kinases. *Mol. Plant* **9**: 289–300.
- Xu, Z.Y., Lee, K.H., Dong, T., Jeong, J.C., Jin, J.B., Kanno, Y., Kim, D.H., Kim, S.Y., Seo, M., Bressan, R.A., Yun, D.J., and Hwang, I.** (2012). A vacuolar β -Glucosidase homolog that possesses glucose-conjugated abscisic acid hydrolyzing activity plays an important role in osmotic stress responses in Arabidopsis. *Plant Cell* **24**: 2184–2199.
- Yamaguchi, Y., Pearce, G., and Ryan, C.A.** (2006). The cell surface leucine-rich repeat receptor for AtPep1, an endogenous peptide elicitor in Arabidopsis, is functional in transgenic tobacco cells. *Proc. Natl. Acad. Sci. U. S. A.* **103**: 10104–10109.
- Yan eff, A., Vitali, V., and Amodeo, G.** (2015). PIP1 aquaporins: Intrinsic water channels or PIP2 aquaporin modulators? *FEBS Lett.* **589**: 3508–3515.
- Yang, Y., Costa, A., Leonhardt, N., Siegel, R.S., and Schroeder, J.I.** (2008). Isolation of a strong Arabidopsis guard cell promoter and its potential as a research tool. *Plant Methods* **4**: 1–15.
- Ye, W., Munemasa, S., Shinya, T., Wu, W., Ma, T., Lu, J., Kinoshita, T., Kaku, H., Shibuya, N., and Murata, Y.** (2020). Stomatal immunity against fungal invasion comprises not only chitin-induced stomatal closure but also chitosan-induced guard cell death. *Proc. Natl. Acad. Sci. U. S. A.* **117**: 20932–20942.
- Yoo, Y.J. et al.** (2016). Interactions between Transmembrane Helices within Monomers of the Aquaporin AtPIP2;1 Play a Crucial Role in Tetramer Formation. *Mol. Plant* **9**: 1004–

- Young, J.J., Mehta, S., Israelsson, M., Godoski, J., Grill, E., and Schroeder, J.I.** (2006). CO₂ signaling in guard cells: Calcium sensitivity response modulation, a Ca²⁺-independent phase, and CO₂ insensitivity of the *gca2* mutant. *Proc. Natl. Acad. Sci. U. S. A.* **103**: 7506–7511.
- Yu, X. et al.** (2019). The Receptor Kinases BAK1/SERK4 Regulate Ca²⁺ Channel-Mediated Cellular Homeostasis for Cell Death Containment. *Curr. Biol.* **29**: 3778-3790.e8.
- Zeb, Q., Wang, X., Hou, C., Zhang, X., Dong, M., Zhang, S., Zhang, Q., Ren, Z., Tian, W., Zhu, H., Li, L., and Liu, L.** (2020). The interaction of CaM7 and CNGC14 regulates root hair growth in Arabidopsis. *J. Integr. Plant Biol.* **62**: 887–896.
- Zhang, F.P., Sussmilch, F., Nichols, D.S., Cardoso, A.A., Brodribb, T.J., and McAdam, S.A.M.** (2018a). Leaves, not roots or floral tissue, are the main site of rapid, external pressure-induced ABA biosynthesis in angiosperms. *J. Exp. Bot.* **69**: 1261–1267.
- Zhang, H. et al.** (2018b). A Plant Phytosulfokine Peptide Initiates Auxin-Dependent Immunity through Cytosolic Ca²⁺ Signaling in Tomato. *Plant Cell* **30**: 652–667.
- Zhang, M. et al.** (2018c). The MAP4 Kinase SIK1 Ensures Robust Extracellular ROS Burst and Antibacterial Immunity in Plants. *Cell Host Microbe* **24**.
- Zhang, S., Pan, Y., Wang, T., Dong, M., Zhu, H., Luan, S., and Li, L.** (2017). Arabidopsis CNGC14 Mediates Calcium Influx Required for Tip Growth in Root Hairs. *Mol. Plant* **10**: 1004–1006.
- Zhang, Z., Hou, C., Tian, W., Li, L., and Zhu, H.** (2019). Electrophysiological Studies Revealed CaM1-Mediated Regulation of the Arabidopsis Calcium Channel CNGC12. *Front. Plant Sci.* **10**: 1–9.
- Zhao, B., Liu, Q., Wang, B., and Yuan, F.** (2021). Roles of Phytohormones and Their Signaling Pathways in Leaf Development and Stress Responses. *J. Agric. Food Chem.* **69**: 3566–3584.
- Zhou, L., Lan, W., Jiang, Y., Fang, W., and Luan, S.** (2014). A calcium-dependent protein Kinase interacts with and activates a calcium channel to regulate pollen tube growth. *Mol. Plant* **7**: 369–376.

APPENDIX

Appendix Table 1: Chemicals and their manufacturers.

Name	Manufacturer
2-Mercaptoethanol	Carl Roth GmbH & Co. KG
2-Propanol	Carl Roth GmbH & Co. KG
(+)-Cis, Trans-Abscisic acid	Duchefa Biochemie B.V.
Acetic acid	Carl Roth GmbH & Co. KG
Acrylamid Bisacrylamid	Carl Roth GmbH & Co. KG
Agarose Standard	Carl Roth GmbH & Co. KG
APS	Carl Roth GmbH & Co. KG
L(+)-Ascorbic acid	Carl Roth GmbH & Co. KG
ATP	Sigma-Aldrich Chemie GmbH
[γ - ³² P] ATP	Hartmann Analytic GmbH
Brilliant Blue R 250	Carl Roth GmbH & Co. KG
Bromphenol blue	Merck KGaA
Calcium chloride dihydrate	Merck KGaA
Cellulase Onozuka R-10	Duchefa Biochemie B.V.
Chloroform	Carl Roth GmbH & Co. KG
3,3'-Diaminobenzidine tetrahydrochloride	Carl Roth GmbH & Co. KG
2',7'-Dichlorofluorescein diacetate	Sigma-Aldrich Chemie GmbH
3',5'-Dimethoxy-4'-hydroxyacetophenone	Sigma-Aldrich Chemie GmbH
1,4-Dithiothreitol (DTT)	Carl Roth GmbH & Co. KG
EDTA	Carl Roth GmbH & Co. KG
Ethanol	Carl Roth GmbH & Co. KG
Ethidiumbromid	Carl Roth GmbH & Co. KG
Gelrite	Duchefa Biochemie B.V.
α -D(+)-Glucose monohydrate	Carl Roth GmbH & Co. KG
Glycerol	Carl Roth GmbH & Co. KG
Glycin	Carl Roth GmbH & Co. KG
Hydrogen peroxide 30%	Carl Roth GmbH & Co. KG

Name	Manufacturer
HEPES	Carl Roth GmbH & Co. KG
Imidazol	Sigma-Aldrich Chemie GmbH
IPTG	Carl Roth GmbH & Co. KG
LB Agar (Luria/Miller)	Carl Roth GmbH & Co. KG
LB Broth (Luria/Miller)	Carl Roth GmbH & Co. KG
D(-)-Mannitol	Carl Roth GmbH & Co. KG
MES	Carl Roth GmbH & Co. KG
Methanol	Carl Roth GmbH & Co. KG
Magnesiumchlorid	Merck KGaA
Mangan (II) chlorid	Sigma-Aldrich Chemie GmbH
Murashige & Skoog Medium Basal Salt	Duchefa Biochemie B.V.
Nitro blue tetrazolium chloride	Sigma-Aldrich Chemie GmbH
Peptone ex meat	Carl Roth GmbH & Co. KG
Potassium acetate	Carl Roth GmbH & Co. KG
Potassium chloride	Carl Roth GmbH & Co. KG
Phytosulfokine	Pepscan
Rotiphorese® Gel 40 (29:1)	Carl Roth GmbH & Co. KG
D(+)-Saccharose	Carl Roth GmbH & Co. KG
SDS	Carl Roth GmbH & Co. KG
Silwett L-77	Leu+Gygax AG
Sodium hypochlorite solution	Carl Roth GmbH & Co. KG
Sodium citrate	Carl Roth GmbH & Co. KG
TALON® Metal Affinity Resin	Takara Bio Europe SAS
TEMED	Carl Roth GmbH & Co. KG
TRI Reagent	Sigma-Aldrich Chemie GmbH
Tris-(hydroxymethyl)-aminomethane	Carl Roth GmbH & Co. KG
Tween 20	Carl Roth GmbH & Co. KG
Urea	Carl Roth GmbH & Co. KG
X-GlcA cyclohexylammonium salt	Duchefa Biochemie B.V.
Yeast extract	Carl Roth GmbH & Co. KG

Appendix Table 2: Solutions and their compositions.

Solution	Composition
Clearing solution	67% (w/v) chloral hydrate 11% (w/v) glycerol
Column buffer MBP-tagged proteins	20 mM Tris/ HCl, pH 7.5 200 mM NaCl 1 mM EDTA
Coomassie staining solution	50% (v/v) MeOH 7% (v/v) acetic acid 0.25% (w/v) Brilliant Blue R250
DAB-staining solution	0.1% (w/v) 3,3'-diaminobenzidine 100 mM sodium phosphate buffer, pH 7.2
Destain solution	40% (v/v) MeOH 7% (v/v) acetic acid 3% (v/v) glycerol
DNA extraction buffer	200 mM Tris, pH7.5 250 mM NaCl 25 mM EDTA 0.5% (w/v) SDS
10X DNA loading dye	50% (v/v) glycerol 10 mM Tris, pH 8.0 0.4% (w/v) bromphenol blue
Elution buffer for HIS-tagged proteins	50 mM sodium phosphate pH 8.0 300 mM NaCl 150 mM imidazole

Solution	Composition
Elution buffer for MBP-tagged proteins	20 mM Tris/ HCl, pH 7.5 200 mM NaCl 1 mM EDTA 10 mM Maltose
Extraction buffer for HIS-tagged proteins	50 mM sodium phosphate pH 7.0 300 mM NaCl
Enzyme Solution (protoplast assay)	1% (w/v) cellulase 0.075% (w/v) pectolyase 9% (v/v) macro nutrient salt solution 0.9% (v/v) micro nutrient salt solution pH 5.6, 330 mosmol/L
High Salt Solution	0.8 M sodium citrate 1.2 M NaCl
Infiltration medium	10 mM MES, pH 5.6 200 µM acetosyringon 0.015% (v/v) Tween 20 0.56 M ascorbate acid 10 mM MgCl ₂
2X Kinase buffer	100 mM HEPES, pH 7.4 2 mM DTT 20 mM MgCl ₂ 20 mM MnCl ₂ 0.4 mM ATP

Solution	Composition
10X Laemmli buffer	1.92 M Glycin 0.25 M Tris 1% (w/v) SDS
Macro nutrient salt solution (protoplast assay)	2.5 mM NH_4NO_3 17.31 mM KNO_3 1.47 mM KH_2PO_4 1.42 mM $\text{MgSO}_4 \cdot 7 \text{H}_2\text{O}$ 3.06 mM $\text{CaCl}_2 \cdot 2 \text{H}_2\text{O}$
Micro nutrient salt solution (protoplast assay)	8.75 mM $\text{MnSO}_4 \cdot \text{H}_2\text{O}$ 81 mM H_3BO_3 26 mM $\text{ZnSO}_4 \cdot 7 \text{H}_2\text{O}$ 4.5 mM KI 1 mM $\text{Na}_2\text{MoO}_4 \cdot 2 \text{H}_2\text{O}$ 0.1 mM $\text{CuSO}_4 \cdot 5 \text{H}_2\text{O}$ 0.1 mM $\text{CoCl}_2 \cdot 6 \text{H}_2\text{O}$
MS-medium	0.215% (w/v) Murashige & Skoog Medium, Basal Salt Mixture 1% (w/v) Saccharose pH 5.7
NBT-staining solution	2 mM nitro blue tetrazolium chloride 20 mM sodium phosphate buffer, pH 6.1

Solution	Composition
4X SDS sample buffer	40% (v/v) glycerol 20% (v/v) β -mercaptoethanol 9% (w/v) SDS 0.4% (w/v) Bromphenol blue 250 mM Tris, pH 6.8
Stomata opening buffer	50 mM KCl 10 mM MES, pH 6.15
50X TAE	2 M Tris 50 mM EDTA, pH 8.0 0.95 M acetic acid
TE-buffer	10 mM Tris, pH 8.0 1 mM EDTA
TF-buffer 1 (transformation buffer)	30 mM potassium acetate 50 mM MnCl_2 100 mM KCl 10 mM CaCl_2 15% (v/v) glycerol
TF-buffer 2 (transformation buffer)	10 mM MOPS, pH 7.0 75 mM CaCl_2 10 mM KCl 15% (v/v) glycerol
Washing solution (protoplast assay)	1 mM $\text{CaCl}_2 \cdot 2 \text{H}_2\text{O}$ 10 mM KCl 10 mM MES, pH 6.5, 330 mosmol/L

Solution	Composition
X-Gluc solution	50 mM sodium phosphate, pH 7.2 0.2% (v/v) Triton X-100 2 mM potassium ferrocyanide 2 mM potassium ferricyanide 2 mM X-GlcA cyclohexylammonium salt
YEP-Medium (liquid)	1% (w/v) peptone 1% (w/v) yeast extract 0.5% (w/v) NaCl pH 7.0
YEP-Medium (solid)	YEP-Medium (liquid) 0.6% Agar

Appendix Table 3: Equipment and their manufacturers.

Type	Name	Manufacturer
Centrifuge	Heraeus Fresco 21	Thermo Fisher Scientific
	Avanti™ J-25	Beckman Coulter Inc.
Growth Chamber		Johnson Controls
French Press	SLM-Aminco FRENCH® Pressure Cell Press	Thermo Fisher Scientific
Gel imaging system	FAS-Digi PRO	NIPPON Genetics EUROPE
Magnetic stirrer	IKA-Combimag RCT	IKA®-Werke GmbH & Co. KG
Microscope	Zeiss LSM 880 with Airyscan	Carl Zeiss Microcopy GmbH
	Olympus BX41 Phase Contrast & Darkfield Microscope	Olympus Europa SE & Co. KG
	Research Stereo Microscope SMZ18	Nikon GmbH
	Leitz Wetzlar Diavert Trinocular Inverted Phase Contrast Microscope	Ernst Leitz Wetzlar GmbH
Mixing	Vortex Genie 2™	Bender & Hobein GmbH
Osmometer	Osmomat 030	Gonotec GmbH
PCR machine	Applied Biosystems™ 2720 Thermal Cycler	Thermo Fisher Scientific

Type	Name	Manufacturer
Spectrophotometer	DU® 530 Life Science UV/Vis Spectrophotometer	Beckman Coulter Inc.
	NanoDrop™ 2000 Spectrophotometer	Thermo Fisher Scientific Inc.
Temperature control and mixing	Thermomixer <i>comfort</i>	Eppendorf AG
	New Brunswick™ Excella® E25	Eppendorf AG
	New Brunswick Scientific G-25 Incubator Shaker	Eppendorf AG

Appendix Table 4: Companies and their registered seat.

Company name	Address
Beckman Coulter Inc.	250 South Kraemer Boulevard, Brea, California 92821-6232, USA
Bender & Hobein GmbH	John-Deere-Straße 5, 76646 Bruchsal, Germany
Carl Roth GmbH + Co. KG	Schoemperlenstr. 1-5, 76185 Karlsruhe, Germany
Carl Zeiss Microcopy GmbH	Carl-Zeiss-Promenade 10, 07745 Jena, Germany
Duchefa Biochemie B.V	A. Hofmanweg 71, 2031 BH Haarlem, The Netherlands
Eppendorf AG	Barkhausenweg 1, 22339 Hamburg, Germany
Ernst Leitz Wetzlar GmbH	Am Leitz-Park 2, 35578 Wetzlar, Germany
Gonotec GmbH	GSG-Hof Reuchlinstr. 10-11, 10553 Berlin, Germany
GSL Biotech LLC	2365 Northside Dr. Suite 560, San Diego, CA 92108, USA
Hartmann Analytic GmbH	Steinriedendamm 15, 23108 Braunschweig, Germany
IKA®-Werke GmbH & Co. KG	Janke & Kunkel-Str. 10, 79219 Staufen, Germany
Johnson Controls Limited	One Albert Quay, Ballintemple, Cork, County Cork T12 X8n6, Ireland
Laboratory Imaging s.r.o.	Za Drahou 171, 102 00 Praha 15, Czech Republic

Company name	Address
Leu+Gygax AG	Fellstraße 1, 5413 Birmenstorf, Switzerland
Merck KGaA	Frankfurter Straße 250, 64293 Darmstadt, Germany
Minitab Ltd.	Brandon Court, Unit E1-E2, Progress Way, Coventry CV3 2TE, United Kingdom
Nikon GmbH	Tiefenbroicher Weg 25, 40472 Düsseldorf, Germany
NIPPON Genetics EUROPE	Mariaweilerstraße 28-30, 52349 Düren, Germany
Olympus Europa SE & Co. KG	Amsinckstraße 63, 20097 Hamburg, Germany
OriginLab Corporation	One Roundhouse Plaza, Suite 303, Northhampton, MA 01060, USA
Pepscan	Zuidersluisweg 2, 8243 RC Lelystad, The Netherlands
QIAGEN GmbH	QIAGEN Strasse 1, 40724 Hilden, Germany
Sigma-Aldrich Chemie GmbH	Frankfurter Straße 250, 64293 Darmstadt, Germany
Takara Bio Europe SAS	34 rue de la Croix de Fer, 78100 Saint-Germain-en-Laye, France
Thermo Fisher Scientific Inc.	168 Third Avenue, Waltham, Massachusetts 02451, USA

Appendix Table 5: Primers to genotype Arabidopsis plants.

Name	Sequence (5' to 3')	Use
Salk LBb1	ACCGCTTGCTGCAACTCTC	Genotyping SALK lines
SAIL LB3	TAGCATCTGAATTTTCATAACCAATCTCG ATACAC	Genotyping SAIL lines
CNGC14 F1	TTCTTATGGACAGAACCTGAG	Genotyping CNGC14
CNGC14 R1	CACGAATTTGAGATCACCTGC	
CNGC15 CC F1	CAAACACACGTGTCTGATCCA	Genotyping CNGC15
CNGC15 CC R1	GGTTCTTCAAGCCCCACCAT	
CNGC16 F1	CTTTACTTACTTGTGAGCCAC	Genotyping CNGC16
CNGC16 R1	CTCATCTGGCAATTGCCTATG	
At4g30360 F4	ATCATCGATCTCATTGCGAC	Genotyping CNGC17
At4g30360 R3	CCACTTATACTGCTCATATCG	
Cas9 F1	CAAGTCTAACTTCGATCTCGC	Check Cas9 presence
Cas9 R1	GAAAGACTGAGCACTAGCACC	

Appendix Table 6: Primers used for Colony PCRs or sequencing.

Name	Sequence (5' to 3')	Use
pENTR_1A_fow	GTTAGTTACTTAAGCTCGGGC	Colony PCR or sequencing of
pENTR_1A_rev	AACATCAGAGATTTTGAGACAC	
sequ. RB-R1	TATCCTGTCAAACACTGATAG	Colony PCR or sequencing of constructs with a reporter gene
GFP F1	GAAGGGCATCGACTTCAAGG	
GFP F1	TTGAAGTCGATGCCCTTCAG	
mCherry F1	CCCGTAATGCAGAAGAAGA	
mCherry R1	TTGGTCACCTTCAGCTTGG	
CRISPR F1	AGTACAGTATAGGCTTGAGCTC	Colony PCR or sequencing of constructs for CRISPR
CRISPR R2	ATGGCATTGTAGGAGCCAC	
SS102	CACCATGTTATCACATCAATCC	
pQE seq F	GGCCCTTTCGTCTTCACCTC	Colony PCR or sequencing of
pQE seq R	GCTCCTGAAAATCTCGCCAA	

Name	Sequence (5' to 3')	Use
pMAL-c5x seq F	TATGCCGTGCGTACTGC	constructs for recombinant proteins
pMAL-c5x seq R	GTTGCTTCGCAACGTTCA	
OT Ubi fow	GCGTTTGGATCGAATCAGCT	Sequencing possible off targets
OT Ubi rev	ACAGGCGGTGAAGAAGAAGA	
OT Fut8 fow	GAAAGGCCCGAGTTCAACAG	
OT Fut8 rev	AGCTTAAGACCCGTGATCCG	

Appendix Table 7: Primers used for *Promoter:GUS* constructs.

Name	Sequence (5' to 3')	Use
ProCNGC14 KpnI F	CCACGGTACCTTCAAGAAATTGGGCGT G	Amplification of promoter sequence of <i>CNGC14</i>
ProCNGC14 EcoRV R	CCATGATATCTGTTTGTA GCA ATAAAAAC	
ProCNGC15 KpnI F	AAGGTACCCTG AACCTAACT TTAGCGTG	Amplification of promoter sequence of <i>CNGC15</i>
ProCNGC15 EcoRV R	ATGATATCGTCTTCTTCTTA TCAAATCCCTGAC	
ProCNGC16 KpnI F2	CAGGTACCTAAATGCTCCATTCACGAG GGTG	Amplification of promoter sequence of <i>CNGC16</i>
ProCNGC16 XhoI R2	TCATCTCGAGTTGGGGGTTGC GTGTGTTTC	

Appendix Table 8: Primers used for fusion protein constructs.

Name	Sequence (5' to 3')	Use
RBOHD BamHI F	GCAGCAGGATCCCGATGAAAATGAGA CGAGGCAATTCAAG	Amplification of coding sequence of RBOHD for pB7WGF2/ pB7WGR2 vector
RBOHD EcoRI R	AGCAGAATTCTCACTTGAAGTTCTCTT GTGGAAGTCAAAC	
RBOHF Not1 F1	CTGAGCGGCCGCATGAAACCGTTCTC AAAGAACGA	Amplification of coding sequence of RBOHF

Name	Sequence (5' to 3')	Use
RBOHF XhoI R1	GATCCTCGAGGTGAAATGCTCCTTGTG AAATTCAA	for pB7FWG2/ pB7RWG2 vector
RBOHF NotI F1	CTGAGCGGCCGCATGAAACCGTTCTC AAAGAACGA	Amplification of coding sequence of RBOHF for pB7WGF2/ pB7WGR2 vector
RBOHF XhoI R2	GACTCTCGAGTTAGAAATGCTCCTTGT GAAATTCAA	

Appendix Table 9: Primers used for recombinant protein constructs.

Name	Sequence (5' to 3')	Use
Nterm RBOHD NcoI F3	TACCATGGTGAAAATGAGACGAGGCAA TT	Amplification of coding sequence of Nterm- RBOHD for pQe60 vector
Nterm RBOHD BamHI R3	ATAGGGATCCTCTCTGCCAATTGTCAA GTATG	
Cterm RBOHD BamHI F3	ACGTGGATCCTCGGAGAGGCTGCTCC GTGC	Amplification of coding sequence of Cterm- RBOHD for pQe60 vector
Cterm RBOHD BglII R3	TAAGATCTGAAGTTCTCTTTGTGGAAG TCA	
Nterm RBOHF NcoI F3	TACCATGGTGAAACCGTTCTCAAAGAA CGAT	Amplification of coding sequence of Nterm- RBOHF for pQe60 vector
Nterm RBOHF BamHI R3	ATATGGATCCCCTTTTCCAATTCTCTTG CATAATGTA	
Intern RBOHF NcoI F4	ATGGCCATGGTTGGAGAAAGAACA AGGTACTTC CG	Amplification of coding sequence of Intern- RBOHF for pQe60 vector
Intern RBOHF BglII R3	GAACAGATCTATCATATTTCTATAATC TTGTGCTGGT	
Cterm RBOHF NcoI F1	CTTGCCATGGAGAAAGATTTGCTTAAC AACATTG	Amplification of coding sequence of Cterm-

Name	Sequence (5' to 3')	Use
Cterm RBOHF BamHI R1	GATT <u>GATCC</u> GAAATGCTCCTTGTGAA ATTCA	RBOHF for pQe60 vector
Nterm PIP2 NcoI F1	GTAT <u>CCATGG</u> TGGCAAAGGATGTGGAA GCCGT	Amplification of coding sequence of Nterm- PIP2;1 for pQe60 vector
Nterm PIP2 BglII R1	CTGC <u>AGATCT</u> TCTGTAGAAAGACCACT TCTTTAGCT	
Loop PIP2;1 NcoI SalI BamHI F2	<u>CATGGGTCGACC</u> CACATTAACCCAGCG GTGACATTTGGGCTATTCTTGGCACGT AAAGTGTCTGTTACCTAGGGCC <u>G</u>	Oligomers for oligomer annealing of Loop- PIP2;1 for pQe60
Loop PIP2;1 NcoI SalI BamHI R2	<u>GATCCGGCCCTAGG</u> TAAACGACACTTTA CGTGCCAAGAATAGCCCAAATGTCACC GCTGGGTTAATGTGGT <u>TCGACC</u>	
Cterm PIP2 NcoI BamHI BglII F2	<u>CATGGGATCC</u> AGAGCTTCAGGTTCTAA GTCTCTTGGATCATTCAGAAGTGCTGC CAACGTCA	Oligomers for oligomer annealing of Cterm- PIP2;1 for pQe60
Cterm PIP2 NcoI BamHI BglII R2	<u>GATCTGACGTTGG</u> CAGCACTTCTGAAT GATCCAAGAGACTTAGAACCTGAAGCT CTGGATCC	
Cterm RBOHD NcoI F	ACGT <u>CCATGG</u> CCTCGGAGAGGCTGCT CCGTGC	Amplification of coding sequence of Cterm- RBOHD for pMAL-c5x vector
HIS EcoRV R	ATAGGATATCTTAGTGATGGTGATGGT GATG	Amplification of 6xHIS for pMAL-c5x vector

Appendix Table 10: Primers used for RT-qPCR.

Name	Sequence (5' to 3')	Use
Aktin qF1	ACATTCCAGCAGATGTGGATCTC	Expression analysis of control housekeeping gene <i>Actin2</i>
Aktin qR1	GATCCCATTCATAAAACCCCAGC	
GAPC qF1	GATTCTACAATGGCTGACAAGAAGA	Expression analysis of control housekeeping gene <i>GAPC</i>
GAPC qR1	ATGAAGGGGTCGTTGACAGC	
RBOHD qPCR F	GATCAAGGTGGCTGTTTACCC	Expression analysis of <i>RBOHD</i>
RBOHD qPCR R	CGAATGGAGATACGGCTCGG	
RBOHF qPCR F	CGGTTCGACTGCTTAAGGTTG	Expression analysis of <i>RBOHF</i>
RBOHF qPCR R	AAACCGCAGGACATTGGACA	
PIP2;1 qF3	GTGTTTTCCACTTGCTCTTTTG	Expression analysis of <i>PIP2;1</i>
PIP2;1 qR3	CACAACGCATAAGAACCTCTTT	

Appendix Table 11: Plant genotypes used in this work.

Organism	Accession/genotype	Reference
<i>Arabidopsis thaliana</i>	Columbia 0 (Col-0)	Timo Staffel (CAU Kiel)
	<i>pskr1-3</i> (SALK_008585)	Kutschmar et al., 2009; Stührwohldt et al., 2011
	<i>pskr2-1</i> (SALK_024464)	Amano et al., 2007; Stührwohldt et al., 2011
	<i>pskr1-3 pskr2-1</i> (SALK_008585, SALK_024464)	Stührwohldt et al., 2011; Hartmann et al., 2013
	<i>PSK2:GUS2, PSK4:GUS2, PSK5:GUS1, PSKR1:GUS4, PSKR2:GUS3</i>	Kutschmar et al., 2009; Stührwohldt et al., 2011
	<i>PSKR1:PSKR1-GFP1.2, 3.1, 4.5, PSKR2:PSKR2-GFP1.3, 3.2, 4.1</i>	Timo Staffel (CAU Kiel)
	<i>PSKR1Ox-2, 12 PSKR2Ox-1, 6 35S:PSKR1-GFP1</i>	Hartmann et al., 2014; Hartmann et al., 2015
	<i>tpst-1</i> (SALK_009847)	Komori et al., 2009
	<i>pip2;1</i>	Da Ines et al., 2010; Prado et al., 2013
	<i>PIP2;1-AA, PIP2;1-DD, PIP2,1- SS</i>	Prado et al., 2013
	<i>cngc14</i> (SALK_206460)	Zhang et al., 2017
	<i>cngc16-2</i> (SAIL_726_B04)	Tunc-Ozdemir et al., 2013
	<i>cngc17</i> (SALK_041923)	Ladwig et al., 2015

Appendix Table 12: Original vectors used in this thesis.

Name	Use	Reference
<i>pENTR™ 1A DS</i>	Entry vector	Thermo Fisher
<i>pH7FWG2</i>	Destination vector	Karimi et al., 2002
<i>pB7WGF2</i>		
<i>pB7RWG2</i>		
<i>pB7WGR2</i>		
<i>pDe CAS9 GentR</i>		Prof. H. Puchta, KIT Karlsruhe
<i>pETDuet-1</i>	Expression vector	Thermo Fisher
<i>pQE-60</i>		QIAGEN GmbH
<i>pMAL-c5X</i>		New England Biolabs
<i>CCPS1+2 CNGC15 pDe CAS9</i>	CRISPR/Cas	Timo Staffel, CAU Kiel
<i>RBOHD pB7RWG2</i>	FRET analysis	Dr. C. Kaufmann, CAU Kiel
<i>RBOHD pH7FWG2</i>		
<i>RLP44 pK7RWG2</i>		Wolf et al. 2014
<i>RLP44 pH7FWG2</i>		
<i>BRI1 pB7RWG2</i>		Ladwig et al. 2015
<i>BRI1 pH7FWG2</i>		
<i>PSKR1 pH7FWG2</i>		
<i>PSKR1 pB7RWG2</i>		

Appendix Table 13: Vectors generated in this work.

Name	Vector	Use
<i>CCPS1+2 CNGC15 pDe CAS9 GentR</i>	<i>pDe CAS9 GentR</i>	CRISPR
<i>CNGC14:GUS</i>	<i>pBGWFS7</i>	Expression analysis
<i>CNGC15:GUS</i>		
<i>CNGC16:GUS</i>		
<i>mRFP-RBOHD</i>	<i>pB7WGR2</i>	FRET analysis
<i>mRFP-RBOHF</i>		
<i>eGFP-RBOHF</i>	<i>pB7WGF2</i>	
<i>eGFP-PIP2;1</i>		
<i>RBOHD/Nterm-6xHIS</i>	<i>pQE-60</i>	Protein expression
<i>RBOHD/Cterm-6xHIS</i>		
<i>RBOHF/Nterm-6xHIS</i>		
<i>RBOHF/Intern-6xHIS</i>		
<i>PIP2;1/Nterm</i>		
<i>PIP2;1/NLC</i>		
<i>MBP-RBOHD/Nterm-6xHIS</i>	<i>pMAL-c5X</i>	
<i>MBP-RBOHD/Cterm-6xHIS</i>		
<i>MBP-RBOHF/Intern-6xHIS</i>		
<i>PIP2;1/Nterm</i>		
<i>PIP2;1/NLC</i>		

Appendix Table 14: RNA sequencing experiment numbers.

Organ	Experiment numbers
root	SRR1046909, SRR1046910, SRR314814
root apical meristem	SRR1260032, SRR1260033, SRR1261509
aerial	SRR847503, SRR847504, SRR847505 SRR847506, SRR548277
leaf	SRR314813, SRR493036, SRR764885 SRR924656, SRR934391, SRR942022 SRR1105822, SRR1105823
carpel	SRR1207194, SRR1207195
receptacle	SRR401413, SRR401414, SRR401415 SRR401416, SRR401417, SRR401418 SRR401419, SRR401420, SRR401421
stage 12 inflorescence	SRR314815, SRR800753, SRR800754
pollen	SRR847501

ACKNOWLEDGEMENT

First, I would like to express my special thanks to Professor Dr. Margret Sauter for giving me the opportunity to do my Ph.D. in her research group Developmental Biology and Physiology of Plants at the University of Kiel. I am grateful for all the support, guidance, helpful advice and encouragement over the past 4 years. I have learned a lot about science and research and have been able to grow personally. Thank you.

I would like to thank all the members of the Sauter lab for their great support, for the stimulating discussions about science, and for all the fun we have had over the past years. My special thanks go to Timo Staffel and Komathy Rajamanickam, who were the best lab partners. Besides the laughing and singing sessions, I could always count on them, which I really appreciate. I would also like to thank Tanja Rehders, who was always there for me with good advice, support and with a good supply of sweets and funny stories. Further, I thank Christine Kaufmann and Michael Motzkus, for their support and advice regarding protein analysis and of course Jay Jethva, my office mate, who provided me with great discussions and the best snacks.

I would also like to thank Jan Michels, who gave me excellent advice on microscopy and Maxim Faroux for his contribution as a master's student.

Finally, I would like to express my deep gratitude to my entire family, my wonderful friends and my partner in crime Felix for faithfully supporting and constantly encouraging me throughout the years. I wouldn't have gotten this far without such a backbone.

EIDESSTATTLICHE ERKLÄRUNG

Hiermit bestätige ich, dass die vorliegende Dissertation „Phytosulfokine receptors mediate stomatal closure in response of abscisic acid by controlling reactive oxygen species levels in guard cells“, abgesehen von der Beratung durch meine Betreuerin Frau Prof. Dr. Margret Sauter, nach Inhalt und Form meine eigene Arbeit ist. Die Dissertation wurde an keiner anderen Stelle im Rahmen eines Prüfungsverfahrens vorgelegt oder veröffentlicht. Die Arbeit ist unter Einhaltung der Regeln guter wissenschaftlicher Praxis der Deutschen Forschungsgemeinschaft entstanden. Mir wurde kein akademischer Grad entzogen.

Kiel, den

Lena Anna Carstens